IN-09

B2245

NASA TECHNICAL TRANSLATION

NASA TT-20078

TEST OF A TRAIL CRYOGENIC BALANCE IN THE ONERA T2 WIND TUNNEL

A. Blanchard, A. Seraudie, M. Plazanet, M.J. Payry

Translation of "Essai de la balance probatoire cyrogénique ONERA dans la soufflérie T2", DERAT Technical Report No. 22/5007 DN - July 1985, 47 pages

(NASA-TT-20078) TEST OF A TRAIL CRYOGENIC BALANCE IN THE ONERA T2 WIND TUNNEL (NASA) 106 p Avail: NTIS HC A06/MF A01 CSCL 14B

N87-24485

Unclas
G3/09 0082245

NATIONAL AERONAUTICS AND SPACE ADMINISTRATION
WASHINGTON D.C. 20546 JULY 1987

STANDARD TITLE PAGE

1. Report No.	2. Government Accession No.	3. Recipient's Catalog No.
NASA TT-20078		

4. Title and Subtitle	5. Report Date
TEST OF A TRIAL CRYOGENIC BALANCE IN THE ONERA T2 WIND TUNNEL	July 1987
	6. Performing Organization Code

7. Author(s)	8. Performing Organization Report No.
A. Blanchard, A. Seraudie, M. Plazanet, M.J. Payry	
	10. Work Unit No.

9. Performing Organization Name and Address	11. Contract or Grant No.
Leo Kanner Associates Redwood City, CA 94063	NASw-4005
	13. Type of Report and Period Covered
	Translation
12. Sponsoring Agency Name and Address	14. Sponsoring Agency Code
National Aeronautics and Space Administration Washington, D.C. 20546	

15. Supplementary Notes

Translation of "Essai de la balance probatoire cryogenique ONERA dans la soufflerie T2", R.T. No. 22/5007 DN, 57 pages, July 1985

16. Abstract

The three component cryogenic balance designed and manufactured by the ONERA Large Means Directorate, was equipped with a light alloy schematic model and tested at the end of 19[illegible] at the T2 wind tunnel in gusts at low temperatures up to 120 K. The tests pertained to the impact of the cryogenic conditions on the behavior of extensometric bridges while cooling the balance-model system mounted in the conditioning device and during gusts with models in the test section. A few tests with thermal disequlibrium between the flow and balance made it possible to confirm the proper operation in the range 120 K - 300 K. This gust system showed that the balance, that was well compensated thermally, may be used in T2 with and without preccoling. For any thermal gradient, the analysis was always performed with the same matrices and the aerodynamic coefficients were obtained with the same precision.

17. Key Words (Selected by Author(s))	18. Distribution Statement
Balance testing - Three component balance - Strain gages - Cryogenic wind tunnel - Transonic wind tunnel	Unclassified-Unlimited

19. Security Classif. (of this report)	20. Security Classif. (of this page)	21. No. of pages	22.
Unclassified	Unclassified	101	

TABLE OF CONTENTS

	PAGES
ANNOTATIONS	ii
INTRODUCTION	1
1 - MOUNTING ON T2 AND PROBLEMS ENCOUNTERED	2
1.1 - Description of Balance and Its Model	2
1.1.1 - Balance and Equipment Production	2
1.1.2 - Calibration and Deformations	4
1.1.3 - Mode: Description and Equipment	5
1.1.4 - Adaptation to T2 Analog Chain	6
1.1.5 - Analysis: Matrices, Aerodynamic Coefficients	7
1.2 - Cooling Box	10
1.2.1 - Description of Cooling Wind Tunnel	11
1.2.2 - Operating Principle	11
1.3 - Summary of Use of T2 Wind Tunnel	12
1.3.1 - Succinct Description	12
1.3.2 - Description of the Development of a Gust	13
1.3.3 - Acquisition, Analysis and Regulation Programs	14
1.4 - Problems Encountered and Improvements Proposed	15
1.4.1 - Model Icing in Test Section	15
1.4.2 - Sealing of Cooling Box	15
1.4.3 - Procedure Adopted for Cryogenic Tests	16
1.4.4 - Drift of Zeros of Strain Bridges	16
2 - DESCRIPTION OF RESULTS	17
2.1 - Test Conditions - Visualizations	17
2.2 - Description of Typical Tests	19
2.3 - Special Effects: Thermal Disequilibrium of Balance	20
2.4 - Test Description	22
2.4.1 - Reynolds Number by Pressure	22
2.4.2 - Reynolds Effect by Temperature	22
CONCLUSION	24
APPENDIX 1 - Model Plus Balance Strain Matrices Used for Analysis	27
APPENDIX 2 - Variation of Strain Bridge Zeros	38
APPENDIX 3 - Test Results	42
REFERENCES	48
LIST OF PLATES	49

ANNOTATIONS

c	mean chord of wing
S	wing surface
M or M_{ref}	Mach number of test
Pi	Generating pressure of test
Ta	Ambient temperature
Ti	Generating temperature of test
Tm	Model temperature
α,i	Angle of attack of model
Rc	Reynolds Number based on mean chord

Balance

X, M1, M2, N1, N2	Bridges of balance
X	drag
Y	side-slip
Z	lift
L	roll (not used)
M	pitch
N	yaw

Stresses on balance

C_{xb}, C_{yb}, C_{zb}, C_{lb}, C_{mb}, C_{nb}	Aerodynamic coefficients in balance index (X_B, Y_B, Z_B)
C_x, C_z, C_m	Aerodynamic coefficients in index associated with flow (X_A, Y_A, Z_A)

TEST OF A TRIAL CRYOGENIC BALANCE IN THE ONERA T2 WIND TUNNEL

A. Blanchard, A. Seraudie, M. Plazanet, M.J. Payry

INTRODUCTION

/9*

Current developments in the cryogenic technique with respect to wind tunnel with a high Reynolds number originate in the design and production of models and measuring means supporting low temperatures.

The T2 wind tunnel of O.N.E.R.A./C.E.R.T. operating in cryogenics since 1981 exceeded the scope of its own development and now requires the use of models for validating the cryogenic concept: the effect of the Reynolds number on aerodynamic coefficients of CAST 7 and CAST 10 airfoils has already been provided by means of local measurements on the airfoil and in the wake (Ref 4,5).

The Large Test Means (G.M.E.) to which we owe the insulation of the T2 wind tunnel, the design and manufacturing of models and the conditioning of cryogenic models is also a balance specialist. The Large Test Means Directorate of O.N.E.R.A. designed and manufactured (Ref. 1 and 2) a trial balance with three components that can undergo temperature cycles after selecting the material and the extensometric gages through tests between 100 K and 300 K on test pieces.

The dimensions and capacities of the balance were selected to be tested in the T2 wind tunnel equipped with its precooling system.

---

*Numbers in the margin indicate pagination in the original text.

After a succinct specification of the means used (balance, model, T2 wind tunnel, conditioning system), the tests conducted during the first half of the month of October 1984 will be presented. Their envelope is given below:

$$0^\circ \leq \alpha \leq 6^\circ$$
$$0.6 \leq M \leq 0.8$$
$$2 \times 10^6 \leq Rc \leq 8 \times 10^6 \text{ (mean chord = 0.103 m)}$$

During these pressure and temperature variations, we observed the behavior of the strain gages during both precoolings and testing. The good behavior of the balance was analyzed on the aerodynamic coefficients of the model.

Finally, all problems encountered are described for both the balance (Zero drift, model ice, etc.) and the precooling system (leaks, ice on displacement system, etc.).

1 - MOUNTING ON T2 AND TEST CONDITIONS /10

1.1 Description of the Balance and of its Model

The selection of the most appropriate components for making balances that function under the conditions peculiar to cryogenic wind tunnels required preliminary testing at Modane by GME (Ref. 1 and 2). These made it possible to select the material and gages sued for making a trial cryogenic balance measuring three components: axial force (X), normal force (Z) and the pitching moment (M).

The study of the structure of this balance, called XZM, was centered in particular on minimizing the thermomechanical effects, caused by the temperature gradients which may be large in cryogenic wind tunnel.

1.1.1 Balance and Equipment Manufacturing

This balance, made of HARVAL 18 maraging steel, called "XZM

Balance for cryogenic wind tunnels", is adapted to low temperature tests (120 K). It is of the "single unit" type with three components: X, A, M, but its structure enables Y, N and L (Ref. 1) to be measured as well.

Its theoretical overall outside dimension is contained in a 24 mm diameter and an overall length of 210 mm. The thinned down areas are separated by fittings, (male tapering at the rear, cylindrical with screw stopping at front), by widely dimensioned parts so as to limit the effect of stresses coming from the clamping points of the sting or fo the model and to allow the installation of electrical resistors and fairings.

Although only designed to measure X, Z, M components, the balance was provided with five bridges which, in addition to their own dynamometric function, are differentiated by the number and arrangement of gages in order to compare their particular behaviors under the influence of the temperature. The first three bridges marked: X, M1, M2, allow the longitudinal components X-Z-M (Cx-Cz-Cm) to be measured. These bridges are made upon of eight gages arranged in a particular fashion to minimize the temperature impact. Two other bridges: N1 and N2, made up of four gages arranged in a "conventional" manner, serve as reference pieces to compare the thermal effects. They can also measure the lateral components Y and R (Ref. 2).

The X bridge is made up of two half bridges, each arranged over two drag dynamometers, which may be measured separately.

The two bridges M1 and M2 are each arranged over forward and rear measuring sections of the balance. The two components Z and M are determined on the basis of the difference and the sum of their two signals.

The two bridges N1 and N2 are positioned over the lateral faces /11 of forward and rear sections. They are used as reference pieces and by comparison with the bridges M1 and M2 they are used to

determine the influence of the temperature and thermal gradients, in particular, on the two types of arrangement.

The L bridge, mentioned in the matrix tables, was not installed.

All bridges are made up of "KARMA" alloy gages of shade SK13 and with a resistance of 350 Ω (Ref. 2).

The thermal equipment of the balance includes two thermocouples, made of Constantan cooper, numbered T1 and T2, are used to determine the local temperatures of the balance.

1.1.2. Calibration and Deformation

Documents (1), (2) and (3) shows details of the studies and results of calibrations performed at Modane by GME. Let us recall the various stages of these researches:

-Study and calculation of the balance structure;

-Manufacturing and equipping the balance in two versions:

."cold" balance,
."reheated" balance;

-Calibration at ambient temperature,
Determination of its dynamometric characteristics;

-Study of the balance behavior in a cryogenic chamber in a "cold" case without gradient,
Measurement of zero variations and of sensitivity as a function of the temperature;

-Zero and sensitivity thermal compensations of balance bridges,
Determination of the effectiveness of these compensations;

-Measurement of the impact of the thermal gradients on the compensated "cold" balance, in particular on the drag bridge which is the most sensitive to these effects;

-Tests on the reheating device, and study of its ability to resist thermal gradients, or their effects.

The qualification tests of the balancer in the T2 cryogenic wind tunnel were expected to be conducted in its "cold" version. Namely, it was to be left to itself and adopted the temperatures imposed by the flow in the precooling chamber, or in the test section.

The sensitivity coefficients measured after compensation are given in the form of matrices, shown in plate ($A_1$1).

The angular elastic deformations of the balance alone, were measured on the dynamometric bench. Since the balance was installed in a sleeve considered to be infinitely rigid. The values are shown in plate ($A_1$3). The axial deformation under the effects of force X was also measured using comparators. The corresponding rigidity is 25,000 N/mm, (Ref. 2). /12

To examine the deformations of the model, we conducted a few extra tests. This allowed us to select new alpha and beta coefficients in the relationship $\Delta\theta = \alpha Z + \beta M$. Details of this transformation will be found in Appendix 1.

After the test campaign at T2, the balance-model system was sent back to Modane for testing. The new coefficients which were found when the model was installed on the balance are close to those used in the test analyses, Appendix 1.

1.1.3. Model: Description and Equipment

The model, outlining a delta wing aircraft, is made of an aluminum alloy. Its fuselage has a diameter of 38 mm, its length

is 270 mm and its span is 220 mm. The maximum chord at the root is 160 mm (Ref. 3).

It is installed on the balance whose downstream end is itself fastened to a streamlined support placed perpendicular to the flow. The model is oriented parallel to the left window of the test section of the T2 wind tunnel and at 180 mm from the window.

The support is itself fastened to this mobile metallic window which makes the wall continuous when the model is in the test section, ready for blowing. Lights help to orient the support, corresponding to model angles of attack of 0 to 6°.

This model-balance-support-window system is integrated with a precooling box fastened laterally to the wind tunnel wall.

The model is equipped with four Constantan copper thermocouples. The T3 thermocouple T3 measures the fuselage temperature, the thermocouples T4, T5, T6 measure the wing temperatures (plate 2).

1.1.4. Adaptation to the T2 Analog Chain

The different bridges of the cryogenic balance are connected to the cable path of the T2 wind tunnel. Each of the 5 bridges wired to an analog ampli-conditioner channel of the measuring chain.

A few differences in the wiring relative to the branching of /13
traditional sensors of the wind tunnel pertain to:

-the excitation voltage control: it is reclosed at the end of the cable path and does not include the extensometric bridge part and its power supply wire "bit". This was to prevent the gage bridge from being destroyed by suddenly increasing the power supply voltage in the event of wire breakage, for example.

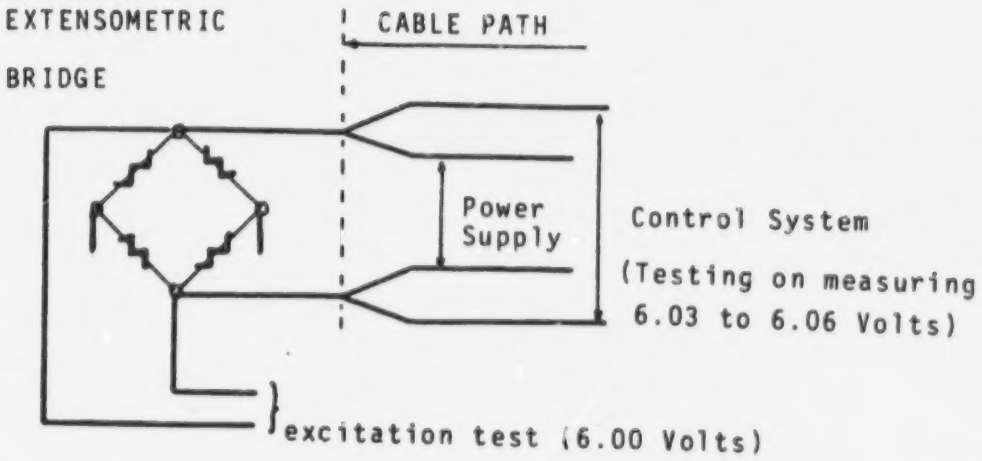

-testing the excitation voltage: the power supply voltage of the extensometric bridges is 6 volts. This test is conducted at the sensor terminals near the wind tunnel and the tested voltage is not very different that that obtained on the measuring chain (the control system does to reach the gage bridge). 6.03 to 6.06 Volts of voltage must be supplied to the conditioning level to obtain 6 Volts on the sensor.

1.1.5 Analysis: Using Matrices and Aerodynamic Coefficient

During calibrations, the stresses applied to the balance and the voltages of the five bridges X, M1, and M2, N1, N2 are measured. This is derived from the sensitivity coefficients table plate A.

If the output voltage of the bridges were perfectly linear with the stresses they are assigned to, and if no interaction occurs, only the main terms would be nonzero:

X - X drag

M1,M2 - Z lift

M1,M2 - M pitch

N1,N2 - Y yawing

N1,N2 - N roll

The roll moment L is not measured, but it stresses the gage bridges slightly. The same is true for other stresses except for the X drag plate ($A^1 1$). Owing to the nonlinearities and interactions, the quadratic terms must be taken into account. Certain configurations deemed less important were not made (Ref. 2).

We express in direction form: /14

$$\begin{bmatrix} X \\ N1 \\ M1 \\ \\ M2 \\ N2 \end{bmatrix} = \left[A'1\right] \begin{bmatrix} X \\ Y \\ Z \\ L \\ M \\ N \end{bmatrix} + \begin{bmatrix} \Delta X \\ \Delta N1 \\ \Delta M1 \\ \\ \Delta M2 \\ \Delta N2 \end{bmatrix}$$

with the quadratic terms

$$\begin{cases} \Delta X = \left[X,Y,Z,L,M,N\right] \cdot \left[B'1\right] \cdot \begin{bmatrix} X \\ Y \\ Z \\ L \\ M \\ N \end{bmatrix} \\ \Delta N2 = \left[X,Y,Z,L,M,N\right] \cdot \left[B'5\right] \cdot \begin{bmatrix} X \\ Y \\ Z \\ L \\ M \\ N \end{bmatrix} \end{cases}$$

To analyze the measuring results, the inverse matrices must be used. They were provided to us by GME, plate $A_1 2$, where the units selected are voltages in micro-Volts, Newton stresses and moments in Newton meters.

The matrices will be used as above with an inversion of the stress and voltage roles. Given for example for the X drag:

$$X = \sum_{j=1}^{6} A(1,j).E(j) + \sum_{i=1}^{n} \left(E(i).\left(\sum_{j=1}^{n} B1(i,j).E(j)\right)\right)$$

using the conventional notation $A(i,j)$ { i line
{ j column

E(i) being the bridge voltages in the selected order.

The stresses are expressed in the trihedron associated with the /15 aircraft used in flight mechanics.

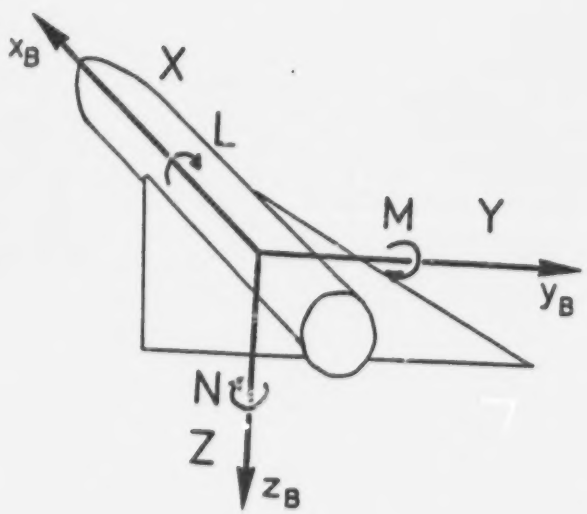

To reduce these stresses and to give dimensionless aerodynamic coefficients, we have calculated a reference surface and a mean chord, shown on the next page:

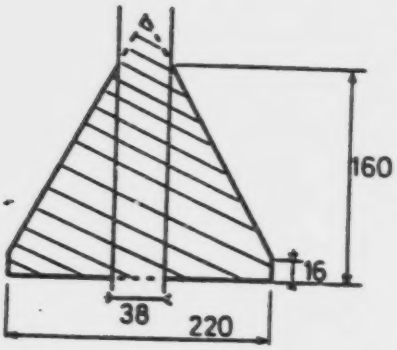

$S = 0{,}022667\ m^2$

$C = 0{,}10303\ m$

The coefficients obtained $\begin{cases} C_{\begin{matrix}X\\Y\\Z\end{matrix}} = \dfrac{\vec{F}}{{}^1/_2\rho_0 V_0^2 S} \\ C_{\begin{matrix}L\\M\\N\end{matrix}} = \dfrac{\vec{M}}{{}^1/_2\rho_0 V_0^2 cS} \end{cases}$

are associated with the balance reference. They must be projected into the aerodynamic reference, accounting for the real incidence of the model, to obtain true aerodynamic coefficients.

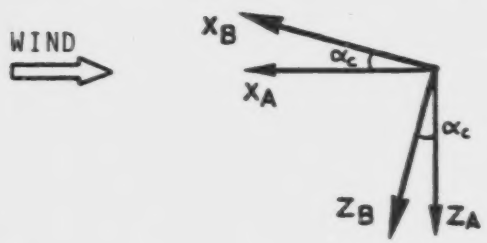

$$C_{Xa} = C_{XB}.\cos\alpha_c + C_{ZB}.\sin\alpha_c$$

$$C_{Za} = -C_{XB}.\sin\alpha_c + C_{ZB}.\cos\alpha_c$$

α_c corrected indicdence (App. 1)

The selection of the aerodynamic reference used in flight mechanics leads to negative lift and drag coefficients for a positive incidence. /16

1.2 Cooling Box

As seen in the previous report (Ref. 6), the T2 gust wind tunnel requires that a precooling system of the model be defined. We therefore designed a first cooling box for the CAST 7 airfoil.

Inspired by the diagram of the box, another box was specially made for the cryogenic balance equipped with its model.

1.2.1 Description of the Cooling Wind Tunnel

It is made up of two parts:

-the cooling circuit made up of the fan, nitrogen injection, discharge system and the reheater of the preceding circuit;

-the cooling airflow associated with the left window of the T2 wind tunnel. It is made of stainless steel and is insulated on the inside by 4 mm of polyurethane foam. This is the element in which the model is lodged for cooling.

The cryogenic balance, equipped with its model, is incorporated with the left window of the test section and the system is displaced inside the cooling box via a guidance made up of two columns-ball bushings. The cooling circuit is enclosed around the model by a slide that moves horizontally and perpendicular to the window model displacement. This slide, located on the upstream horn side, assures the continuity and isolation of the precooling circuit.

All these displacements are performed manually.

After cooling, the model-window unit is positioned in the test section and is blocked by a high speed locking system.

1.2.2 Operating Principle

A threshold regulation was used to bring the model to a selected temperature (between 120 and 300 K) and to keep it at its value before "injecting" it into the wind tunnel test section.

The nitrogen injection is controlled by two HERION electrovalves controlled by the regulation computer. The

discharge system provides a pressure of about ten millibars in the circuit.

Two computers were used to perform the regulation and data acquisition on T2.

1.3 Use of the T2 Wind Tunnel /17

1.3.1 Succinct Description

T2 is a pressurized transonic wind tunnel whose return circuit and services are shown schematically on plate 5.

The test section has a practically square section of 0.39 x 0.37 m^2.

In cryogenic operation, the flow is cooled by injecting liquid nitrogen directly into the return circuit. A 20 m^3 storage tank supplies a pressurized test tank up to 13 bars, which serves the wind tunnel injectors, arranged over two circles. The injection is therefore performed peripherally, normal to the flow, at the wall of an element located immediately downstream from the mixing chamber of the motor air and of the driven fluid.

The discharge is provided via pressurization in the wind tunnel, between the test section and the injector bend.

The wind tunnel operates by gusts. The duration of these, about one minute, depends to a certain extent on the motor rate required for testing and on the high pressure air reserve available.

The operating range of the T2 wind tunnel covers a Mach number range that extends from the lower subsonic range (OM = 0.3) to the transonic range (M = 1). The generating pressure may vary by 1.5 absolute bars to a maximum value of 100 K and 300 K, leading to Reynolds numbers of 4 to 30 million for an airfoil with a 180 mm chord.

Finally, the test section is equipped with self-adjustable walls made of Invar.

1.3.2 Description of the Development of a Gust

The wind tunnel operation is controlled by a system with 2 computers, one used for controlling the bust, the other used for measurement acquisition during the test, plate 6. The flow chart presented actually corresponds to the usual operation of the wind tunnel. For these balance tests, the model introduction phase was modified as follows:

1 - Test preparation phase consisting of cooling the model and initializing the control and acquisition programs, then introducing the model into the test section (plate 7).

2 - Establishing a gust in which a flow is initiated for a small Mach and low pressure, but at ambient temperature. A liquid nitrogen flow rate is injected that is triple the equilibrium value, making the temperature drop quickly. This flow rate is then gradually reduced, the computer controlling the regulation at the required temperature level.

The Mach number and pressure are then increased to the required values by an action programmed over the motor air flow and over the discharge flow rate. The temperature is maintained constant by increasing the nitrogen flow rate corresponding to that of the motor air flow rate.

3 - The third stage is the stabilized gust where the test parameters are maintained at nominal values using a closed loop regulation of the pressure and of the temperature. This is the phase in which the measurements per se are performed. /18

For this test campaign, the model operation was not motorized. It is performed manually prior to actually starting the gust (phase 1), and with all associated drawbacks.

The shaded area on plate 7 corresponds to to the time during which the cold model is found in the test section. There is not flow because the air is at ambient temperature. The times indicated on this plate are given only for illustration of the order of magnitude of the duration of each phase. This parameter varies with the test conditions.

1.3.3 Acquisition - Regulation - Analysis Programs

The temperature level selected for cooling the balance is obtained by regulating the nitrogen levels injected into the precooling circuit. This regulation includes the value of the temperatures measured on the model, on the balance and in the flow. The temperature acquisition is performed every 3 to 5 seconds (during phase 1). The measured values are placed on a disk file: Gust test number.

Then during phase 2, when the gust is formed and the generating conditions are stabilized, the data acquisition is performed on a magnetic tape by ACQ06. The acquisition rate is 1,000 points per second over 16 channels. The acquisition program maintains on a tape only 50 scannings per second (average over 20 points) forming blocks of 3,200 values (mV values).

The gust is regulated in the usual manner based on the conditions required for the test: Mach, pressure, temperature.

Finally, it is possible to store on disk the regulation parameters remaining in memory of the computer, in; the form of the RE test number file:

The analysis programs are used for obtaining the result of a test within minutes after the burst:

-"TRVV" makes it possible to plot the parameter variations during the cooling process as a function of time,

-"TRBAL" recovers the test parameters of the test on tape and plots them as a function of time,

-"TRREG" plots the control parameters of the test.

The values stored on the magnetic tape are in mV. The "zero"s of the channels taken in the preceding 10 second were removed before the test actually began.

1.4 Problems Encountered and Improvements Made /19

All problems encountered in this test campaign pertain to cryogenics. Most of the tests for which the model was cooled are questionable.

1.4.1 Icing the Model and Introducing it into the Test Section

The manual displacement of the model between the cooling box and the test section, should be done before the gust begins because of the size of the window displaced and the stresses created by the pressures, even at a small Mach. This introduction principle is bad, because the model, precooled in the chamber, becomes the coldest point of the wind tunnel which is still at ambient temperature. The model and the balance are then attraction poles for humidity.

In draining the circuit, before each cryogenic gust, with dry air used for operating the wind tunnel, the quantity of ice deposited on the model is decreased.

1.4.2 Sealing the Cooling Box

The test section of the cooling circuit (plate 3) is made up of four walls:

-upper and lower fixed walls,

-lateral walls which are two faces of a slide moved after positioning the model and its window for precooling (plate 3). The large clearance required for operating the slide (unilateral insulation of its walls -> repulled when cold) does not provide enough sealing.

The connection between the outside envelope of the cooling test section and the wind tunnel test section gate is not impervious. It also allows wet air to be input.

All "leaks" and the cooling of the attached circuit over a fairly long period of time should cause ice on the model and the displacement system, despite the slight overpressure prevailing in the circuit (nitrogen injection). Some tests were stopped after cooling, because the model could not be placed in the test section because of ice and frost accumulating in the displacement system. It therefore seems excluded to redo the tests without improving the sealing of this conditioning system.

1.4.3 Procedure Adopted for Cryogenic Tests

It was however possible to improve these tough test conditions by reducing the humidity rate of the cooling system:

-before dropping the temperature, by forming a long sweep with gaseous nitrogen injection, and with the reheating system branched simultaneously, to discharge as far as possible the humidity contained in the circuit and its isolation:

-after each cryogenic gust, the model and the entire conditioning circuit are brought back up to ambient temperature. Another improvement consists of draining the T2 wind tunnel circuit before each cryogenic gust, as described in section 1.4.1. /20

1.4.4 Derivative of Bridge Zeros

Right from the first cooling operations performed on the

balance in the precooling circuit, we noticed a variation in the bridge zeros as a function of time. The five first days of the test campaign, large variations were observed (plate $A_2 1$): while returning to ambient temperatures after each test, the values obtained were not more than those recorded before the gust or cooling. This difference became more marked with the number of tests performed. On plate $A_2 1$, we showed this variation, during the test campaign (15 days): we observe a variation of several hundreds of millivolts on the bridge zeros; only the X bridge did not undergo such variations.

These curves also show that the variations diminish during the second test week. There is a stabilization at clearly different values than those at the beginning at the end of the test campaign.

Systematic daily checks were conducted on the balance-model system mounted in the test section of the wind tunnel:

-with weights of 320 g and 5,470 Kg placed at 95 mm in front of the center of force reduction; the model assembly in the test section made it possible to check by weighing only bridges N1 and N2.

-with a resistor (R - 210 Ω) causing a bridge disequilibrium: this is a sensitivity check of each of them. We were thus able to verify that the delta E caused by this delta R remained constant despite the zero deflections.

In addition to these verifications, the excitation voltages were adjusted carefully before each test.

2 - DESCRIPTION OF THE RESULTS

2.1 Test Conditions

These tests were combined under 4 angles of attack:

alpha = 0°; 1.5°; 3.65°; 5.70°

for Mach numbers between 0.6 and 0.8. The pressures varied between 1.5 bars and 3 bars and the temperatures between 120 K and ambient temperature. The high and low pressure tests are not very numerous. Many gusts were performed at ambient temperature and at low pressure.

A few tests were conducted with thermal disequilibrium, either hot model and cold flow, or cold model and flow at Ta, to assess its impact on the balance measurement.

This group of tests and their conditions are marked in the tables placed in Appendix 3, as well as the results obtained: bridge voltages, stresses on balance, aerodynamic coefficients.

A few visualizations were performed at 0° and 4° angle of attack for M = 0.75 and M - 0.8; they are shown in plates 8,9 and 10. We used the usual mixture (vaseline oil and lamp-black mixture) deposited on the wing prior to the gust. /21

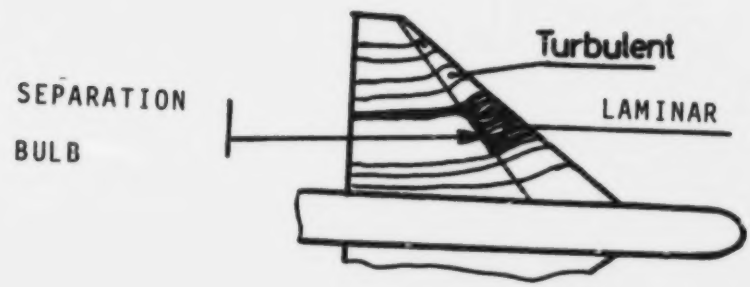

At M = 0.75, alpha = 0°, Ti = Ta, Pi = 1.6 b (plate 8), the boundary layer is turbulent over virtually the entire upper surface of the wing from the leading edge (a laminar zone is perceived over the upper wing: regrouping of mixture on edge of dihedral).

Plates 9 and 10 correspond to an angle of attack of 0°. We

see three dimensional effects form: magnifications of the end tip demonstrate the appearance of typical vortices of a swept-back wing. All wall lines are well marked (separation line, reseparation, etc.,). Plate 10 pertains to a higher Mach number; the apex vortex outline is very distinguishable along the leading edge.

2.2 Description of Typical Tests

These tests were selected at M = 0.75, Pi = 1.7 b and Ti = 180 K for 2 angles of attack alpha = 0° (test 22) and alpha = 3.43° (test 39).

For these two cases, we plotted the temperature variation on the model and balancer (plates 11 and 17), as well as their bridge tension values during the precooling phase (plates 12 and 18): the aluminum alloy model cools very rapidly. T3, T4, T5 and T6 just about follow the variation of the cooling Ti. Conversely, the balance takes a great deal of time to reach the recommended value (about 20 minutes). The temperature deviation between the front and back of the balance passes through a maximum value (thermal disequilibrium on X drag bridge).

The gage bridge tensions change considerably and want, it seems, to stabilize near different values than those of the beginning, corresponding to the temperature of the balance: it is nearly these values which are assumed to be zero, just before the test.

For the test, we first plot (plate 13) the regulation conditions (Pi, Ti, M), the temperature variation on the model and balance (plates 14 and 19), the variations in the extensometric bridge tensions (plates 15 and 20), then the corresponding aerodynamic coefficients in the aircraft reference mark (plates 16 and 21) as a function of time.

Temperatures: when the generating conditions of the test are

reached (t - 40 s), the model which was not reheated very much returned to the design temperature. The balance is not sensitive to these variations and its thermocouples T1 and T2 remain approximately at the test value.

Bridge gages: the tensions change in good proportions based on /22 the temperature rise in the wind tunnel. This corresponds to the balance loading. The aerodynamic coefficients established with the generating conditions do not change during the test. In the same Mach, pressure and temperature case, but with a larger angle of attack (test 39), we observe a good behavior of the balance loaded nearly four times more along Z (the lift passing from 63 N to 280 N).

2.3 Special Effects: Thermal Disequilibrium of the Balance

In addition to the conventional variation tests of the Mach number and of the angle of attack for various pressures and temperatures, a few gusts were made to observe the behavior of the balance in thermal disequilibrium relative to the flow.

The first test was conducted at M = 0.757, Pi = 1.63 b, alpha = 0° (test 28), at ambient temperature, the model cooled to 200 K. The generating conditions are plotted on plate 12.

The model temperatures are just about established on Tiv right from the beginning of the stabilized bust (plate 23). Conversely, the balance operates in thermal disequilibrium relative to the flow with a longitudinal temperature gradient on the drag bridge of some ten degrees. This temperature deviation is not noticeable on the plotting curves for bridge tensions and aerodynamic coefficients (plates 24 and 25). The results obtained on the aerodynamic coefficients are very close to those obtained for the same test with ambient temperature model (plate A_{34} - tests 16, 17 and 28).

The second comparison with and without thermal disequilibrium

was made for a case with low temperatures (difference between Ta and 120 K) and high balance loading in Z (M = 0.756, Pi = 1.64 b, alpha = 3.43°, tests 36 and 37).

Test 36 was conducted with a thermal balance satisfying Ti n ≃ 120 K and the precooled model toward 125 K (plates 26, 27 and 28). Test 37 was conducted with the same generating gust conditions, but without precooling the model (plates 29, 30 and 31). The longitudinal gradient (T1,T2) remains small but the temperature difference between the balance and the flow is very large (≃ 170°). In this case where the balance remains near ambient temperature, the model is established in temperature by the flow during the test. We then see a very slight variation on the bridges N1 and N2 (plate 30) which results in a small difference in the aerodynamic coefficients C_Z and C_m (plate 31).

The table below shows the results obtained on the aerodynamic coefficients for these comparative tests: /23

M = 0,75 | α = 3,43°

N° Essai	C_X	C_Z	C_m	
36	-3.3×10^{-2}	-2.69×10^{-1}	-9.75×10^{-2}	Ti = 120K Pi = 1,6b Tm = 120K
37	$-3,07 \times 10^{-2}$	-2.66×10^{-1}	-9.48×10^{-2}	Ti = 120K Pi = 1,6b Tm = Ta
35	$-2,98 \times 10^{-2}$	$-2,6 \times 10^{-1}$	$-9,38 \times 10^{-2}$	Ti = Ta Pi = 3b Tm = Ta

These tests show that the thermally compensated balance may be used in T2 without precooling with the same accuracy for measuring the aerodynamic coefficients by keeping the same matrices for analysis.

2.4 Test Description

All tests performed on the cryogenic balance, the numerical results of which are given in Appendix 3 are gathered on the aerodynamic coefficient curves (Cx, Cz, Cm) plotted as a function of the Mach number (plates 32 to 43), as a function of the angle of attack (plates 44 to 46) and in polar form of plate 47.

The first tests at ambient temperature were conducted at four Mach numbers and four angles of attack:

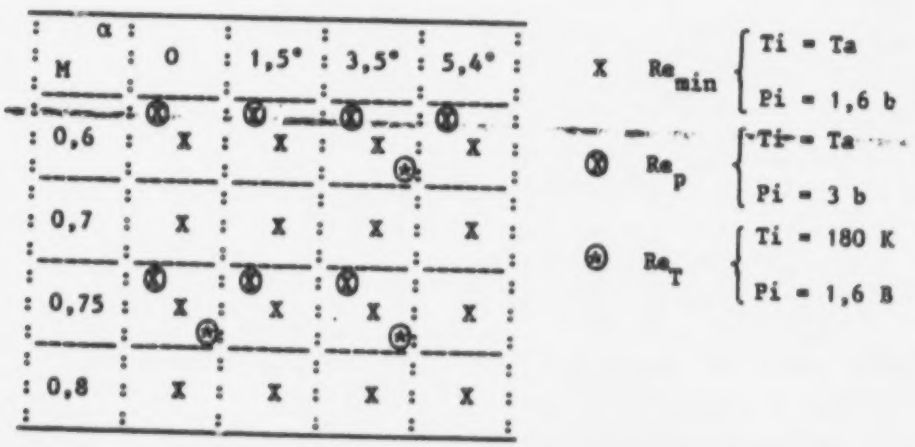

All Cx, Cz, Cm curves as a function of M indicate an increase in the aerodynamic coefficients with an increase in the Mach M number for the same angle of attack. These same coefficients plotted as a function of the angle of attack give aligned /24
experimental points, for the same Mach number.

A few cases were selected for which the Reynolds number was increased by the pressure or temperature:

-pressurized tests up to 3 bars, Ti = Ta
-cryogenic testss at 180 K and 120 K, Pi = 1.6 b

2.4.1 Reynolds Effect by Pressure

Gusts at ambient temperature and 3 bars of a generating pressure were conducted for two Mach numbers at all angles of attack, except for the highest where the loads supportable by the balance could have been exceeded by the Z bridge.

In Cz and Cm , at M = 0.6 as well as at M = 0.75, the experimental points obtained are correctly placed on the curves obtained at low pressure. Conversely, the pressure creates in all cases a drop in the aerodynamic drag coefficient Cx: this may be interpreted by an effect of the Reynolds number on the boundary layer development on the wing. In natural transition as in triggered transition, the Reynolds effect on an airfoil (Ref. 1, 2, 3) results in a decrease in the drag coefficient. This is confirmed by the plottings as a function of the angle of attack alpha (plates 44, 45, and 46): the dotted curves at M = 0.75 and 0.6 are below those obtained at a small Reynolds number (plate 44).

2.4.2 Reynolds Effect by Temperature

The tests at low temperatures were conducted with the same thermal balance first, then without cooling the balance-model system. The icing problems elicited in section (1.4.1) found during tests with a model-cold balance, create differences in the values obtained for aerodynamic coefficients.

As for pressure effects, the results obtained on Cz and Cm deviate very little from tests at ambient temperature. Conversely, for Cx, we see major differences, certainly due due the Reynolds effect and to icing on the model (opposite variation direction).

A few interesting points were obtained by introducing the balance-model at ambient temperature into the T2 circuit for a cold gust. In such a case, there was no ice deposit on the model

cooled by the flow and the decrease in the drag coefficient due to the Reynolds effect cannot be masked by a spurious effect. The decrease in Cx is inversely proportional to the Reynolds number: plate 38 (Ti = 180 K and Ti = 120 K with hot model at M = 0.75 and alpha = 3.43°).

It was possible to obtain a correct agreement on the test results by accounting for the deformations of the balance-model system. The corrective coefficients are given in Appendix 1.

CONCLUSION /25

The development of large cryogenic wind tunnels revealed instrumentation problems, particularly for stress measurements. ONERA therefore understood this study, on a trail cryogenic balance of moderate dimensions adapted to the T2 wind tunnel. Numerous investigations conducted at Modane by GME on the architecture of the balance and its equipment concentrated on minimizing the thermomechanical effects. Two versions were studied: "cold balance" and "reheated balance"; they both gave good results during the various calibrations in the cryogenic chamber. The temperature compensation of the various bridges seemed particularly successful.

For the final qualification tests in the T2 cryogenic wind tunnel, a schematic model of a fighter plane and its support were manufactured, as well as precooling means associated with the wind tunnel. The rough pattern of the model is associated with the low cost of its production. This involves controlling the behavior of the balance and the precision of the instrumentation under realistic operating conditions. In particular, it was interesting to note the temperature variations in the balance, the amplitude of the bridges, their stabilities during the gust.

During this study campaign, a certain number of problems occurred. The main ones are:

-Major variations of zeros of 4 in 5 bridges during the first week, the sensitivities remaining constant in other cases.

-Large bending of the model than expected. It was necessary to redetermine the angle of attack correction coefficients.

-Poor sealing of the precooling chamber. Ice formation on model and blocking of translation system.

-Incorrect procedure of introducing model into test section.

These different points would be improved if a similar study were conducted in the T2 wind tunnel.

Despite these problems, numerous sensitive points were brought to light:

-acceptable time for cooling balance;

-the measurements could be performed with the desired accuracy (the main limitation being a resolution of 5 mv of the multiplexer of the acquisition chain);

-the X bridge is unusually stable, whereas it was likely, a priori, to vary the most. (This result is due to the stresses developed by GME to minimize the thermomechanical effects);

-the measuring result is independent of the temperature taken /26 on by the balance;

-moderate thermal gradients may be accepted, without altering the calibration coefficients.

After these tests,the model and the balance were returned to Modane to test the deformations of the system, the calibration coefficients of the bridges, the zero differences, to inspect the gage bondings and the system covering which could have been

damaged by the humidity deposited by the ice.

The tests of the cryogenic prototype balance ∅ 24 mm of ONERA in the wind tunnel T2 confirmed the reliability of a 5 component balance (X, Y, Z, M, N) of this dimension for use in a cryogenic wind tunnel.

The concept of a cold balance proves to work correctly. It was demonstrated also that the balance can be used without precooling in a wind tunnel with short gusts such as T2.

These results may not be generalized to balances with larger capacities without reservations. Actually, the experiment conducted at ambient temperature shows that the balances were more sensitive to gradient effects when they had large dimensions. Further developments are therefore planned by GME.

APPENDIX 1

1 - Balance Calibration: Matrices (A_1, A_2)

2 - Model + balance deformations: checks after testing

O.N.E.R.A.	GME	RSF - 29 7/0791 GY	Drawn by H. OUERNA	Date July 82	

ORIGINAL PAGE IS OF POOR QUALITY

XZM CRYOGENIC BALANCE
SENSITIVITY COEFFICIENTS
in μV/kg and mkg or $\mu V/kg^2$ and mkg^2

$U_0 = 6{,}000\ V$

Bridges / Stress	(X)		(M_1)		(M_2)		(N_1)		(N_2)	
X	+369,0	100	0	0	0	0	0	0	0	0
Y	-0,06	<0,1	+0,30	0,6	+0,05	0,1	-46,43	99,9	+45,93	99,9
Z	-3,52	9,1	+30,00	64,4	-29,48	59,5	-0,06	<0,1	+0,23	0,3
L	0	0	-0,4	<0,1	+29,0	2,9	-5,2	0,3	+0,4	0,1
M	+21,0	4,5	+645,5	100	+607,0	100	-4,5	0,2	-3,0	0,2
N	+17,0	1,2	-4,8	0,8	+0,6	0,1	+947,0	100	+946,0	100
X^2	0	0	0	0	0	0	0	0	0	0
Y^2	+0,010	0,7	0	0	0	0	0	0	0	0
Z^2	+0,016	1,1	0	0	0	0	0	0	0	0
L^2	-15,90	2,7	0	0	+0,20	<0,1	0	0	0	0
M^2	-2,70	1,2	0	0	0	0	0	0	0	0
N^2	+2,30	1,0	0	0	-0,20	0,2	0	0	0	0
XY *										
XZ	+0,012	<0,1	0	0	0	0	0	0	0	0
XL *										
XM	0	0	0	0	0	0	0	0	0	0
XN *										
YZ *										
YL *										
YM *										
YN	-0,70	1,0	0	0	0	0	0	0	0	0
ZL	0	0	0	0	0	0	0	0	-0,15	0,2
ZM	+0,47	0,7	0	0	0	0	0	0	0	0
ZN *										
LM	+0,3	~0	0	0	0	0	+0,3	~0	+0,6	<0,1
LN *										
MN *										

ORIGINAL PAGE IS
OF POOR QUALITY

INVERSE MATRIX

No. 1672 of 2/21/89

Tensions in microVolts
Stresses (Newton)
Moments (Newton.meter)

RSE n=1672 du 21/2/89

(ampli : gain 1000 ---> milliVolts)

G=9.8009 m/s**2

Main Matrix A

-X-	-N1-	-M1-	***	-M2-	-N2-	
.2682239E-01	-.2480879E-03	.1269548E-02	0.	-.1630188E-02	-.2206469E-03	*drag X
0.	-.1064069E+00	-.1058869E-03	0.	.9103161E-03	.1065182E+00	*slip Y
0.	.9182866E-03	.1668150E+00	0.	-.1690812E+00	.1676724E-04	*lift Z
0.	0.	0.	19.8009	0.	0.	*roll L
0.	.4832326E-04	.8101419E-02	0.	.8235689E-02	-.1334765E-04	*pitch M
0.	.9166206E-02	-.4495014E-06	0.	.3003022E-04	.9188672E-02	*yaw N

Matrix B1: Second terms on X drag

-X-	-N1-	-M1-	***	-M2-	-N2-	
0.	-.8253201E-10	-.1499268E-07	0.	.1519639E-07	-.1506974E-11	*bridge X
0.	-.1963044E-06	-.3034311E-08	0.	.2200992E-08	.2833072E-07	*bridge N1
0.	0.	-.2600232E-06	0.	.4023744E-06	.9440823E-10	*bridge M1
0.	0.	0.	0.	0.	0.	*****
0.	0.	0.	0.	.9798636E-07	.3330722E-10	*bridge M2
0.	0.	0.	0.	0.	.5896614E-07	*bridge N2

Matrix B2: Second terms on Y side-slip

0.	0.	0.	0.	0.	0.	*bridge X
0.	.2839833E-10	-.4934805E-14	0.	.3296838E-12	.5696331E-10	*bridge N1
0.	0.	.2146838E-18	0.	-.2868513E-16	-.4956265E-14	*bridge M1
0.	0.	0.	0.	0.	0.	*****
0.	0.	0.	0.	.9581960E-15	.3311174E-12	*bridge M2
0.	0.	0.	0.	0.	.2860551E-10	*bridge N2

Matrix B3: Second terms on Z lift

0.	0.	0.	0.	0.	0.	*bridge X
0.	-.9395869E-08	.1635031E-11	0.	-.1092329E-09	-.1887345E-07	*bridge N1
0.	0.	-.7113042E-16	0.	.9504141E-14	.1642141E-11	*bridge M1
0.	0.	0.	0.	0.	0.	*****
0.	0.	0.	0.	-.3174756E-12	-.1097079E-09	*bridge M2
0.	0.	0.	0.	0.	-.9477760E-08	*bridge N2

Matrix B4: Second terms on L roll UNUSED

0.	0.	0.	0.	0.	0.	*bridge X
0.	0.	0.	0.	0.	0.	*bridge N1
0.	0.	0.	0.	0.	0.	*bridge M1
0.	0.	0.	0.	0.	0.	*****
0.	0.	0.	0.	0.	0.	*bridge M2
0.	0.	0.	0.	0.	0.	*bridge N2

Matrix B5: Second terms on M pitch

0.	0.	0.	0.	0.	0.	*bridge X
0.	.4576584E-09	-.7963991E-13	0.	.5320571E-11	.9192972E-09	*bridge N1
0.	0.	.3464656E-17	0.	-.4629324E-15	-.7998624E-13	*bridge M1
0.	0.	0.	0.	0.	0.	*****
0.	0.	0.	0.	.1546376E-13	.5343709E-11	*bridge M2
0.	0.	0.	0.	0.	.4616474E-09	*bridge N2

Matrix B6: Second terms on N yaw

0.	0.	0.	0.	0.	0.	*bridge X
0.	.1668784E-11	-.2903991E-15	0.	.1940068E-13	.3352081E-11	*bridge N1
0.	0.	.1263339E-19	0.	-.1688014E-17	-.2916580E-15	*bridge M1
0.	0.	0.	0.	0.	0.	*****
0.	0.	0.	0.	.5638631E-16	.1948504E-13	*bridge M2
0.	0.	0.	0.	0.	.1683329E-11	*bridge N2

XZM CRYOGENIC BALANCE
ELASTIC DEFORMATIONS

STRESS COMPONENT	ELONGATION Δx in μm/N	ANGLES in 10^{-6} rd /N or Nm		
		φ	θ	ψ
X	+ 0,04	0	0	0
Y	0	0	0	+ 2,6 ± 0.2
Z	0	0	− 2,6 ± 0,4	0
L	0	+ 340	0	+ 32 ± 2
M	0	0	+ 280 ± 5	0
N	0	+ 40 ± 2	0	+ 400 ± 5

Axial rigidity of entire balance: 25,000 N/mm

ORIGINAL PAGE IS OF POOR QUALITY

O.N.E.R.A. | GME | RSF - 31 | 7/0791 GY | Drawn by | Date July 82

ORIGINAL PAGE IS
OF POOR QUALITY

Angle of Attack-Model Correction Including Deformations of Latter and of Balance

It is assumed that the real angle of attack of the model placed in a flow is the algebraic sum of the displayed angle of attack without wind (therefore without stress), and of the angle of attack variation $\Delta\theta_B$ due to the deformation of the balance plus that of its support, as well as of the angle of attack variation $\Delta\theta_M$ due to the model deformation:

$$\left\{\begin{array}{l}\boxed{\text{incidence} = \text{displayed incidence} + \text{deformation}} \\ \text{where } \textbf{déformation } \boxed{\Delta\theta_L = \Delta\theta_B + \Delta\theta_M}\end{array}\right. \qquad \text{(I)}$$

R : center of reduction
of balance stresses

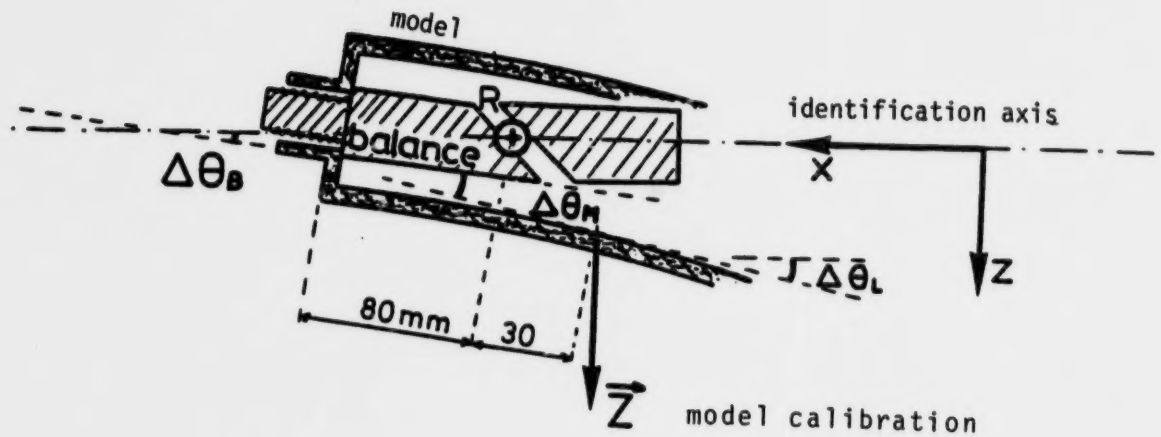

$\Delta\theta_B$: angle of model-balance/identification clamping
$\Delta\theta_M$: model/axis angle of clamping
$\Delta\theta_L$: model/identification axis of mounting

Note:

$\Delta\theta_M$ & $\Delta\theta_L$ are a function of x-axis $\left\{\begin{array}{l}\Delta\theta_M\ (x) \\ \Delta\theta_L\ (x)\end{array}\right.$.

It is assumed that the local angle of attack of the model is /33

$A_1 5$

It is also assumed that the local angle of attack of the model is given by the measured angle of attack $\Delta\theta_L$ at the application point of the stress resultant. All variations of angle θ, and all stresses (X, Z) are in the plane (x-z). Therefore, only the pitch moment M will be included.

The calibrations performed at the Modane center by GME, after the test campaign at T2 are of two types:

-stresses applied to the sleeve of the balance considered to be infinitely rigid (plate A-1) (independent forces and moment). These calibrations give the alpha and beta coefficients of the relationship

$$\Delta\theta_B = \alpha Z + \beta M \qquad \text{(II)}$$

$$\alpha = -4{,}33 \times 10^{-5} \text{ rd/Kg}$$

$$\beta = 307 \times 10^{-5} \text{ rd/m.Kg}$$

-stresses applied 30 mm behind the balance reduction center R, on the mounted model (plate A-2).

This calibration gives the overall coefficient:

$$\frac{\Delta\theta_L}{Z} = 13{,}4 \times 10^{-5} \text{ rd/Kg}$$

(in this case the moment equals 0.03 x Z).

If the model were infinitely rigid like any sleeve, we would have:

$$\Delta\theta = (-4.33 + 0.03 \times 307) \times 10^{-5} \times Z$$

$$= 4.88 \times 10^{-5} \times Z$$

The deformation specific to the model is therefore far from being negligeable.

To calculate the deformation due to the model, we will assume /34 that the angle of attack variation $\Delta\theta_M$ follows a law similar to that established for $\Delta\theta_B$ (relationship II). We will let:

$$\boxed{\Delta\theta_M = \alpha' Z + \beta' M'} \qquad \text{(III)}$$

where M' is the moment calculated relative to the fuselage clamping:

$$M' = M + (0{,}08).Z$$

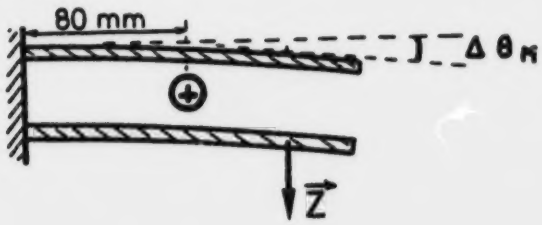

This relationship may therefore be expressed:

$$\Delta\theta_M = (\alpha' + 0{,}08\beta').Z + \beta' M$$

By carrying over relationships (II) and (III) to equation (I), we obtain the following relationship:

$$\boxed{\Delta\theta_L = (\alpha + \alpha' + 0{,}08\beta').Z + (\beta + \beta').M} \qquad \text{(IV)}$$

The value of the four coefficients ($(\alpha, \alpha', \beta$ and $\beta')$ is to be deduced from tests performed at Modane. We have seen that the alpha and beta coefficients are directly known from the calibration on the balance sleeve (plate A19); α' and β' are unknown, they are to be determined by calibration on a full model. Only an overall value is provided to us by tests reported (plate A110). Actually, the force Z is applied 30 mm behind the balance reduction center, it produces a pitching moment M = 0.03 Z. With this expression for the moment, we may rewrite the expresses (IV):

$$\frac{\Delta\theta_L}{Z} = (\alpha + 0{,}03\beta) + (\alpha' + 0{,}11\beta') = 13{,}4 \times 10^{-5} \text{ rd/Kg}$$

i.e. $$\boxed{\gamma = (\alpha' + 0{,}11\beta') = 8{,}52 \times 10^{-5} \text{ rd/Kg}}$$

In the first approximation, we may assume that the coefficient /35 α' is close to zero. This assumption may be mechanically justified because the fuselage has a weak point near its clamping (metal cutout), the rear part is reinforced by the wing.

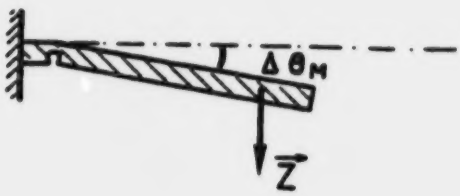

The angle $\Delta\theta_M$ is therefore directly proportional to M'

$$\Delta\theta_M = \beta' M' \text{ with } \boxed{\beta' = \frac{\gamma}{0,11} = 77,45 \times 10^{-5} \text{ rd/m.Kg}}$$

Relationship (IV) becomes:

$$\Delta\theta_L = (1,87 \times 10^{-5} \text{ rd/kg}).Z + (384 \times 10^{-5} \text{ rd/m.Kg}).M$$

or $$\Delta\theta_L = (1,91 \times 10^{-6} \text{ rd/N}).Z + (392 \times 10^{-6} \text{ rd/m.N}).M$$

S.I. unit

It may be directly observed on the coefficients value, the deformation percentage due to the model and that due to the balance.

Relationships (II) and (III) are expressed:

$$\Delta\theta_B = (-4,42 \times 10^{-6} \text{ rd/N}).Z + (313 \times 10^{-6} \text{ rd/m.N}).M$$

$$\Delta\theta_M = (+6,32 \times 10^{-6} \text{ rd/N}).Z + (79 \times 10^{-6} \text{ rd/m.N}).M$$

Checking the Formula /36

A18

Before the departure of the cryogenic model for Modane, and just after the test campaign at T2, a few verifications were made of the order of magnitude of the corrective angle of attack coefficients due to deformations: the results are shown on plate A-3.

A few verifications can be made:

Loads toward front of model

- $Z = -235$ N, $M = 17{,}76$ mN $\rightarrow$ $\theta_{L\ \text{calculated}} = 22'$ (24' measured)
  ($\Delta\theta_B = 22{,}68'$, $\Delta\theta_M = -0{,}28'$)
- $Z = -196$ N, $M = +14{,}8$ mN $\rightarrow$ $\theta_{L\text{calculated}} = 18{,}6'$ (20' measured)
  ($\Delta\theta_B = 18{,}9'$, $\Delta\theta_M = -0{,}24'$)

Loads toward rear of model

- $Z = -235$ N, $M = -26{,}22$ mN $\rightarrow$ $\theta_{L\text{calculated}} = -36{,}8'$ (-33,8' measured)
  ($\Delta\theta_B = -24{,}64'$, $\Delta\theta_M = -12{,}23'$)
- $Z = -196$ N, $M = -21{,}85$ mN $\rightarrow$ $\theta_{L\text{calculated}} = -30{,}7'$ (-27,7' measured)
  ($\Delta\theta_B = -20{,}53'$, $\Delta\theta_M = -10{,}19'$)

We can now see that the agreement of the results is nearly correct, knowing that the deformation tests conducted at DERAT do not have the precision of those obtained at Modane, but give a good idea of the orders of magnitude. These checks justify, a posteriori, the use of the coefficients found at DERAT for analyzing the tests, based on the overall deformations of the model-balance.

ONERA — GMC — Drawn by: L. DURAND — Date: 18 1 7.

CYROGENIC WIND TUNNEL TEST RIG

ELASTIC DEFORMATIONS IN θ — $A_1 9$

θ in 10^{-5} rd.

STRESSES APPLIED TO BALANCE

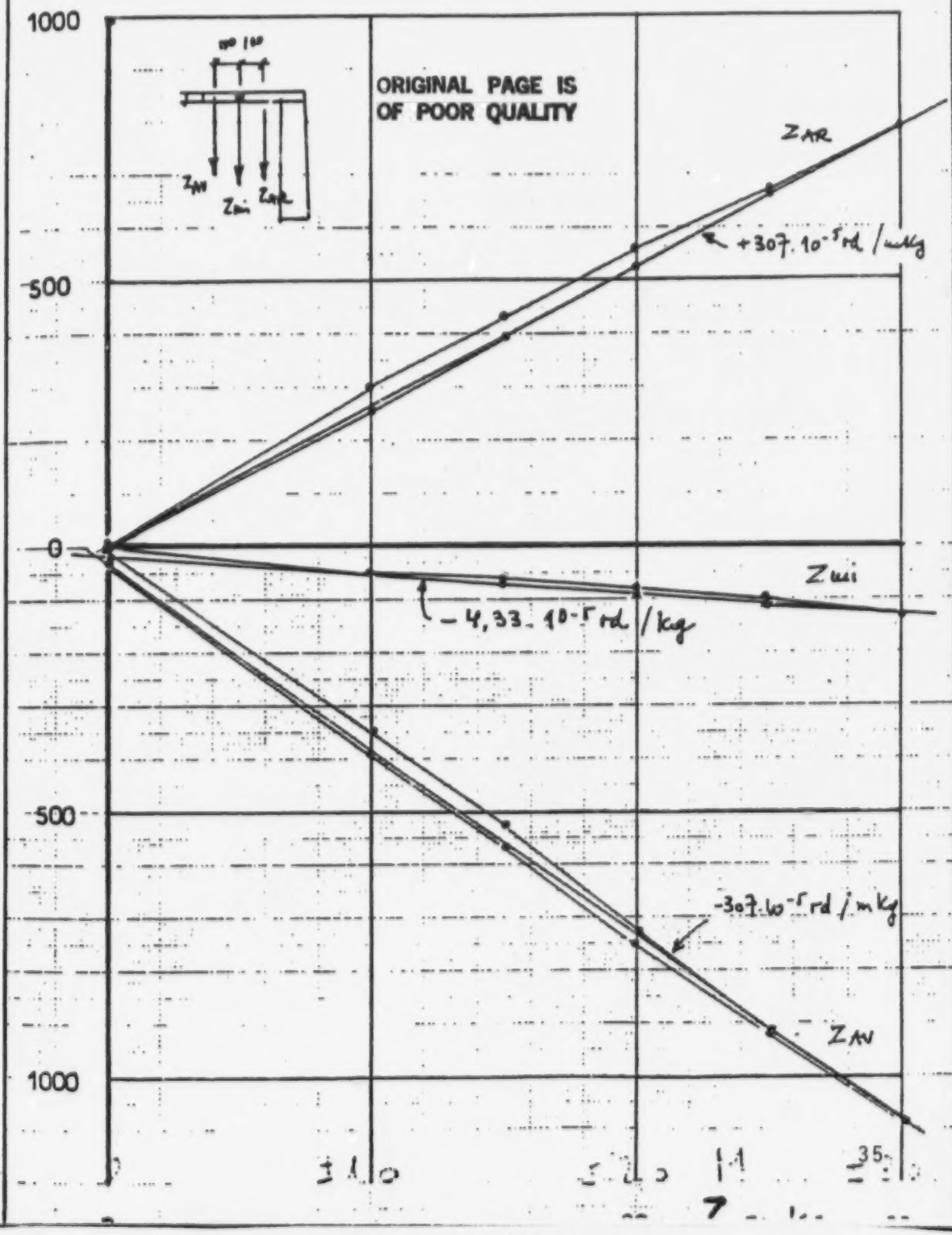

T2

T2 CRYOGENIC SIND TUNNEL TEST RIG
ELASTIC DEFORMATIONS IN θ

STRESSES APPLIED TO MODEL

ONERA

ORIGINAL PAGE IS OF POOR QUALITY

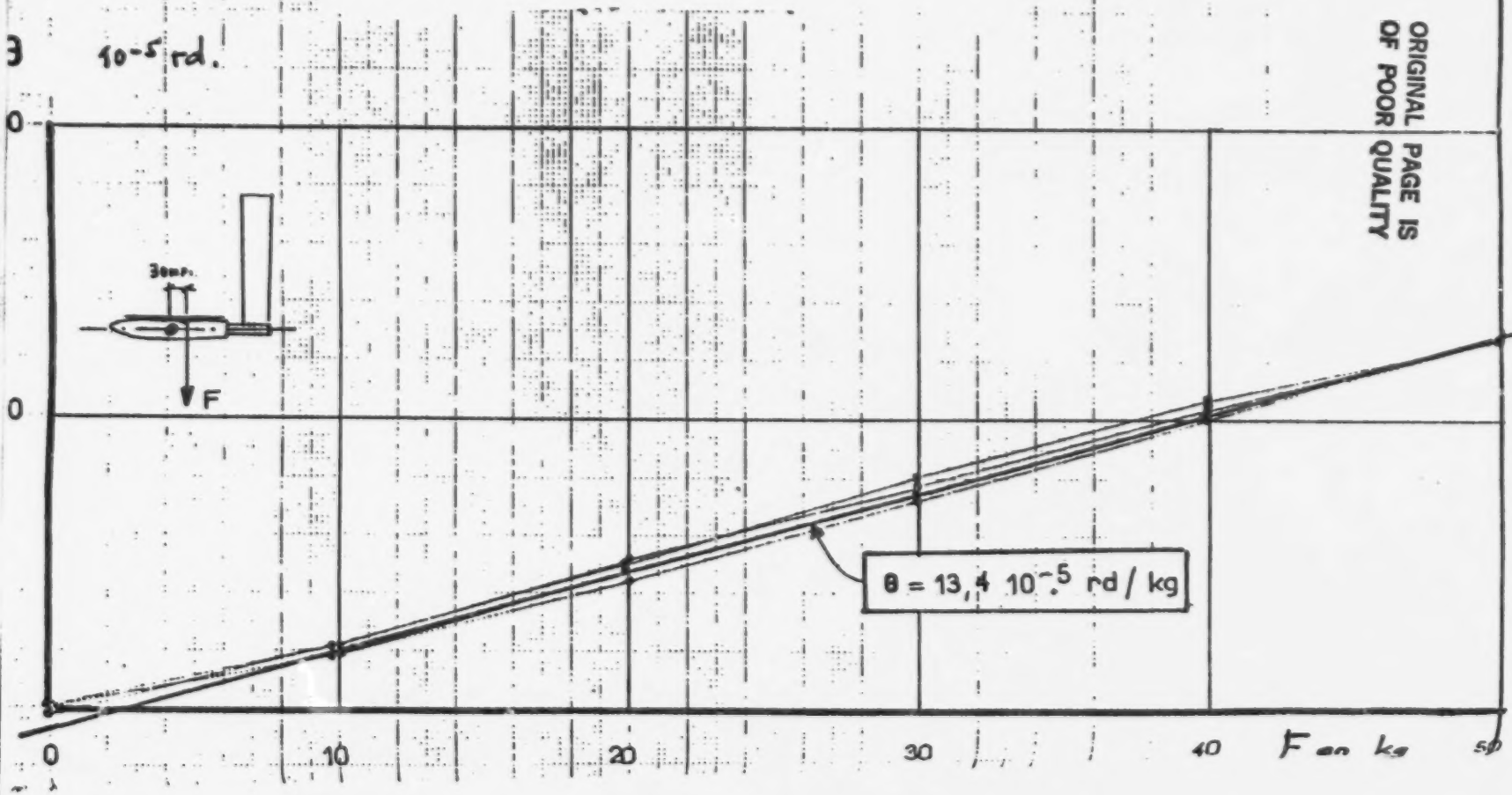

ORIGINAL PAGE IS
OF POOR QUALITY

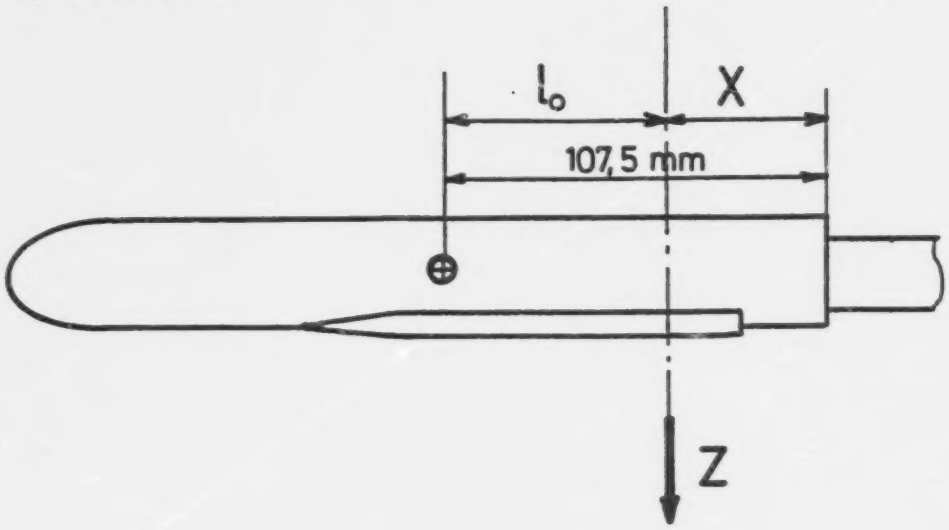

Z (N)	X_{BF} (mm)	l_o (mm)	M (m.N)	$\theta_{measured}$
-196	88	19,5	-3,822	4'
	41	66,5	-13,034	-15,2'
	-4	111,5	-21,85	-27,7'
	+183	-75,5	+14,798	+20'
-235,2	-4	111,5	-26,225	-33,8'
	+183	-75,5	+17,758	+24'

APPENDIX 2

-Variation of Bridge Zeros as a Function of Time

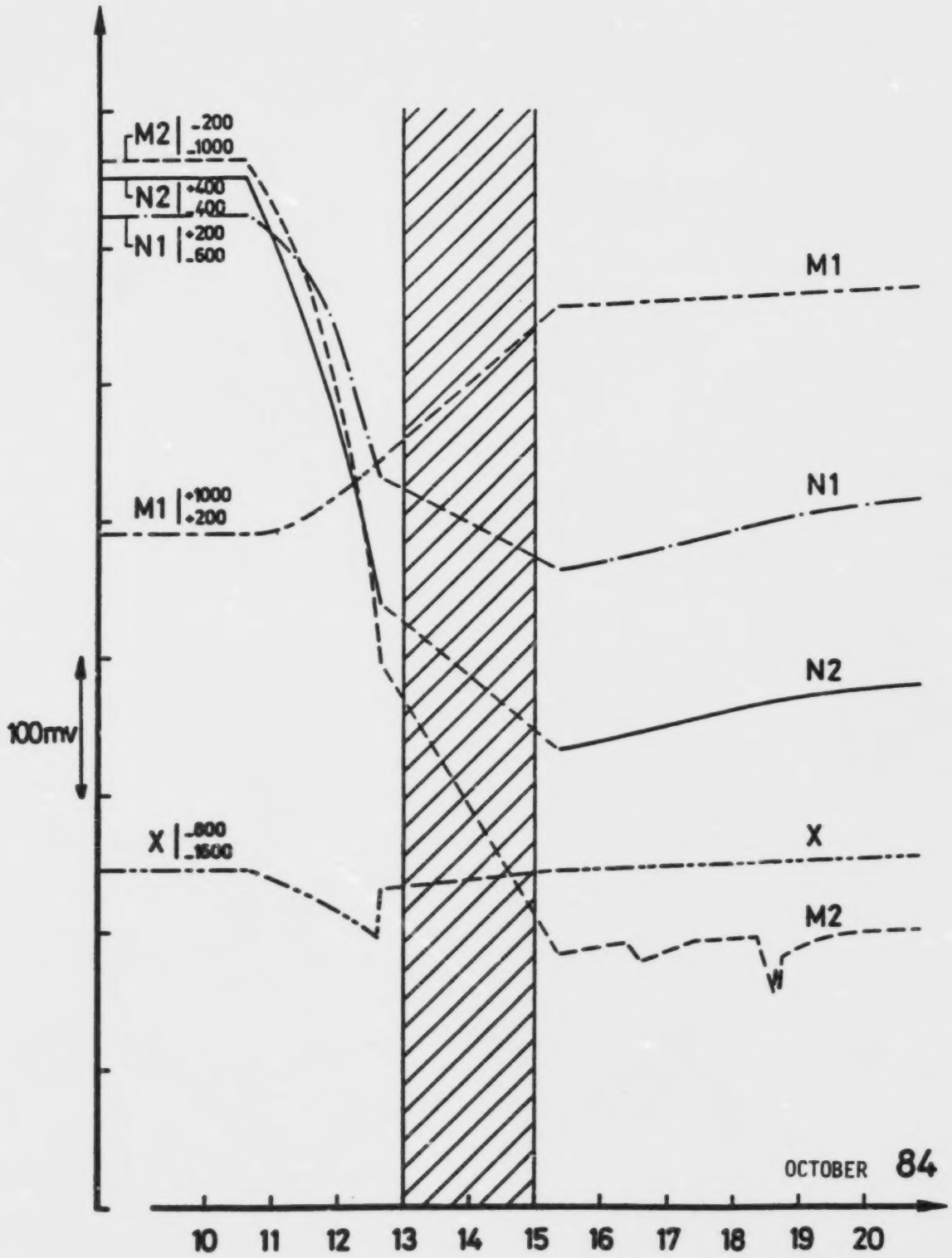
M2 -200 -1000
N2 +400 -400
N1 +200 -600
M1 +1000 +200
X -800 -1500
100mv
M1
N1
N2
X
M2
OCTOBER 84
10 11 12 13 14 15 16 17 18 19 20

Table of Bridge Zeros

Date	Time		T1	T2	X	M1	M2	N1	N2	Remarks
					Incidence = -0,11					
10/10/84										
Wednesday		Control			-1355	690	-235	124	352	- T.amb
	15h10	RF10	295	295	-1355	690	-235	122	350	----
			241	267	-1360	695	-249	142	366	+l.cryo
	17h55	RF11	252	249	-1360	700	-230	125	344	****
			211	223	-1358	709	-225	131	343	****
	18h15	RF12	208	219	-1360	701	-224	130	345	****
			133	145	-1356	717	-200	135	399	****
	16h30	RF13	294	295	-1385	710	-345	70	220	----
11/10/84			142	154	-1355	742	-315	75	255	****
Thursday		Control	295	295	-1395	714	-329	68	214	----
	9h				-1388	722	-499	-27	29	----
12/10/84		Control			-1399	725	-482	-35	70	----
Friday	11h	RF14	293	294	-1370	737	-573	-50	55	----
			134	145	-1350	769	-560	-60	85	****
	14h20	F10	Te	Te	-1398	754	-589	-60	45	----
	15h	F11	Te	Te	-1405	750	-596	-63	44	----
	15h20	F12	Te	Te	-1393	749	-601	-65	41	----
	15h40	F13	Te	Te	-1382	745	-604	-64	40	----
	16h	F14	Te	Te	-1370	745	-605	-68	38	----
	16h15	F15	Te	Te	-1374	749	-606	-70	35	----
Week-End										
	9h	Control			-1355	655	-815	-135	-66	----
15/10/84	11h10	F16	Te	Te	-1354	855	-816	-135	-65	----
Monday	11h50	F17	Te	Te	-1354	855	-816	-135	-65	----
	14h40	F18	Te	Te	-1355	855	-815	-133	-65	----
	15h10	F19	Te	Te	-1351	857	-814	-135	-66	----
	15h50	F20	Te	Te	-1352	858	-810	-135	-67	----
	17h15	F21	Hot model		-1354	855	-810	-132	-65	----
	17h50	RF22	250	271	-1351	840	-825	-135	-70	****
			172	183	-1355	890	-830	-146	-45	****
		F22	177	181	-1350	894	-822	-145	-44	****
	5mn	after gust	200	200	-1348	899	-824	-146	-49	****
	9h	Control			-1351	859	-807	-126	-58	----
16/10/84	11h40	RF23	283	289	-1360	835	-805	-115	-60	----
Wednesday			171	181	-1355	892	-819	-135	-35	****
		F23	179	180	-1353	899	-815	-135	-34	****
	15h	Controle			-1351	855	-823	-122	-52	----
	15h[illegible]	F24	Hot model		-1355	859	-819	-120	-50	----
	16h20	RF25	244	266	-1352	835	-854	-115	-55	****
			108	118	-1354	905	-860	-145	-15	****
		F25	149	145	-1359	933	-845	-137	-20	****
	After gust				-1365	929	-842	-130	-25	****
	17h	F26	210	183	-1348	915	-840	-130	-34	****
	17h25	F27	220	196	-1347	906	-840	-130	-38	****
	17h50	F28	cold model		-1350	918	-840	-139	-35	****
	[illegible]	Controle			[illegible]	[illegible]	[illegible]	[illegible]	[illegible]	[illegible]

ORIGINAL PAGE IS
OF POOR QUALITY

		F27	22							
	17h50	F28	imag. froide	-1350	918	-868	-139	-45	****	
	17h00	Controle	238	218	-1366	918	-818	-141	-45	****

Table of Bridge Zeros (Continued)

Date	Time		T1	T2	X	M1	M2	N1	N2	Remarks
		Change in angle of attack i = 3,65								
17/10/84 Wednesday	10h	Control			-1349	861	-808	-117	-50	----
	11h15	F29	Ta	Ta	-1351	864	-810	-115	-45	----
	11h30	F30	Ta	Ta	-1350	863	-810	-115	-48	----
	11h40	F31	Ta	Ta	-1351	862	-810	-115	-49	----
	14h30	F32	Ta	Ta	-1350	861	-810	-114	-45	----
	15h	F33	Ta	Ta	-1350	863	-810	-113	-45	----
	15h30	F34	Ta	Ta	-1350	860	-809	-114	-46	----
	16h	F35	Ta	Ta	-1350	862	-806	-114	-48	----
	17h20	RF36	290	298	-1350	860	-805	-115	-50	----
			109	120	-1340	905	-835	-130	-10	****
		F36	131	126	-1354	920	-831	-125	-5	****
18/10/84 Thursday	9h	Control			-1349	863	-804	-104	-38	----
	10h	F37	hot model		-1350	865	-804	-103	-38	----
	10h15	F38	hot model		-1350	880	-805	-105	-40	----
	10h55	RF39	284	278	-1352	865	-805	-105	-40	----
			171	182	-1350	905	-820	-111	-11	****
		F39	178	181	-1350	909	-819	-109	-10	****
	11h15	RF40	186	184	-1359	900	-820	-110	-10	****
			166	170	-1350	910	-820	-110	-5	****
		F40	196	182	-1353	920	-819	-110	-9	****
	15h40	F43	Ta	Ta	-1354	870	-844	-99	-30	----
	15h45	F44	hot model		-1355	870	-831	-99	-30	----
	15h50	F45	hot model		-1350	875	-828	-100	-33	----
		Change in angle of attack i = 5,70								
	17h10	F46	Ta	Ta	-1353	868	-840	-100	-30	----
	17h25	F47	Ta	Ta	-1353	866	-835	-100	-30	----
	17h35	F48	Ta	Ta	-1352	865	-829	-100	-30	----
	18h	F49	Ta	Ta	-1352	867	-819	-100	-30	----
	18h10	F50	Ta	Ta	-1352	866	-820	-100	-30	----
		Change in angle of attack i = 1,47								
19/10/84 Friday	10h	Control			-1348	860	-803	-91	-25	----
	14h30	F51	Ta	Ta	-1350	864	-804	-90	-25	----
	14h45	F52	Ta	Ta	-1350	865	-804	-90	-25	----
	14h50	F53	Ta	Ta	-1350	864	-803	-90	-25	----
	14h55	F54	Ta	Ta	-1350	865	-801	-90	-25	----
	15h05	F55	Ta	Ta	-1350	865	-801	-90	-26	----
	15h20	F56	Ta	Ta	-1350	865	-800	-90	-28	----
		Change in angle of attack i = 0								
	16h	F57	Ta	Ta	-1350	865	-800	-90	-26	----

ORIGINAL PAGE IS
OF POOR QUALITY

APPENDIX 3

Summary of tests
Bridge tensions }
Stresses on balance} during tests
Aerodynamic coefficients

ORIGINAL PAGE IS
OF POOR QUALITY

Test Summary

$A_3 1$

File	Mref	P_1	T_1	Re	% cor.	Remarks
			incidence = -0.11 degrees			
BA0010	.701	1.43	293.	1.99E+06	- 17	
BA0011	.705	1.54	295.	2.01E+06	- 17	
BA0012	.705	1.57	296.	2.07E+06	- 18	
BA0013	.756	1.68	296.	2.28E+06	- 20	
BA0014	.604	1.42	298.	1.76E+06	- 15	
BA0015	.807	1.72	297.	2.41E+06	- 25	
BA0016	.757	1.65	294.	2.27E+06	- 20	
BA0017	.757	1.65	295.	2.26E+06	- 20	
BA0018	.758	2.44	299.	3.30E+06	- 25	P1 = 2.5 bars
BA0019	.757	3.00	299.	4.03E+06	- .27	P1 = 3 bars
BA0020	.605	3.00	300.	3.51E+06	- .14	P1 = 3 bars
BA0021	.757	1.62	177.	4.42E+06	- .21	hot model
BA0022	.755	1.66	180.	4.41E+06	-.21	
BA0023	.603	1.52	180.	3.49E+06	-.15	
BA0024	.755	1.64	119.	7.96E+06	- .20	hot model
BA0025	.753	1.63	119.	7.98E+06	- .19	
BA0026	.754	1.64	119.	7.94E+06	-.20	
BA0027	.601	1.48	119.	6.18E+06	-.15	
BA0028	.757	1.64	296.	2.25E+06	- 20	cold model
			incidence = 3.65 degrees			
BA0029	.603	1.52	294.	1.81E+06	3.71	
BA0030	.705	1.61	295.	2.11E+06	3 44	
BA0031	.755	1.64	296.	2.24E+06	3 38	
BA0032	.758	1.65	296.	2.24E+06	3 49	
BA0033	.807	1.72	296.	2.42E+06	3 39	
BA0034	.606	2.99	299.	3.51E+06	3 33	P1 = 3 bars
BA0035	.758	2.99	300.	4.03E+06	3.14	P1 = 3 bars
BA0036	.754	1.64	119.	7.93E+06	3.39	
BA0037	.756	1.64	119	7.98E+06	3 40	hot model
BA0038	.756	1.64	296.	2.24E+06	3.38	
BA0039	.755	1.64	180.	4.39E+06	3.38	
BA0040	.601	1.42	180.	3.28E+06	3.32	
BA0043	.754	1.64	295.	2.24E+06	3.39	
BA0044	.753	1.64	179.	4.39E+06	3.40	hot model
BA0045	.602	1.49	180	3.41E+06	3 42	hot model
			incidence = 5.70 degrees			
BA0046	.602	1.52	295.	1.80E+06	5.50	
BA0047	.704	1.61	296.	2.10E+06	5.41	
BA0048	.755	1.64	296.	2.23E+06	5 54	
BA0049	.806	1.71	296.	2.40E+06	5.52	
BA0050	.605	2.99	299.	3.51E+06	5 53	P1 = 3 bars
			incidence = 1.47 degrees			
BA0051	.606	1.50	296.	1.79E+06	1 39	
BA0052	.706	1.59	295.	2.08E+06	1.39	
BA0053	.757	1.63	297.	2.21E+06	1 52	
BA0054	.807	1.70	297	2.36E+06	1.45	
BA0055	.757	2.99	299	4.03E+06	1 50	P1 = 3 bars
BA0056	.606	3.00	299	3.50E+06	1 52	P1 = 3 bars
			incidence = 0 degrees			

ORIGINAL PAGE IS
OF POOR QUALITY

Bridge Tensions s (mU)

File	Ex	Em1	Em2	En1	En2
BA0010	-570.	-267.	-43.	15.	10.
BA0011	-619.	-290.	-42.	15.	11.
BA0012	-627.	-295.	-41.	15.	11.
BA0013	-794.	-420.	-62.	15.	11.
BA0014	-445.	-176.	-20.	3.	3.
BA0015	-1012.	-626.	-103.	25.	15.
BA0016	-786.	-417.	-66.	19.	10.
BA0017	-785.	-419.	-66.	20.	10.
BA0018	-1150.	-605.	-100.	28.	18.
BA0019	-1404.	-722.	-123.	35.	22.
BA0020	-873.	-344.	-53.	25.	17.
BA0021	-739.	-408.	-63.	17.	10.
BA0022	-858.	-458.	-79.	7.	9.
BA0023	-526.	-194.	-34.	6.	8.
BA0024	-736.	-397.	-70.	27.	7.
BA0025	-864.	-370.	-56.	18.	7.
BA0026	-928.	-380.	-60.	16.	9.
BA0027	-568.	-160.	-24.	10.	3.
BA0028	-789.	-398.	-54.	9.	8.
BA0029	-289.	-830.	156.	10.	1.
BA0030	-414.	-1203.	192.	14.	3.
BA0031	-510.	-1469.	198.	15.	4.
BA0032	-517.	-1480.	197.	14.	5.
BA0033	-715.	-1931.	179.	22.	5.
BA0034	-526.	-1576.	301.	14.	4.
BA0035	-845.	-2566.	337.	17.	6.
BA0036	-536.	-1451.	192.	11.	4.
BA0037	-460.	-1431.	200.	26.	2.
BA0038	-510.	-1481.	196.	10.	4.
BA0039	-607.	-1487.	186.	6.	0.
BA0040	-363.	-781.	139.	5.	0.
BA0043	-508.	-1464.	213.	14.	0.
BA0044	-467.	-1434.	212.	18.	0.
EA0045	-269.	-792.	155.	12.	1.
BA0046	-178.	-1201.	268.	6.	-3.
BA0047	-261.	-1721.	337.	8.	-5.
BA0048	-332.	-2084.	353.	10.	-5.
BA0049	-504.	-2690.	334.	15.	-3.
BA0050	-269.	-2286.	509.	6.	-6.
BA0051	-415.	-417.	44.	10.	5.
BA0052	-580.	-626.	46.	12.	6.
BA0053	-705.	-796.	36.	15.	6.
BA0054	-930.	-1106.	2.	23.	10.
BA0055	-1254.	-1401.	54.	25.	14.
BA0056	-788.	-797.	82.	19.	12.
BA0057	-774.	-422.	-60.	15.	11.

Stresses on Balance (Newton) & (m.Newton)

File	Drag	Slip	Lift	Roll	Pitch	Yaw
BA0010	-15.58	-.50	-37.23	0.00	-2.51	.13
BA0011	-16.93	-.39	-41.23	0.00	-2.69	.13
BA0012	-17.15	-.41	-42.28	0.00	-2.73	.13
BA0013	-21.78	-.29	-59.68	0.00	-3.91	.13
BA0014	-12.13	-.00	-25.93	0.00	-1.59	.03
BA0015	-27.86	-1.01	-86.97	0.00	-5.91	.21
BA0016	-21.55	-.86	-58.39	0.00	-3.92	.15
BA0017	-21.53	-.97	-58.67	0.00	-3.94	.15
BA0018	-31.54	-.97	-83.93	0.00	-5.72	.24
BA0019	-38.50	-1.22	-99.58	0.00	-6.86	.29
BA0020	-23.80	-.79	-48.41	0.00	-3.23	.21
BA0021	-20.29	-.66	-57.34	0.00	-3.82	.14
BA0022	-23.52	.26	-63.09	0.00	-4.36	.08
BA0023	-14.31	.28	-26.50	0.00	-1.85	.07
BA0024	-20.17	-2.03	-54.37	0.00	-3.79	.17
BA0025	-23.59	-1.16	-52.22	0.00	-3.46	.13
BA0026	-25.31	-.75	-53.26	0.00	-3.58	.13
BA0027	-15.42	-.75	-22.72	0.00	-1.50	.07
BA0028	-21.61	-.01	-57.33	0.00	-3.67	.09
BA0029	-9.29	-.80	-164.70	0.00	-5.44	.06
BA0030	-13.43	-.80	-233.00	0.00	-8.16	.09
BA0031	-16.55	-.78	-278.50	0.00	-10.28	.11
BA0032	-16.76	-.62	-280.20	0.00	-10.37	.11
BA0033	-23.07	-1.37	-352.30	0.00	-14.17	.15
BA0034	-17.45	-.61	-313.80	0.00	-10.29	.11
BA0035	-28.57	-.52	-485.00	0.00	-18.02	.13
BA0036	-17.21	-.44	-274.30	0.00	-10.17	.09
BA0037	-15.14	-2.17	-272.40	0.00	-9.94	.15
BA0038	-16.57	-.26	-280.10	0.00	-10.38	.08
BA0039	-19.16	-.19	-279.40	0.00	-10.51	.04
BA0040	-11.16	-.32	-153.80	0.00	-5.18	.03
BA0043	-16.52	-1.04	-280.20	0.00	-10.10	.08
BA0044	-15.37	-1.57	-275.00	0.00	-9.87	.10
BA0045	-8.70	-.97	-158.40	0.00	-5.14	.07
BA0046	-7.23	-.57	-245.70	0.00	-7.52	.02
BA0047	-10.74	-.82	-344.00	0.00	-11.16	.02
BA0048	-13.56	-1.02	-407.30	0.00	-13.97	.04
BA0049	-19.73	-1.28	-505.20	0.00	-19.04	.07
BA0050	-12.77	-.68	-467.50	0.00	-14.33	.02
BA0051	-11.79	-.41	-76.92	0.00	-3.01	.08
BA0052	-16.54	-.59	-112.10	0.00	-4.69	.09
BA0053	-20.17	-.75	-138.80	0.00	-6.15	.11
BA0054	-26.69	-1.15	-184.80	0.00	-8.95	.17
BA0055	-36.09	-.84	-242.90	0.00	-10.91	.20
BA0056	-22.50	-.50	-146.80	0.00	-5.78	.16
BA0057	-21.25	-.38	-60.32	0.00	-3.92	.13

Coefficients in Balance Reference Mark

File	Cxb	Cyb	Czb	Clb	Cmb	Cnb
BA0010	-1.935E-02	-6.236E-04	-4.625E-02	0.000E+00	-3.026E-02	1.545E-03
BA0011	-1.936E-02	-4.445E-04	-4.714E-02	0.000E+00	-2.986E-02	1.463E-03
BA0012	-1.925E-02	-4.579E-04	-4.747E-02	0.000E+00	-2.972E-02	1.447E-03
BA0013	-2.898E-02	-2.818E-04	-5.728E-02	0.000E+00	-3.647E-02	1.236E-03
BA0014	-1.805E-02	-1.136E-06	-3.857E-02	0.000E+00	-2.293E-02	4.294E-04
BA0015	-2.409E-02	-8.761E-04	-7.521E-02	0.000E+00	-4.965E-02	1.721E-03
BA0016	-2.105E-02	-8.381E-04	-5.704E-02	0.000E+00	-3.716E-02	1.426E-03
BA0017	-2.098E-02	-9.483E-04	-5.716E-02	0.000E+00	-3.724E-02	1.438E-03
BA0018	-2.078E-02	-6.385E-04	-5.510E-02	0.000E+00	-3.644E-02	1.509E-03
BA0019	-2.063E-02	-6.780E-04	-5.337E-02	0.000E+00	-3.567E-02	1.507E-03
BA0020	-1.748E-02	-5.795E-04	-3.554E-02	0.000E+00	-2.300E-02	1.520E-03
BA0021	-2.013E-02	-6.561E-04	-5.689E-02	0.000E+00	-3.684E-02	1.336E-03
BA0022	-2.286E-02	2.903E-04	-6.130E-02	0.000E+00	-4.114E-02	7.474E-04
BA0023	-2.090E-02	4.093E-04	-3.871E-02	0.000E+00	-2.628E-02	1.014E-03
BA0024	-1.981E-02	-1.999E-03	-5.340E-02	0.000E+00	-3.611E-02	1.653E-03
BA0025	-2.339E-02	-1.148E-03	-5.177E-02	0.000E+00	-3.330E-02	1.260E-03
BA0026	-2.498E-02	-7.391E-04	-5.256E-02	0.000E+00	-3.428E-02	1.222E-03
BA0027	-2.313E-02	-1.132E-03	-3.408E-02	0.000E+00	-2.179E-02	1.020E-03
BA0028	-2.115E-02	-7.619E-06	-5.610E-02	0.000E+00	-3.485E-02	8.280E-04
BA0029	-1.354E-02	-1.165E-03	-2.401E-01	0.000E+00	-7.699E-02	8.848E-04
BA0030	-1.479E-02	-8.829E-04	-2.566E-01	0.000E+00	-8.724E-02	9.869E-04
BA0031	-1.626E-02	-7.713E-04	-2.737E-01	0.000E+00	-9.799E-02	1.017E-03
BA0032	-1.642E-02	-6.065E-04	-2.745E-01	0.000E+00	-9.857E-02	1.010E-03
BA0033	-1.999E-02	-1.191E-03	-3.052E-01	0.000E+00	-1.192E-01	1.235E-03
BA0034	-1.283E-02	-4.518E-04	-2.307E-01	0.000E+00	-7.345E-02	7.492E-04
BA0035	-1.533E-02	-2.764E-04	-2.602E-01	0.000E+00	-9.382E-02	6.611E-04
BA0036	-1.700E-02	-4.358E-04	-2.709E-01	0.000E+00	-9.749E-02	8.202E-04
BA0037	-1.488E-02	-2.134E-03	-2.677E-01	0.000E+00	-9.484E-02	1.409E-03
BA0038	-1.625E-02	-2.511E-04	-2.746E-01	0.000E+00	-9.880E-02	7.869E-04
BA0039	-1.885E-02	-1.866E-04	-2.747E-01	0.000E+00	-1.004E-01	3.564E-04
BA0040	-1.745E-02	-5.008E-04	-2.404E-01	0.000E+00	-7.855E-02	4.378E-04
BA0043	-1.628E-02	-1.021E-03	-2.762E-01	0.000E+00	-9.663E-02	7.457E-04
BA0044	-1.519E-02	-1.551E-03	-2.717E-01	0.000E+00	-9.463E-02	9.626E-04
BA0045	-1.301E-02	-1.444E-03	-2.370E-01	0.000E+00	-7.462E-02	1.051E-03
BA0046	-1.057E-02	-8.400E-04	-3.593E-01	0.000E+00	-1.068E-01	3.425E-04
BA0047	-1.108E-02	-9.061E-04	-3.007E-01	0.000E+00	-1.199E-01	2.658E-04
BA0048	-1.336E-02	-1.003E-03	-4.012E-01	0.000E+00	-1.336E-01	3.565E-04
BA0049	-1.718E-02	-1.115E-03	-4.400E-01	0.000E+00	-1.609E-01	6.175E-04
BA0050	-9.406E-03	-4.990E-04	-3.444E-01	0.000E+00	-1.024E-01	1.113E-04
BA0051	-1.725E-02	-6.058E-04	-1.126E-01	0.000E+00	-4.283E-02	1.137E-03
BA0052	-1.837E-02	-6.520E-04	-1.244E-01	0.000E+00	-5.058E-02	1.024E-03
BA0053	-1.994E-02	-7.445E-04	-1.373E-01	0.000E+00	-5.901E-02	1.074E-03
BA0054	-2.336E-02	-1.006E-03	-1.617E-01	0.000E+00	-7.600E-02	1.443E-03
BA0055	-1.937E-02	-4.508E-04	-1.303E-01	0.000E+00	-5.682E-02	1.057E-03
BA0056	-1.651E-02	-3.695E-04	-1.077E-01	0.000E+00	-4.121E-02	1.167E-03
BA0057	-2.096E-02	-3.724E-04	-5.949E-02	0.000E+00	-3.749E-02	1.272E-03

ORIGINAL PAGE IS
OF POOR QUALITY

		-7.445E-0				
BA0054	-2.336E-02	-1.006E-03	-1.617E-01	0.000E+00	-7.600E-02	1.443E-03
BA0055	-1.937E-02	-4.508E-04	-1.303E-01	0.000E+00	-5.682E-02	1.057E-03
BA0056	-1.651E-02	-3.695E-04	-1.077E-01	0.000E+00	-4.121E-02	1.167E-03
BA0057	-2.096E-02	-3.724E-04	-5.949E-02	0.000E+00	-3.749E-02	1.272E-03

Aerodynamic Coefficients (Aero Index)

File	Mref.	Pi	Ti	Re	incid.	i.cor.	Cx	Cz	Cm
BA0010	.701	1.43	293.	1.89E+06	-.11	-.17	-1.921E-02	-4.631E-02	-2.026E-02
BA0011	.705	1.54	295.	2.03E+06	-.11	-.17	-1.922E-02	-4.720E-02	-2.986E-02
BA0012	.705	1.57	296.	2.07E+06	-.11	-.18	-1.910E-02	-4.753E-02	-2.972E-02
BA0013	.756	1.68	296.	2.28E+06	-.11	-.20	-2.070E-02	-5.735E-02	-3.647E-02
BA0014	.604	1.48	296.	1.76E+06	-.11	-.15	-1.795E-02	-3.862E-02	-2.293E-02
BA0015	.807	1.72	297.	2.41E+06	-.11	-.25	-2.376E-02	-7.532E-02	-4.965E-02
BA0016	.757	1.65	294.	2.27E+06	-.11	-.20	-2.085E-02	-5.711E-02	-3.716E-02
BA0017	.757	1.65	295.	2.26E+06	-.11	-.20	-2.078E-02	-5.723E-02	-3.724E-02
BA0018	.758	2.44	299.	3.30E+06	-.11	-.25	-2.046E-02	-5.519E-02	-3.644E-02
BA0019	.757	3.00	299.	4.03E+06	-.11	-.27	-2.037E-02	-5.347E-02	-3.567E-02
BA0020	.605	3.00	300.	3.51E+06	-.11	-.19	-1.736E-02	-3.560E-02	-2.300E-02
BA0021	.757	1.62	177.	4.42E+06	-.11	-.20	-1.993E-02	-5.696E-02	-3.684E-02
BA0022	.755	1.66	180.	4.41E+06	-.11	-.21	-2.263E-02	-6.139E-02	-4.114E-02
BA0023	.603	1.52	180.	3.49E+06	-.11	-.15	-2.080E-02	-3.877E-02	-2.628E-02
BA0024	.755	1.64	119.	7.96E+06	-.11	-.20	-1.962E-02	-5.347E-02	-3.611E-02
BA0025	.753	1.63	119.	7.98E+06	-.11	-.19	-2.322E-02	-5.185E-02	-3.330E-02
BA0026	.754	1.64	119.	7.94E+06	-.11	-.20	-2.480E-02	-5.265E-02	-3.428E-02
BA0027	.601	1.48	119.	6.18E+06	-.11	-.15	-2.304E-02	-3.414E-02	-2.179E-02
BA0028	.757	1.64	296.	2.25E+06	-.11	-.20	-2.096E-02	-5.617E-02	-3.485E-02
BA0029	.603	1.52	294.	1.81E+06	3.65	3.51	-2.821E-02	-2.388E-01	-7.699E-02
BA0030	.705	1.61	295.	2.11E+06	3.65	3.44	-3.017E-02	-2.552E-01	-8.724E-02
BA0031	.755	1.64	296.	2.24E+06	3.65	3.39	-3.241E-02	-2.723E-01	-9.799E-02
BA0032	.756	1.65	296.	2.24E+06	3.65	3.39	-3.261E-02	-2.731E-01	-9.857E-02
BA0033	.807	1.72	296.	2.42E+06	3.65	3.29	-3.749E-02	-3.035E-01	-1.192E-01
BA0034	.606	2.99	299.	3.51E+06	3.65	3.38	-2.643E-02	-2.295E-01	-7.345E-02
BA0035	.758	2.99	300.	4.03E+06	3.65	3.19	-2.980E-02	-2.589E-01	-9.382E-02
BA0036	.754	1.64	119.	7.93E+06	3.65	3.39	-3.300E-02	-2.694E-01	-9.749E-02
BA0037	.756	1.64	119.	7.98E+06	3.65	3.40	-3.072E-02	-2.663E-01	-9.484E-02
BA0038	.756	1.64	296.	2.24E+06	3.65	3.39	-3.244E-02	-2.732E-01	-9.880E-02
BA0039	.755	1.64	180.	4.39E+06	3.65	3.38	-3.503E-02	-2.731E-01	-1.004E-01
BA0040	.601	1.42	180.	3.28E+06	3.65	3.52	-3.216E-02	-2.389E-01	-7.855E-02
BA0043	.754	1.64	295.	2.24E+06	3.65	3.39	-3.260E-02	-2.748E-01	-9.663E-02
BA0044	.753	1.64	179.	4.39E+06	3.65	3.40	-3.127E-02	-2.703E-01	-9.463E-02
BA0045	.602	1.49	180.	3.41E+06	3.65	3.52	-2.753E-02	-2.358E-01	-7.462E-02
BA0046	.602	1.52	295.	1.80E+06	5.70	5.50	-4.498E-02	-3.566E-01	-1.068E-01
BA0047	.704	1.60	296.	2.10E+06	5.70	5.41	-4.773E-02	-3.779E-01	-1.199E-01
BA0048	.755	1.64	296.	2.23E+06	5.70	5.34	-5.065E-02	-3.982E-01	-1.336E-01
BA0049	.806	1.71	296.	2.40E+06	5.70	5.22	-5.712E-02	-4.366E-01	-1.609E-01
BA0050	.605	2.99	299.	3.51E+06	5.70	5.33	-4.134E-02	-3.420E-01	-1.024E-01
BA0051	.606	1.50	296.	1.79E+06	1.47	1.39	-1.998E-02	-1.121E-01	-4.283E-02
BA0052	.706	1.59	296.	2.08E+06	1.47	1.35	-2.130E-02	-1.239E-01	-5.058E-02
BA0053	.757	1.63	297.	2.21E+06	1.47	1.32	-2.309E-02	-1.368E-01	-5.901E-02
BA0054	.807	1.70	297.	2.38E+06	1.47	1.25	-2.688E-02	-1.612E-01	-7.600E-02
BA0055	.757	2.99	299.	4.03E+06	1.47	1.20	-2.209E-02	-1.299E-01	-5.682E-02
BA0056	.606	3.00	299.	3.50E+06	1.47	1.32	-1.899E-02	-1.073E-01	-4.121E-02
BA0057	.756	1.63	298.	2.21E+06	0.00	-.09	-2.086E-02	-5.952E-02	-3.749E-02

ORIGINAL PAGE IS
OF POOR QUALITY

REFERENCES

1. DUBOIS M.
Feasibility on strain gauge balances for cryogenic wind tunnels at ONERA
Cryogenic Technology Review Meeting (ETW)
NLR, Amsterdam 15-17 September 1982.

2. DUBOIS M.
Three component trial cryogenic balance. Results of first dynamometric and thermal calibrations.
Final summary report No. 7/079/GY January 1983.

3. BAZION M.
Cryogenic Wind Tunnel Instrumentation
AGARD/FDP Cryogenic Technology for Wind Tunnel Testing
V.K.I. 22-56 April 1985.

4. MIGNOSI, A., SERAUDIE A., BLANCHARD A., BREIL J.F.,
First test report of a CAST 10 airfoil (C = 180) in natural transition, performed in the T2 cryogenic transonic wind tunnel in the presence of self-adaptable walls.
R.T. OA NO. 59/1685 AND (DERAT NO. 4/5019 DN) March 1985.

5. MIGNOSI A., SERAUDIE A., DOR J.B.,
First cryogenic tests of the CAST 7 airfoil (C = 150) at T2 wind tunnel. R.T. OA NO. 57/16805 AND (DERAT No. 3/5019 DN) January 1984.

6. SERAUDIE A, PAYRY M.J.
Development of precooling system for airfoils adapted to T2 cryogenic testing. R.T. DA No. 56/16805 AND (DERAT NO. 2/5019 DN) October 1983.

/55

LIST OF PLATES

PLATES	
1	Three component cryogenic balance
2	Cryogenic balance equipped with its model
3	Diagram of cooling box
4	Cooling box and model in T2
5	Diagram T2 wind tunnel - Test airflow section
6	Flow chart of gust development
7	Development of a gust with cryogenic balance
8	Parietal visualization M = 0.75 Ti = Ta alpha = 0°
9	Parietal visualization M = 0.75 Ti = Ta alpha = 4°
10	Parietal visualization M = 0.8 Ti = Ta alpha = 4°
11	Cooling (test 22): variation of model-balance temperatures
12	Cooling (test 22): variation of bridge tensions
13	Variation of gust conditions (tests 22)
14	Variation of balance-model temperatures during gust (test 22)
15	Variation of bridge tensions during gust (test 22)
16	Variation of aerodynamic balance coefficients (test 22)
17	Cooling (test 39): variation of model-balance temperatures
18	Cooling (test 39): variation of bridge tensions
19	Variation of balance-model temperatures during gust (test 39)
20	Variation of bridge tensions during gust (test 39)
21	Variation of balance aerodynamic coefficients (test 39)
22	Variations in burst conditions (test 28) /56
23	Variation in balance-model temperatures during gusts (test 28)
24	Variation in bridge tensions during gust (test 28)
25	Variation in balance aerodynamic coefficients (test 28)

PLATES

26 Variation in balance-model temperatures during gust (test 36)

27 Variation in bridge tensions during gust (test 36)

28 Variation in balance aerodynamic coefficients (test 36)

29 Variation in balance-model temperatures during gust (test 37)

30 Variation in bridge tensions during gust (test 37)

31 Variation in balance aerodynamic coefficients (test 37)

32 Variation in Cx as a function of the Mach number (alpha = -0.18°)

33 Variation in Cx as a function of the Mach number (alpha = -0.18°)

34 Variation in Cm as a function of the Mach number (alpha = -18°C)

35 Variation of Cx as a function of the Mach number (alpha = 1.33°)

36 Variation of Cz as a function of the Mach number (alpha - 1.33°)

37 Variation of Cm as a function of the Mach number (alpha = 1.33°)

38 Variation of Cx as a function of the Mach number (alpha 3.43°)

39 Variation of Cx as a function of the Mach number (alpha - 3.43°C)

40 Variation of Cm as a function of the Mach number (alpha = 3.43°)

41 Variation of Cx as a function of the Mach number (alpha = 5.42°) /57

42 Variation of Cz as a function of the Mach number (alpha = 5.42°)

43 Variation of Cm as a function of the Mach number (alpha = 5.42°)

44 Variation of Cx as a function of the angle of attack (Ti = Ta)

PLATES

45	Variation of Cx as a function of the angle of attack (Ti = Ta)
46	Variation of Cm as a function of the angle of attack (Ti = Ta)
47	Polar (Ti = Ta)

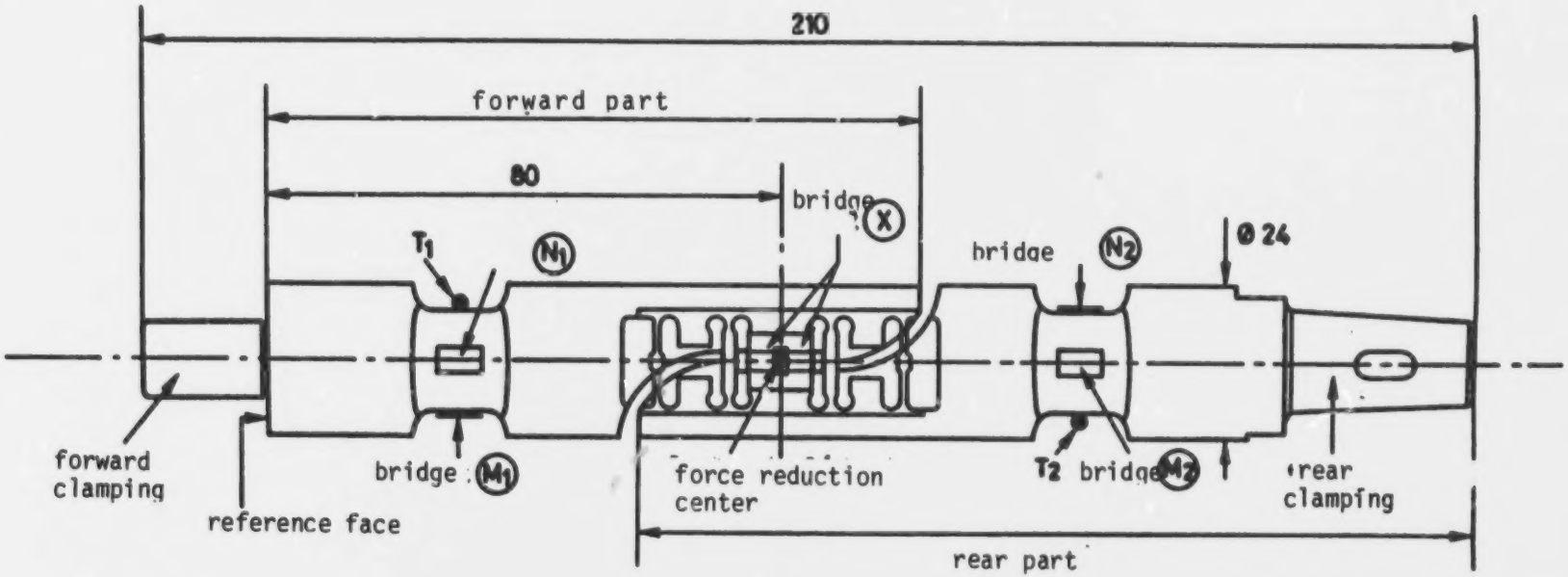

○ : strain gage bridges

● : Constantin-copper thermocouples

Pl. 1

X_Z_M CRYOGENIC BALANCE

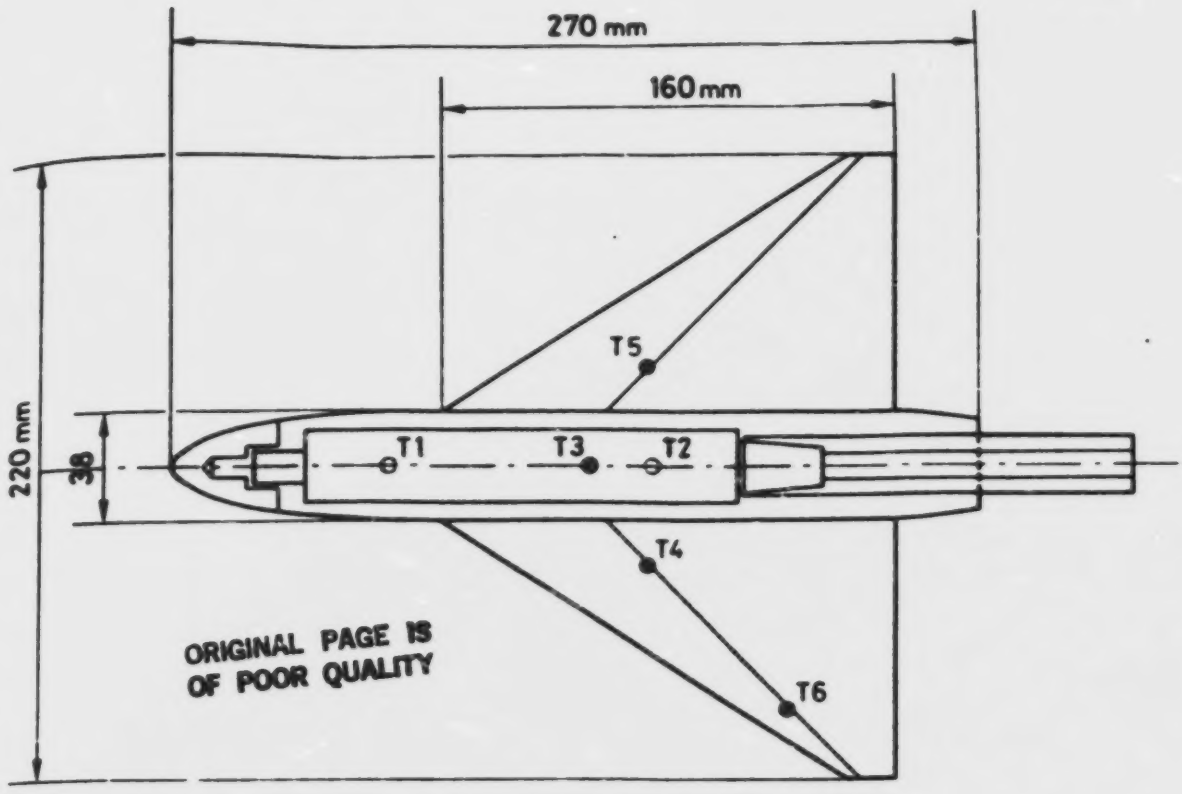

○ Thermocouples of balance

● Thermocouples of model

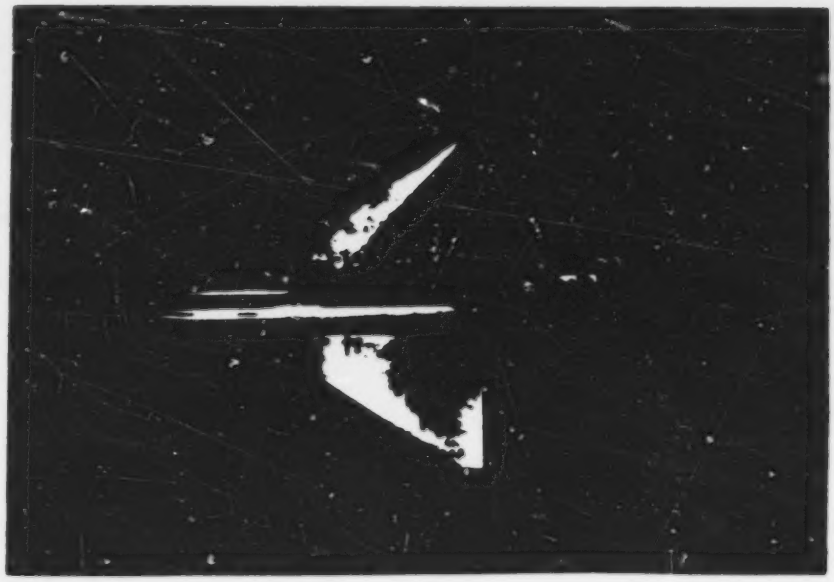

FIG 2 - CRYOGENIC BALANCE EQUIPPED WITH ITS MODEL.

ORIGINAL PAGE IS
OF POOR QUALITY PL. 3

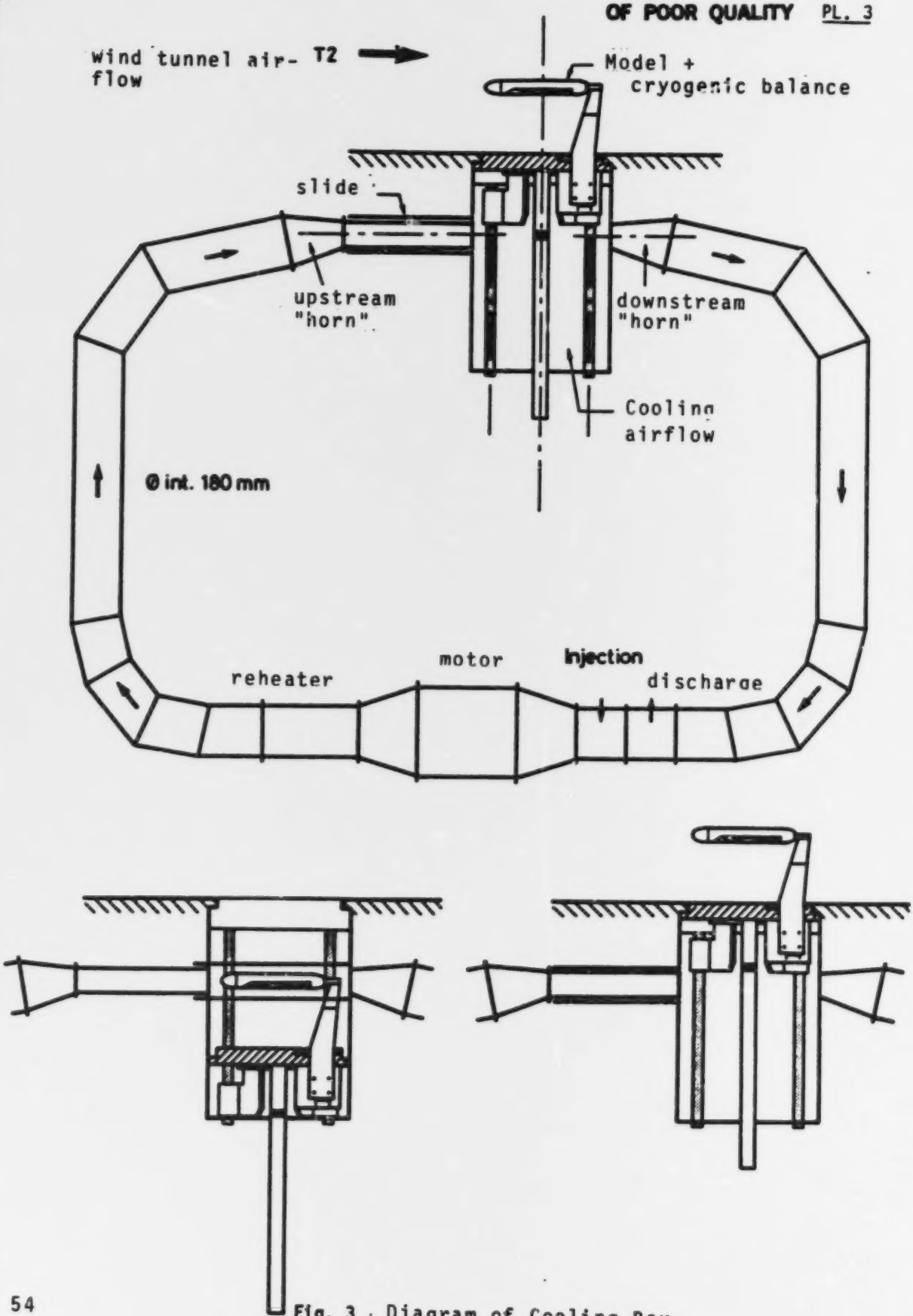

Fig. 3 · Diagram of Cooling Box

ORIGINAL PAGE IS
OF POOR QUALITY

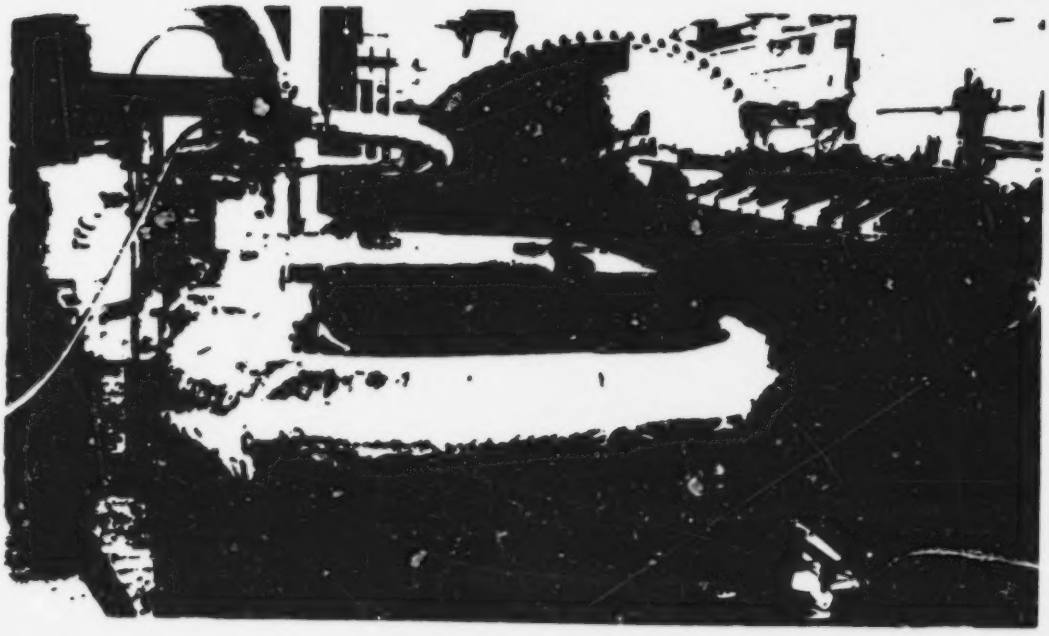

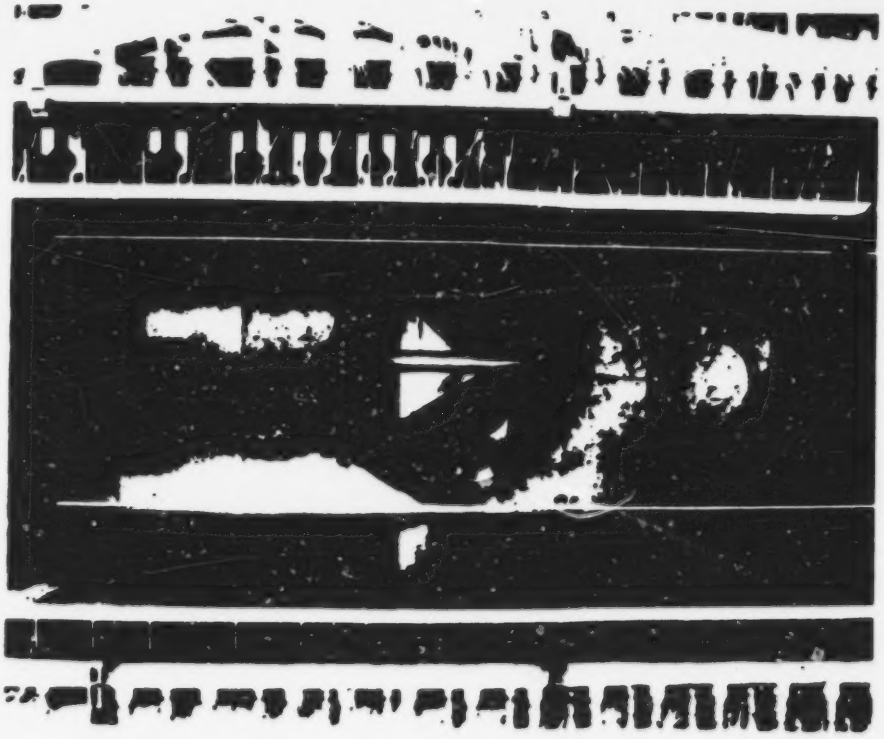

Figure 4 - Cryogenic Precooling.

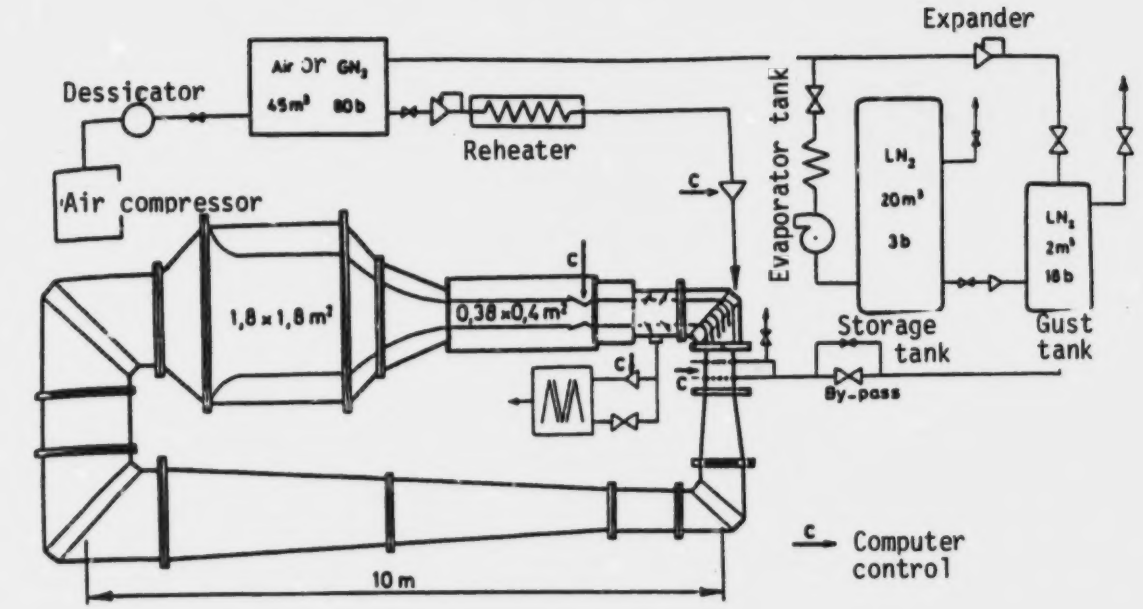

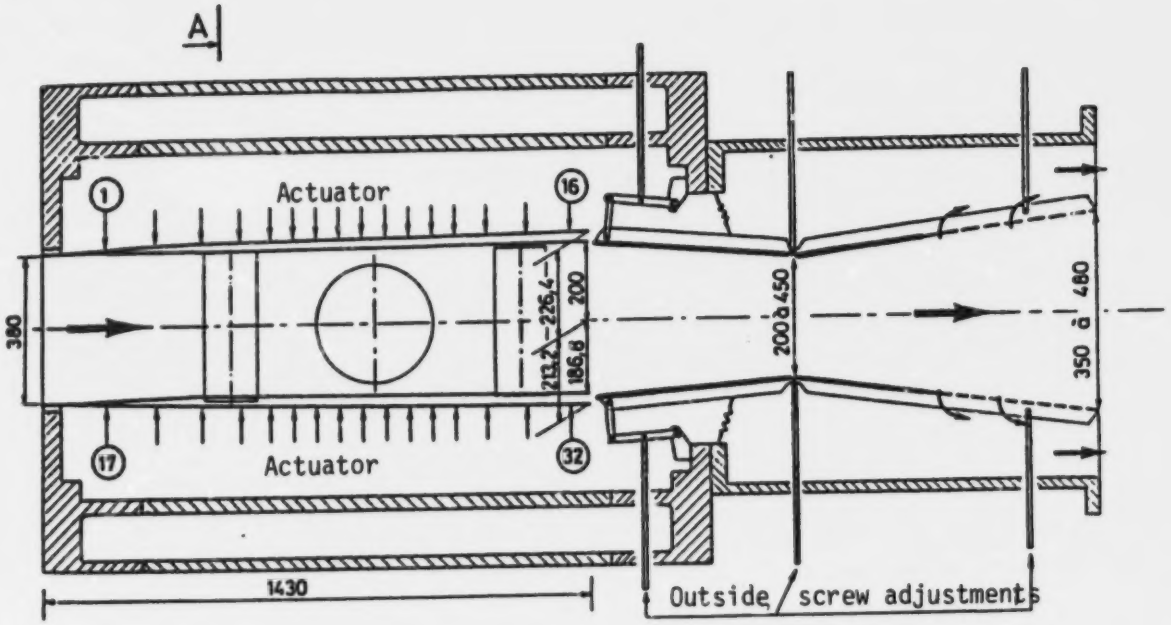

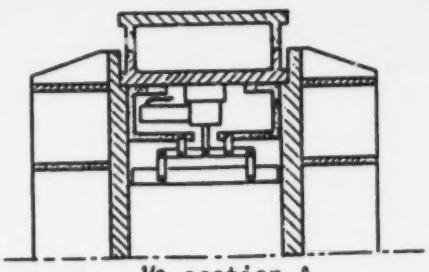

½ section A

Fig. 5 - Diagram of T2 Wind Tunnel - Test Section

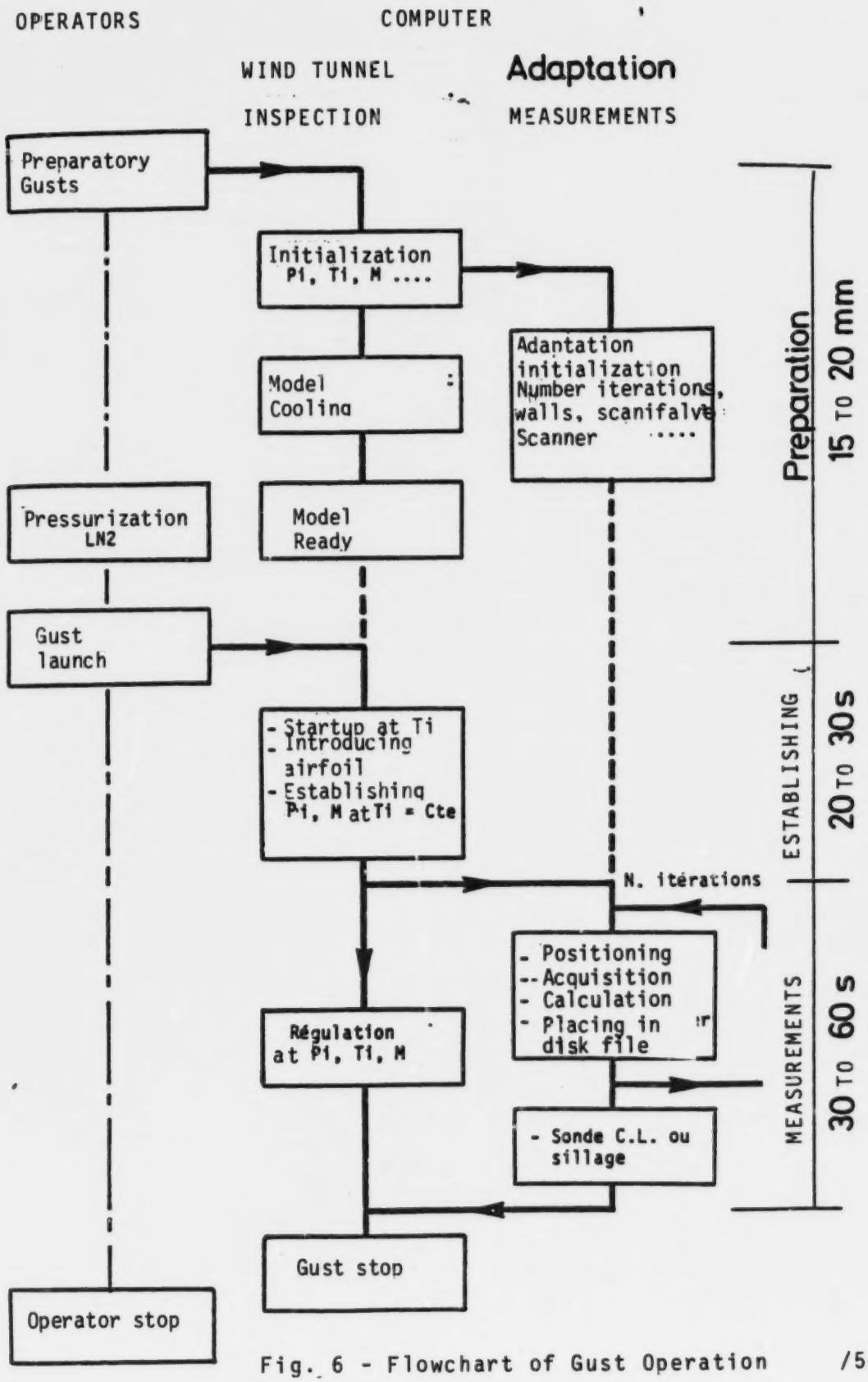

Fig. 6 - Flowchart of Gust Operation

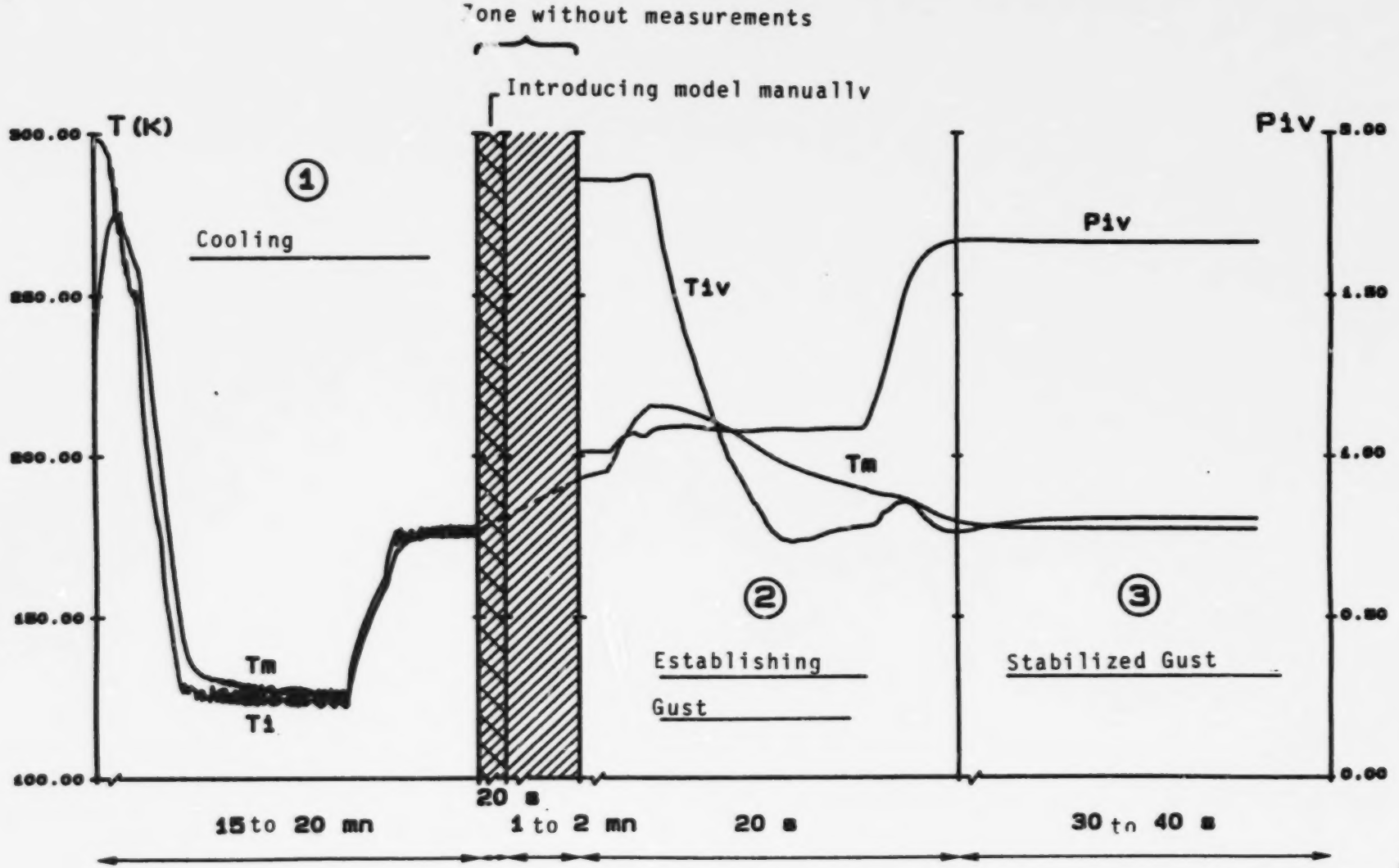

Fig. 7 - Gust Development with Cryogenic Balance

PL. 7

ORIGINAL PAGE IS
OF POOR QUALITY

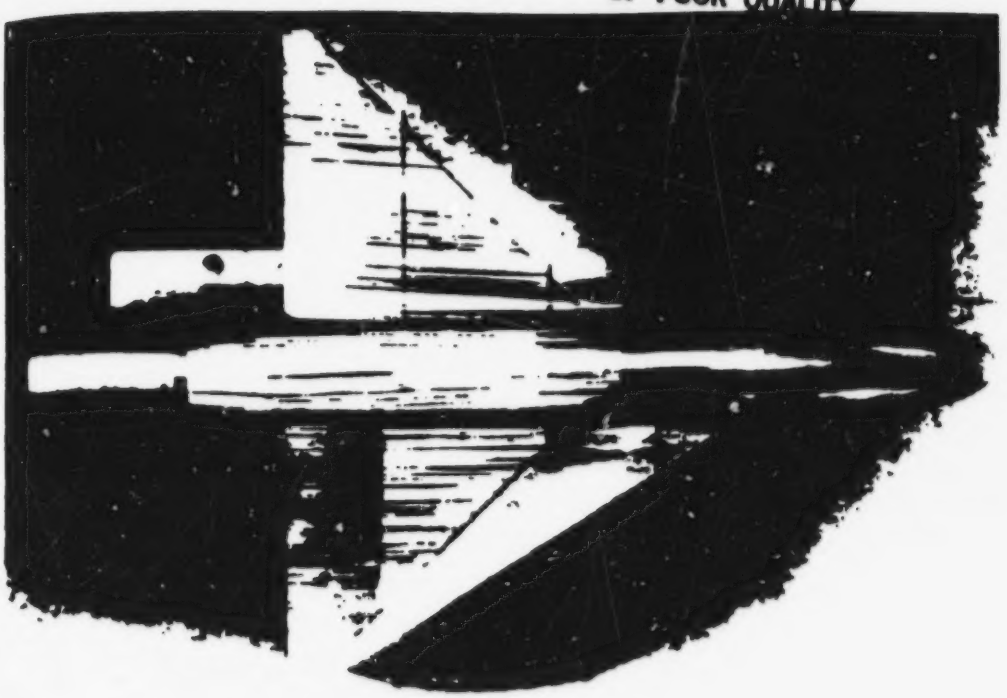

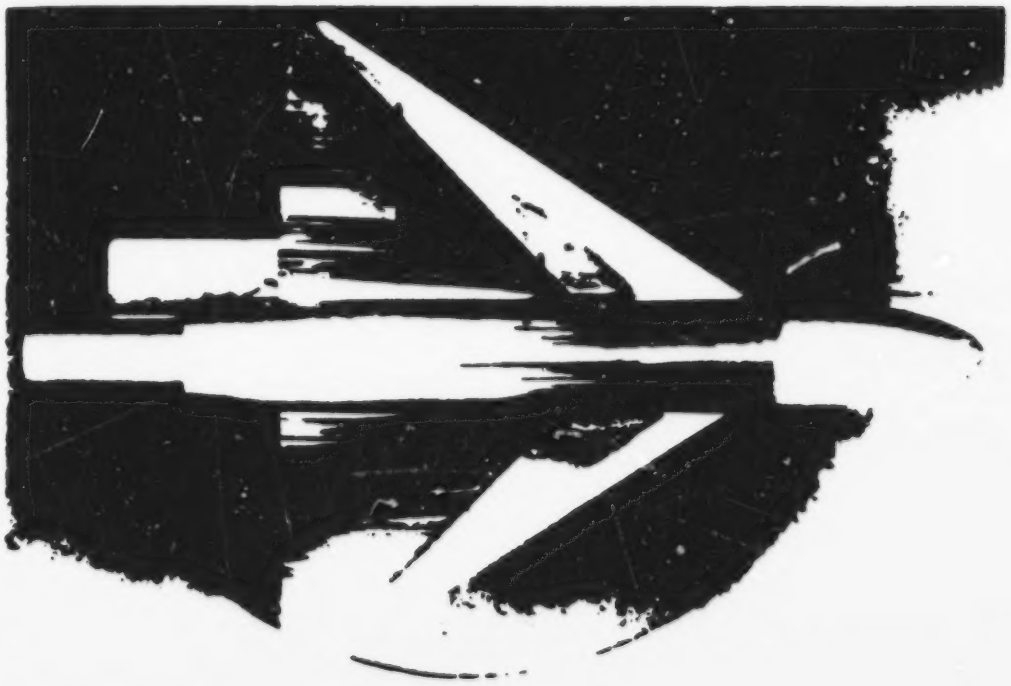

ORIGINAL PAGE IS
OF POOR QUALITY

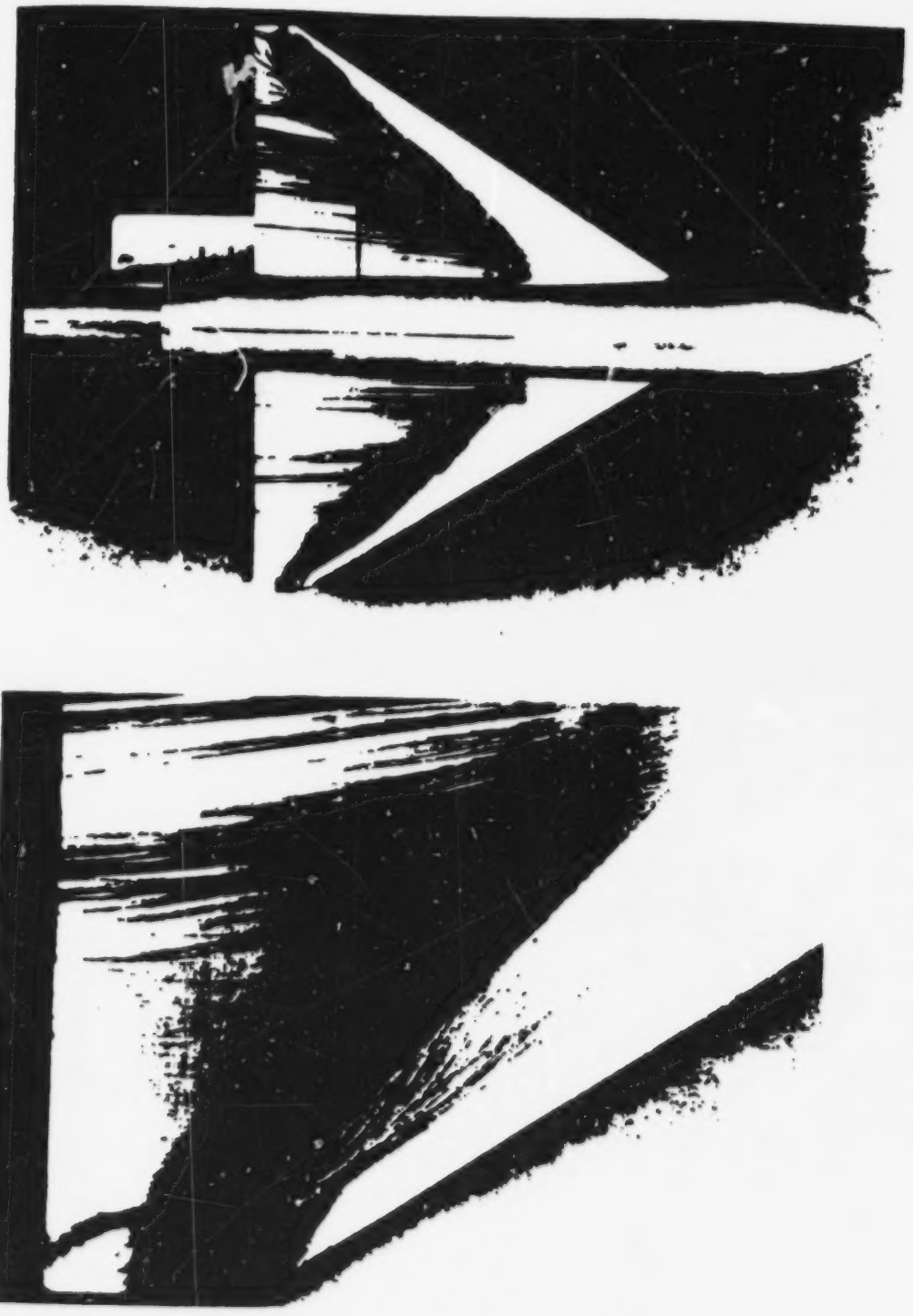

Fig. 9 - VISUALIZATION : M = 0,75 $T_j = T_A$ $\alpha = 4°$

ORIGINAL PAGE IS
OF POOR QUALITY

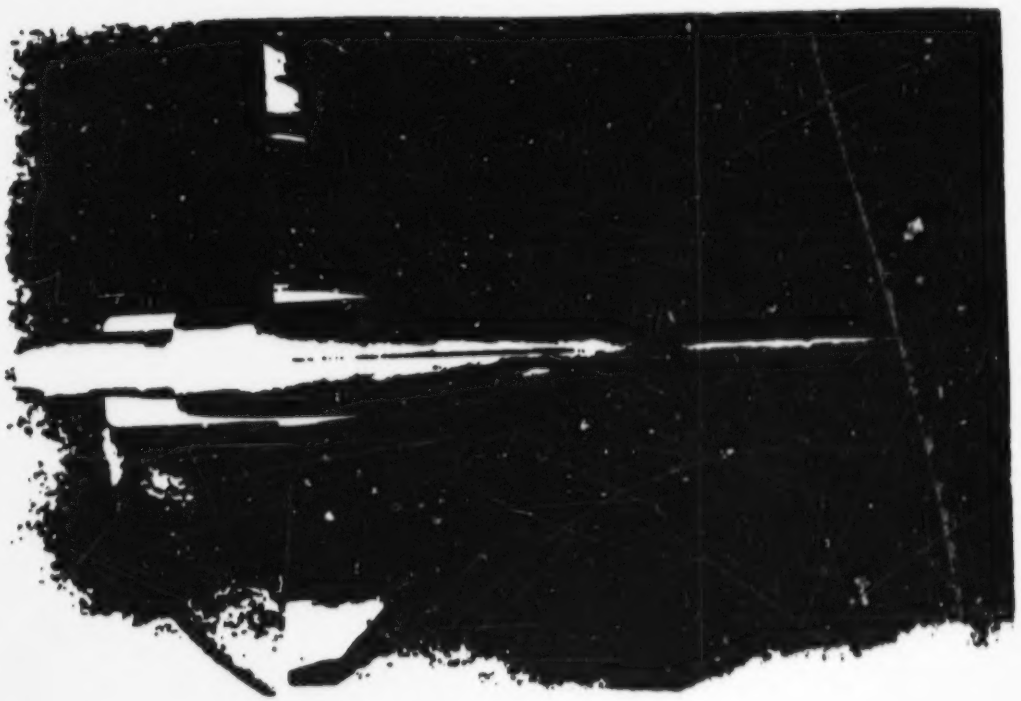

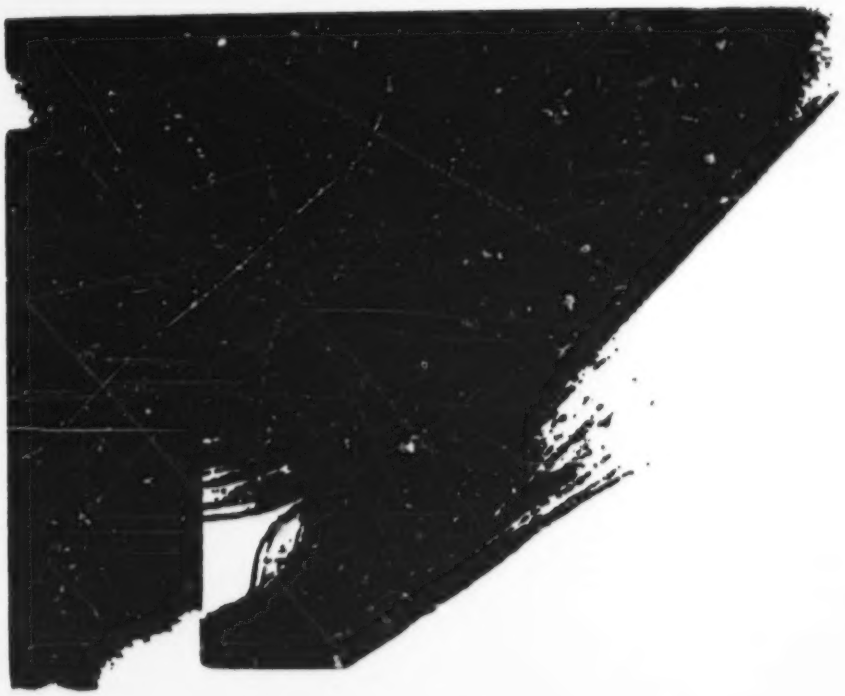

Fig. 10 - VISUALIZATION : M 0,8 $T_i = T_A$ ...

TYPICAL TESTS

M = 0,75	$\alpha = 0°$	Ti = 180 K	Plates 11 to 16
M = 0,75	$\alpha = 3{,}43°$	Ti = 180 K	Plates 17 to 21

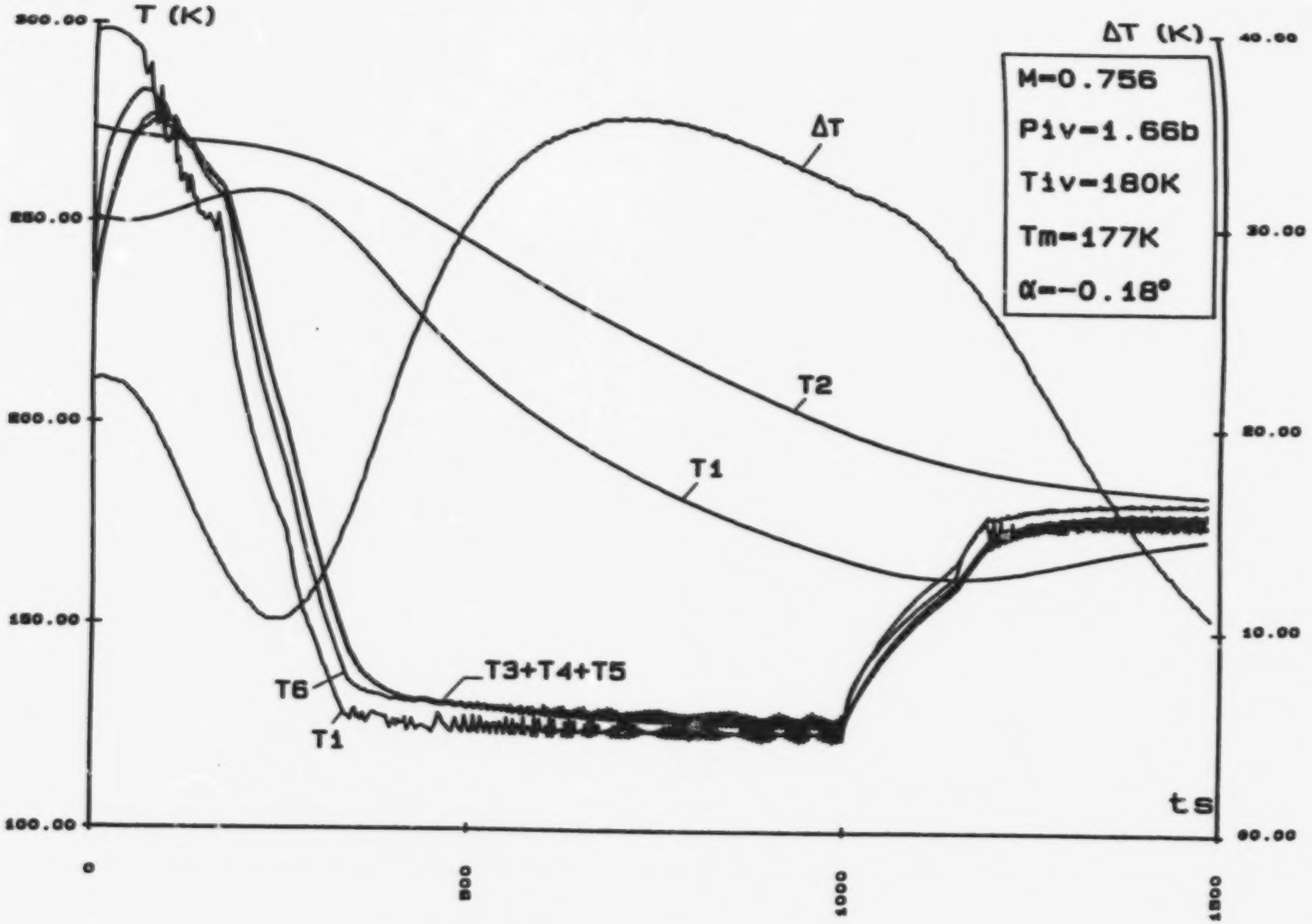

ORIGINAL PAGE IS
OF POOR QUALITY

Fig. 11 - Cooling (test 22): variation of model-balance temperatures

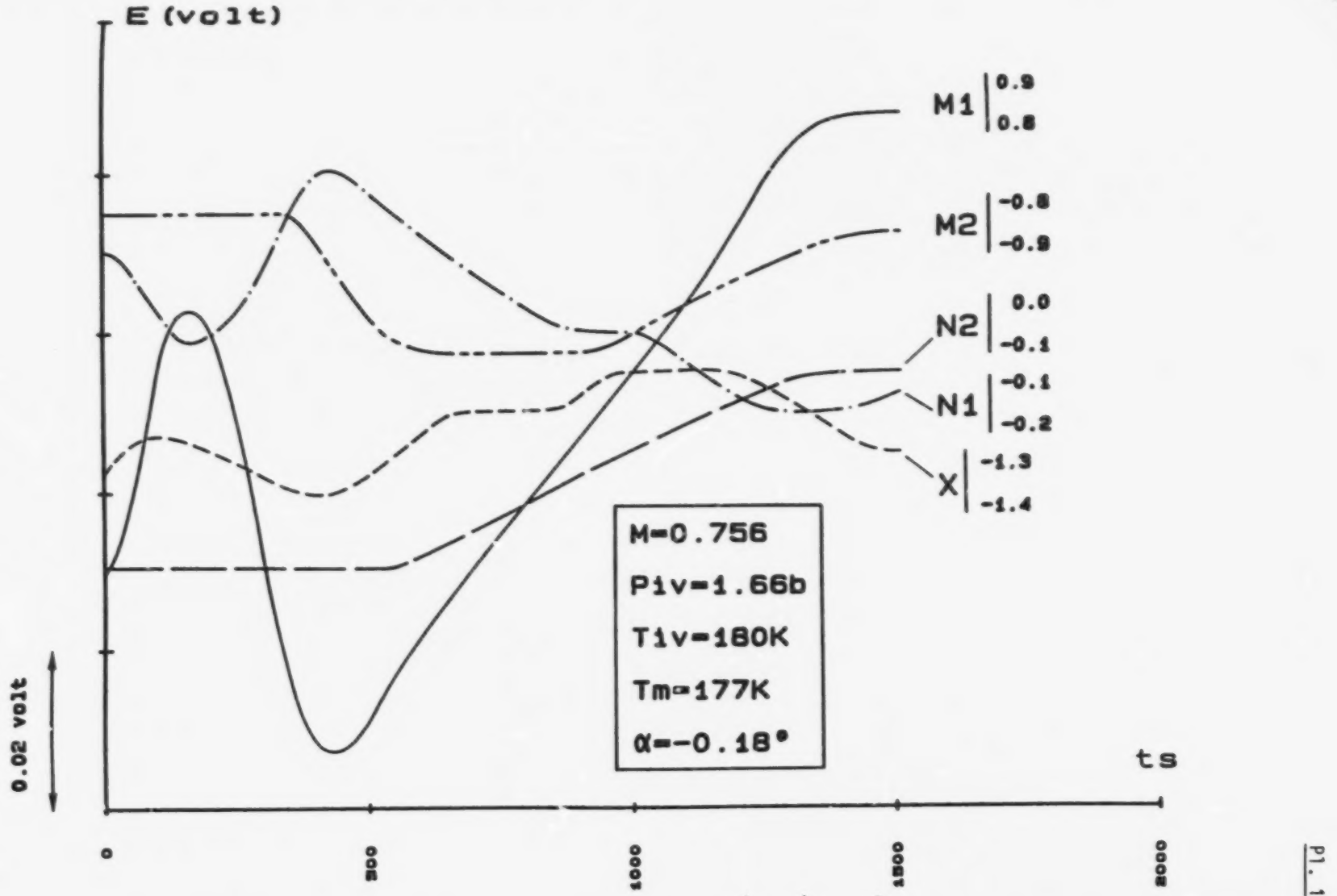

Pl. 12

Fig. 12 - Cooling (test 22): varation of bridge tensions

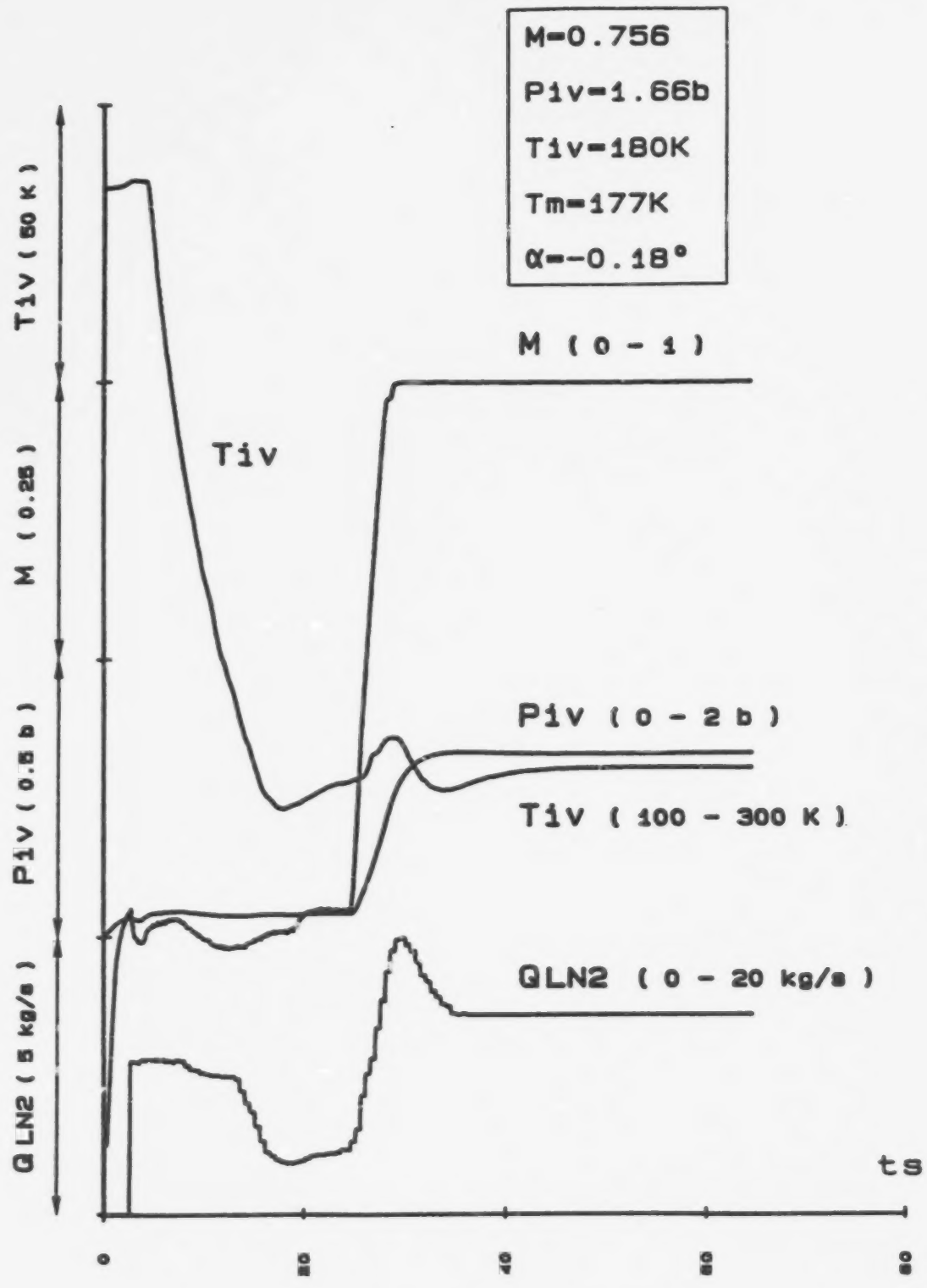

Fig 13 - Variation of Gust Conditions (Test 22)

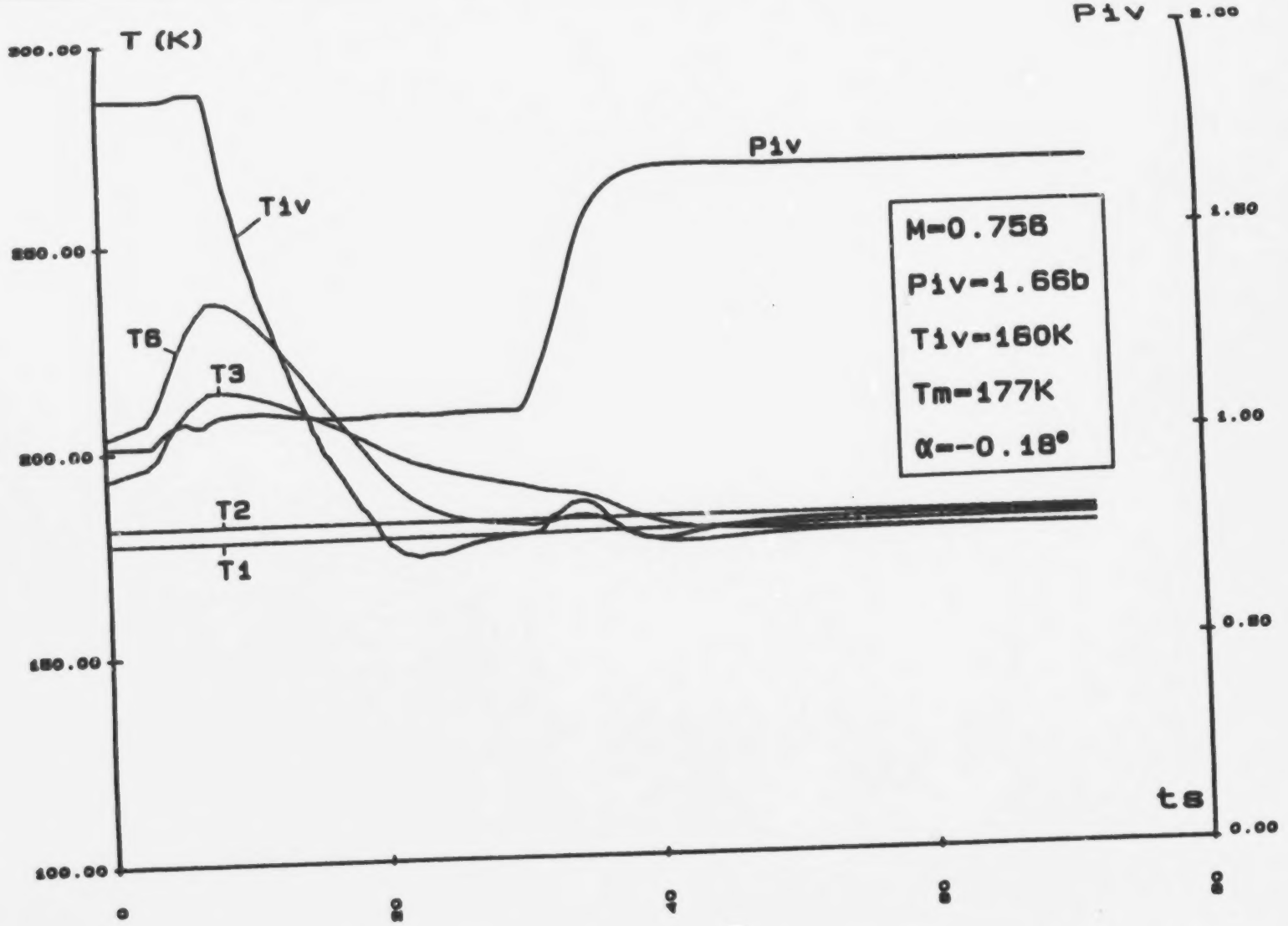

Fig. 14 - Variation of Balance-Model Temperatures During Gust (Test 22)

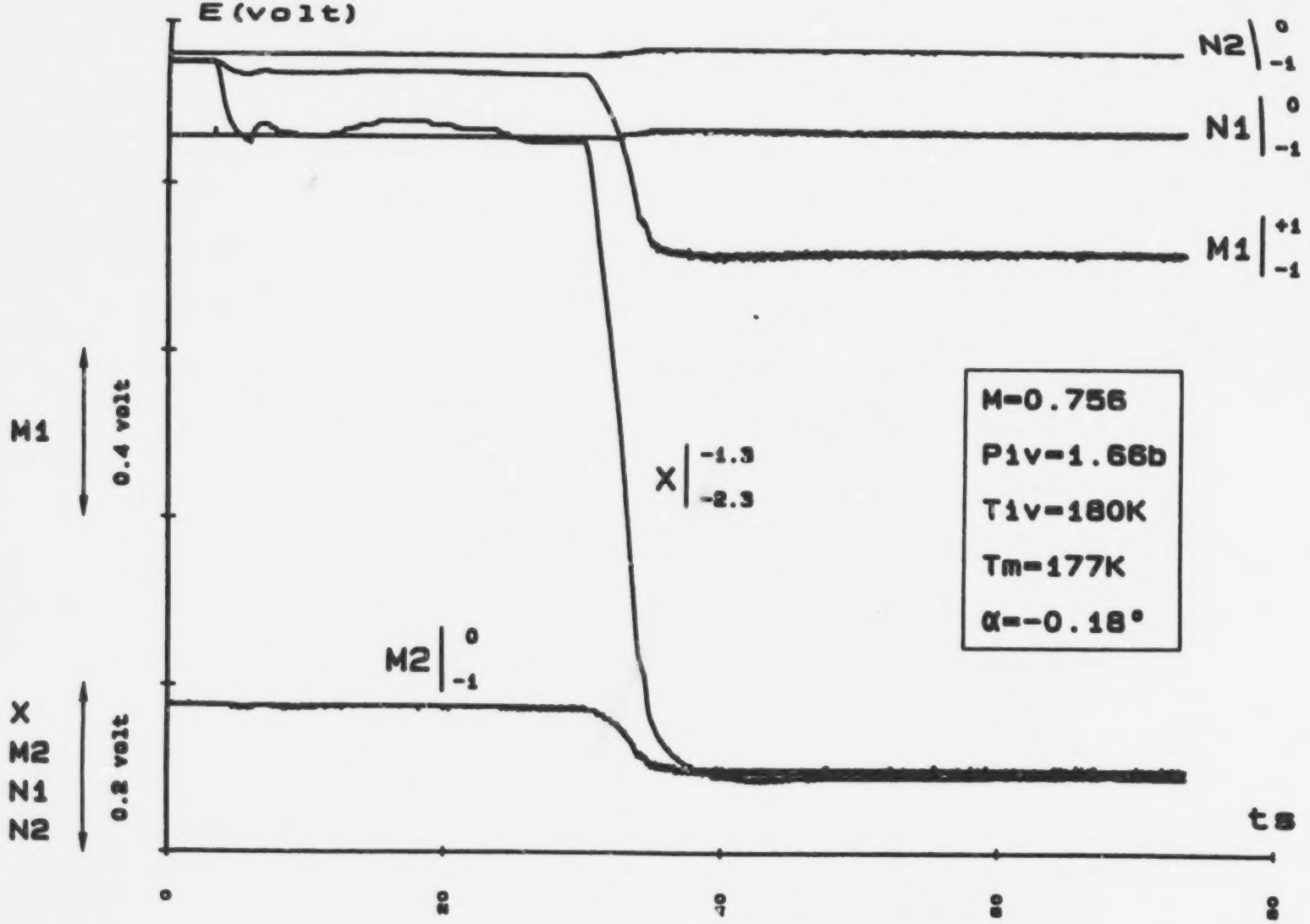

Fig. 15 - Variation of Bridge Tensions During Gust (Test 22)

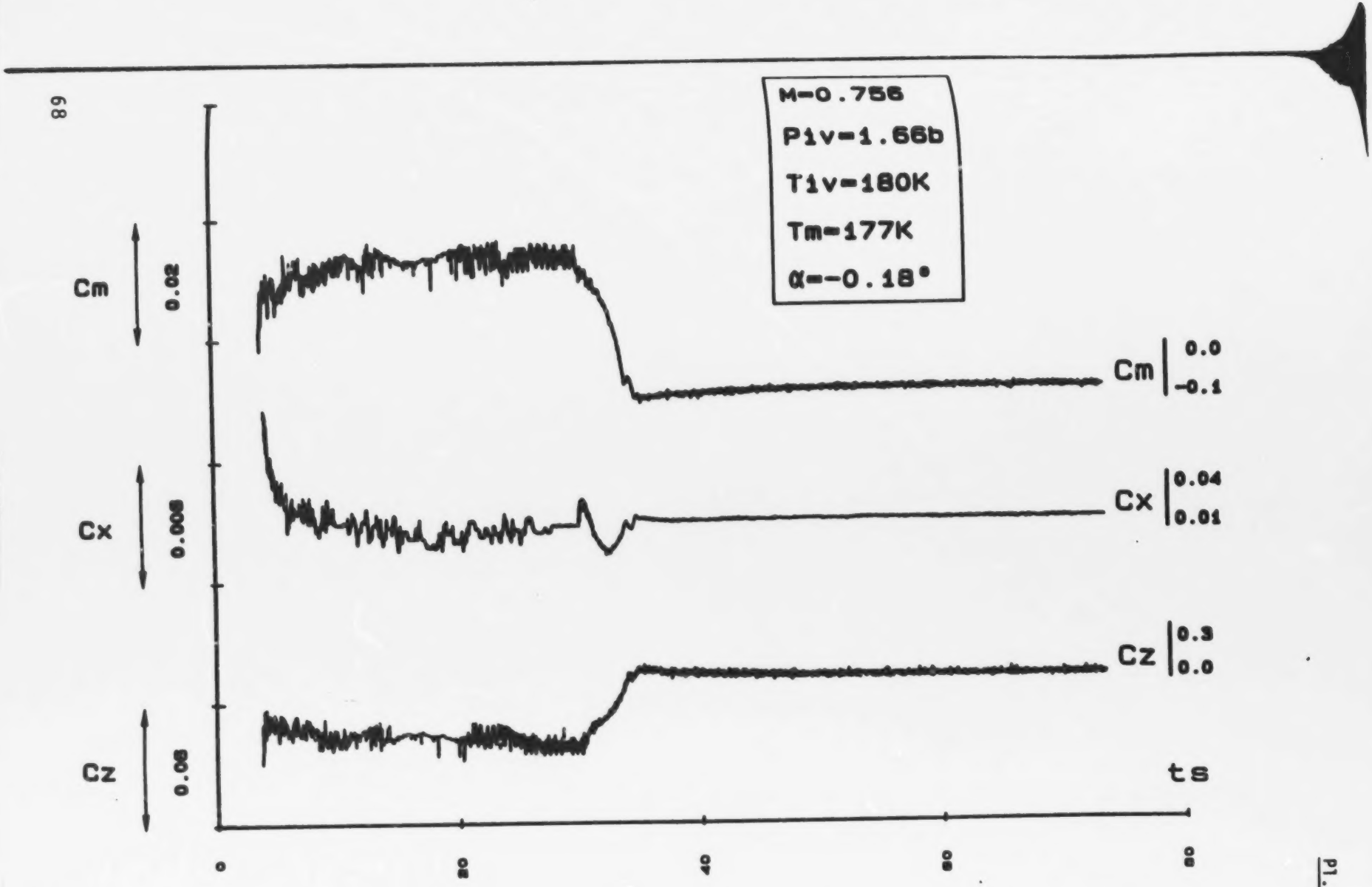

Fig. 16 - Variation of Balance Aerodynamic Coefficients (Test 22)

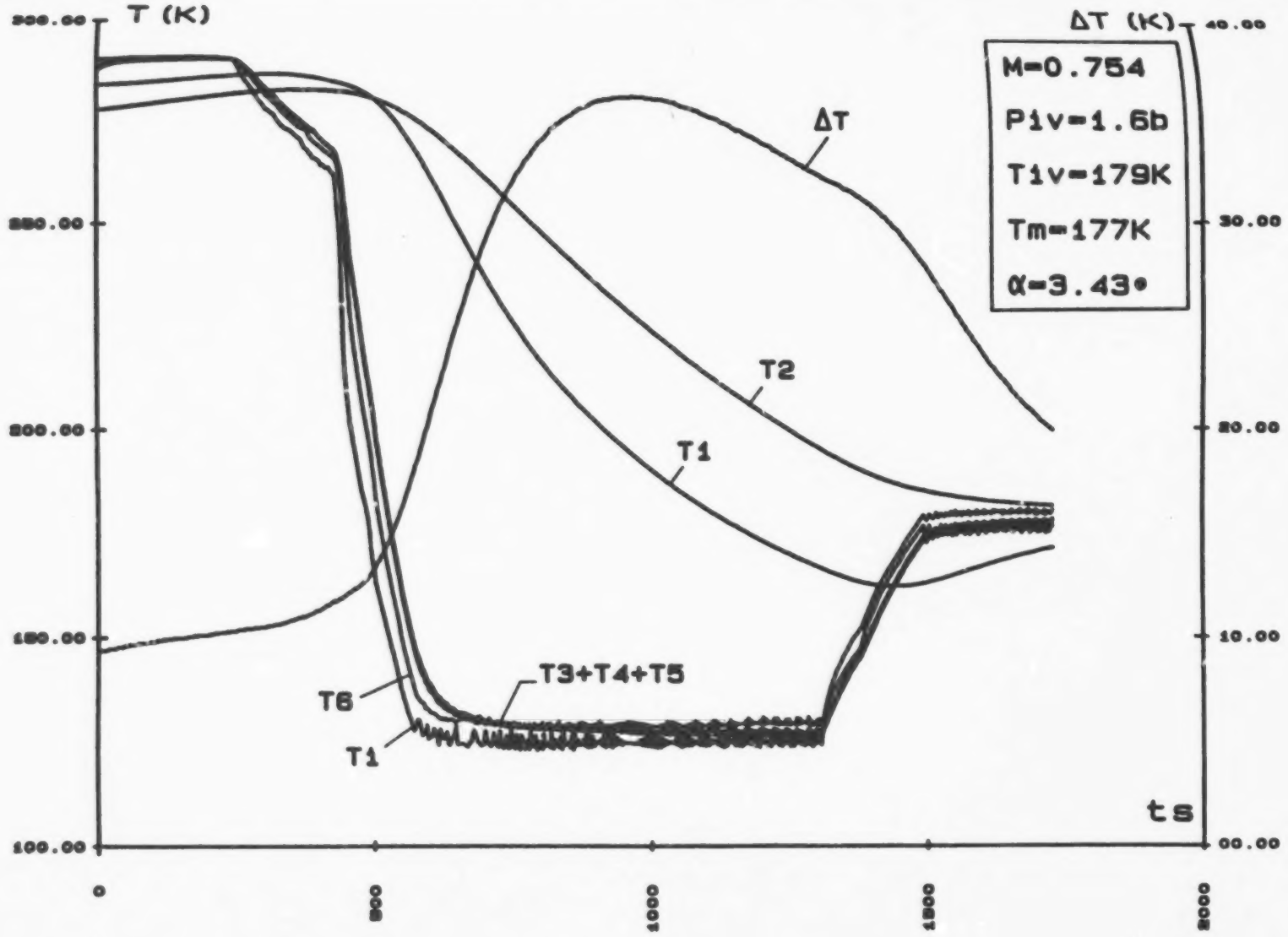

Pl. 17

Fig. 17 - Cooling (Test 39): Variation of Model-Balance Temperatures

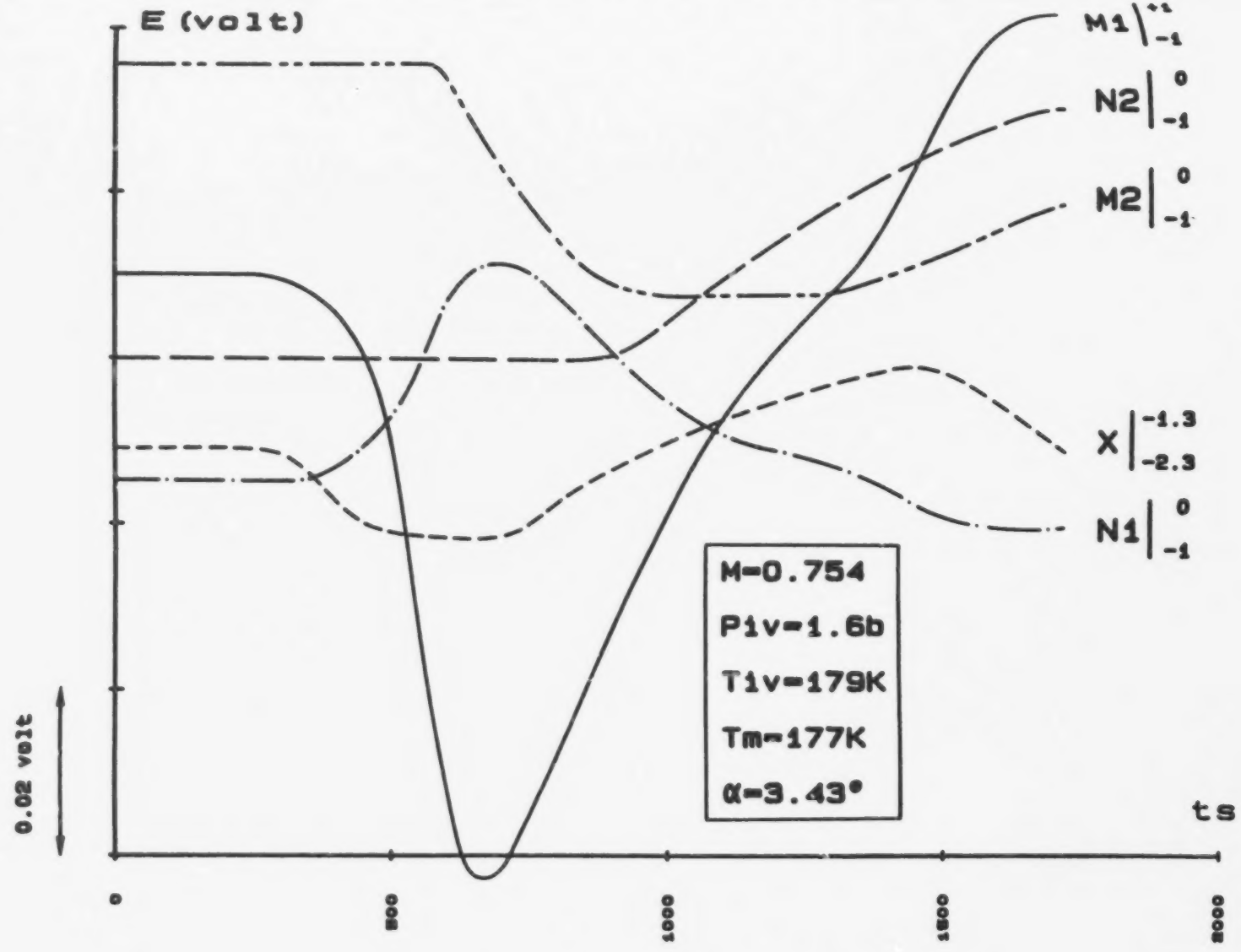

Pl. 18

Fig. 18 - Cooling (Test 39): Variation of Bridge Tensions

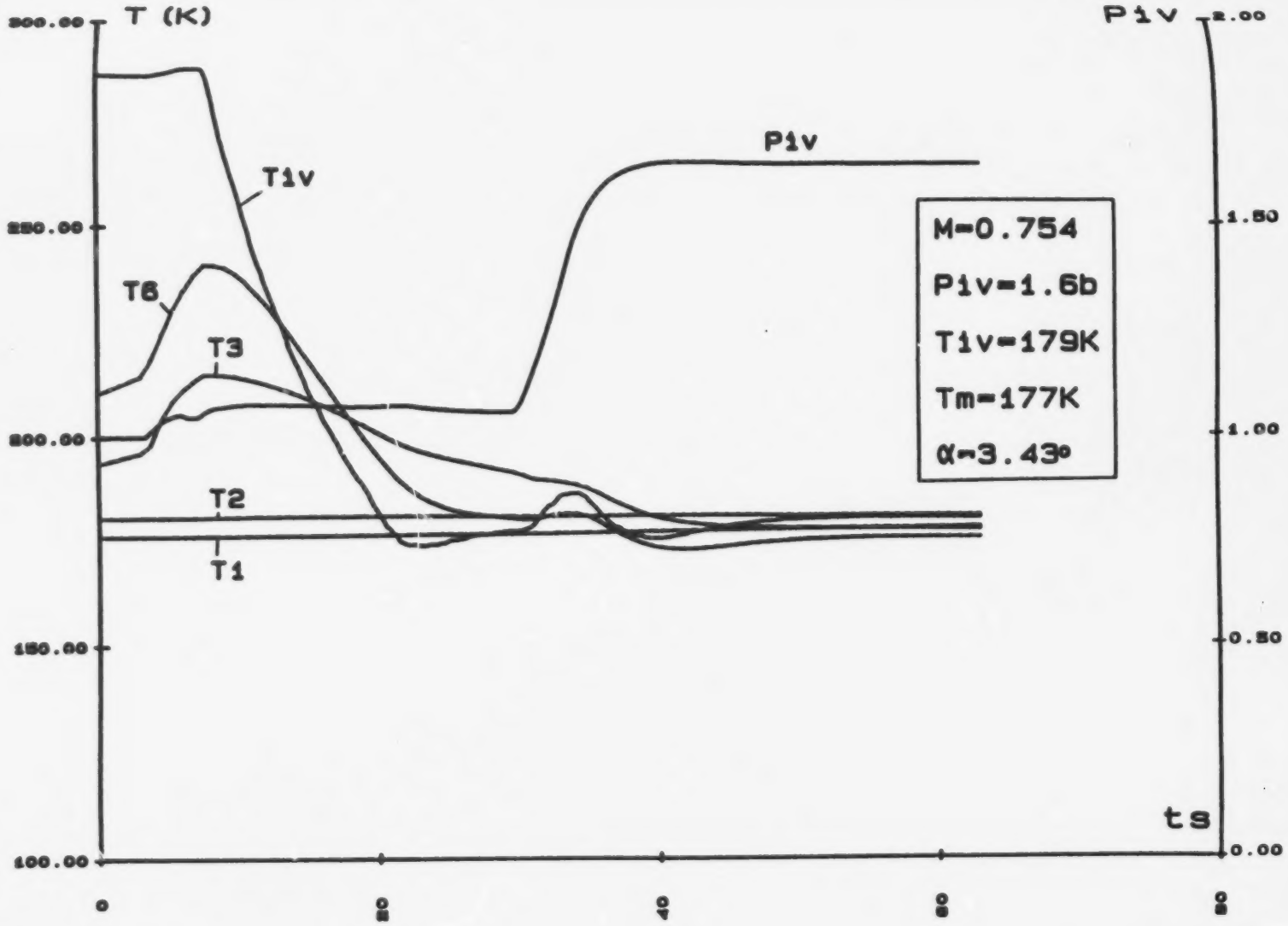

Pl. 19

Fig. 19 - Variation of Balance-Model Temperatures During Gust (Test 39)

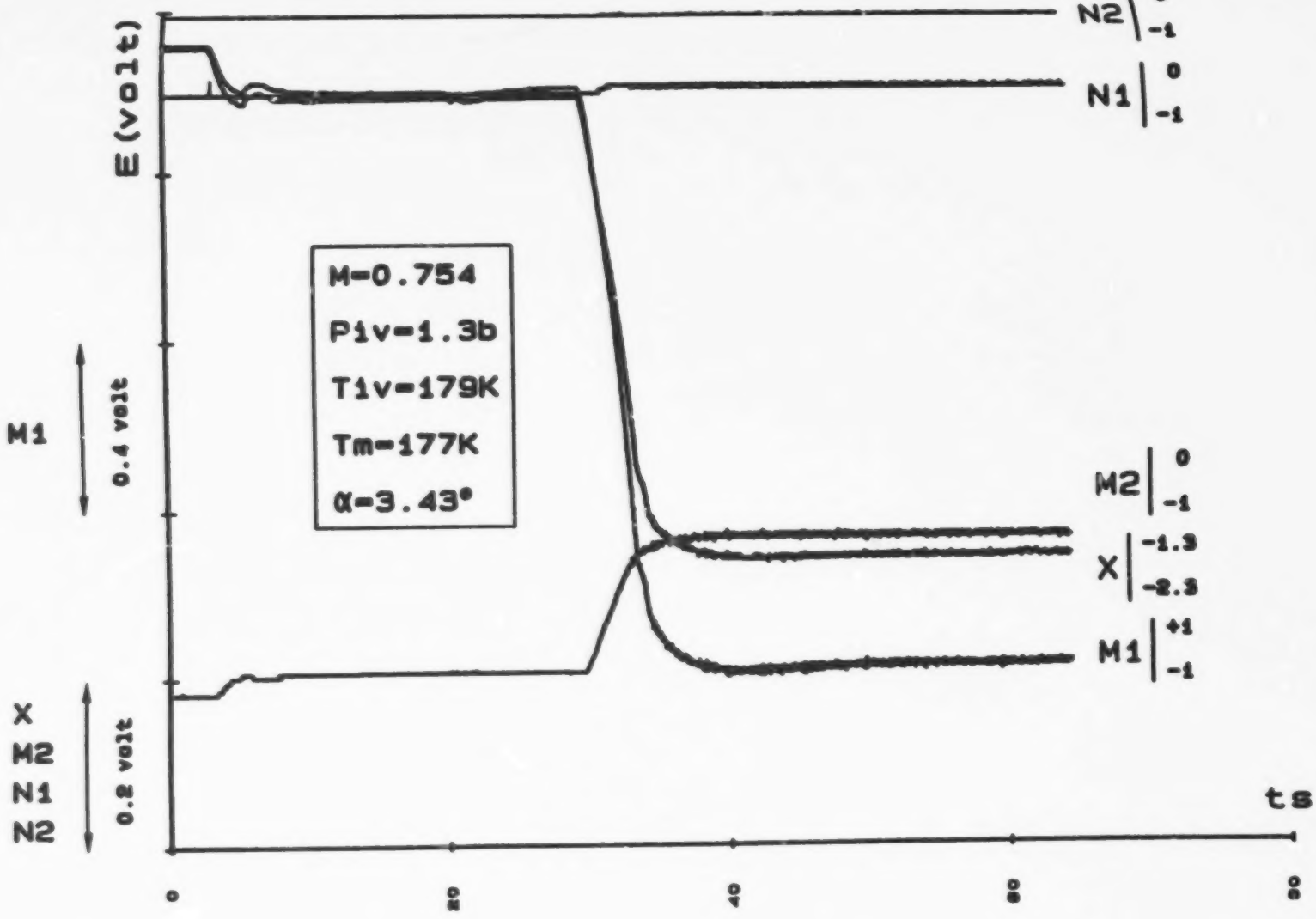

Fig. 20 - Variation of Bridge Tensions During Gust (Test 39)

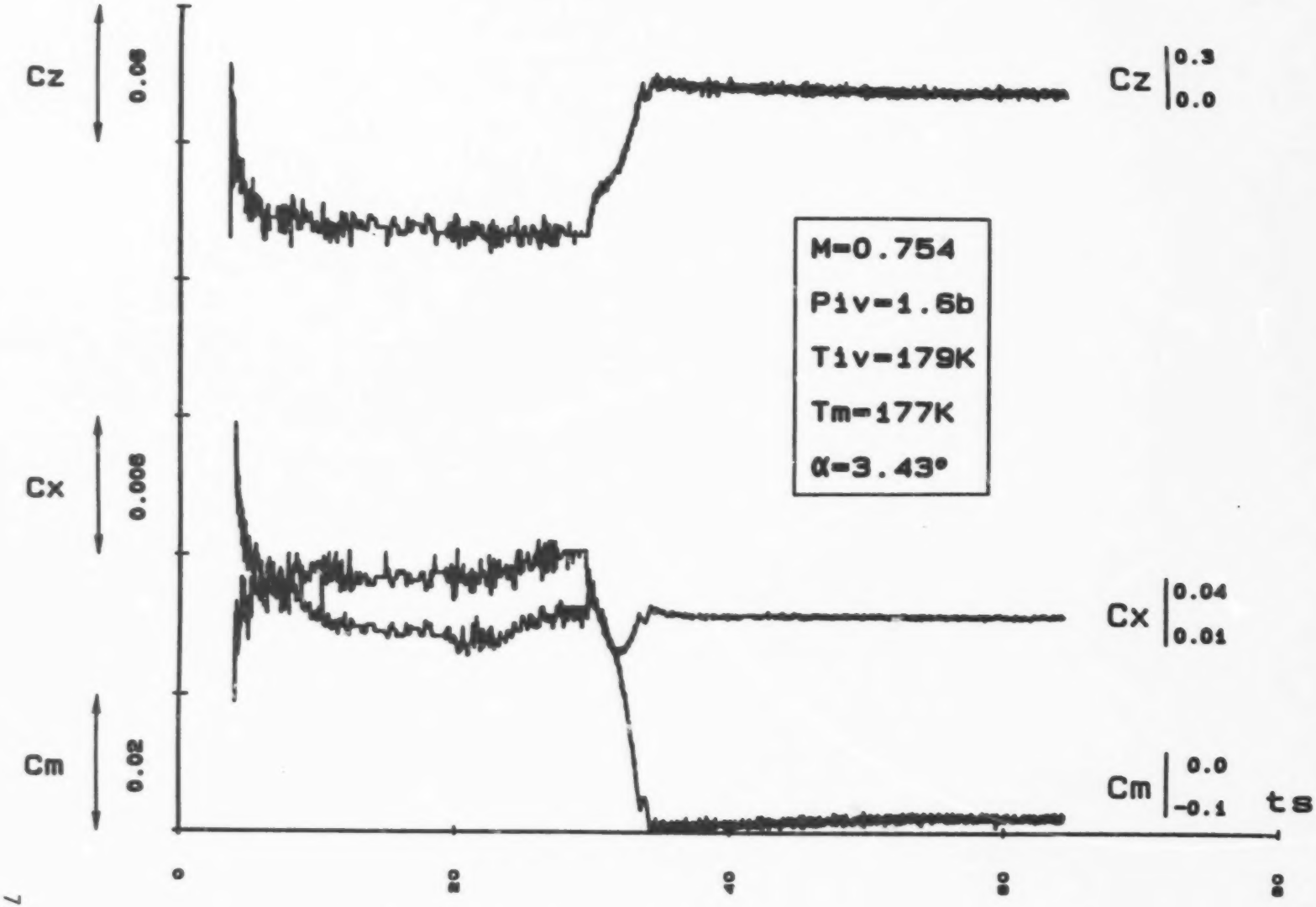

Fig. 21 - Variation of Balance Aerodynamic Coefficients (Test 39)

SPECIAL EFFECTS:

Thermal Disequilibrium of Balance

-Ti = Ta Cooled Model (plates 22 to 25)
-Ti = 120 K Model at Ta (plates 26 to 31)

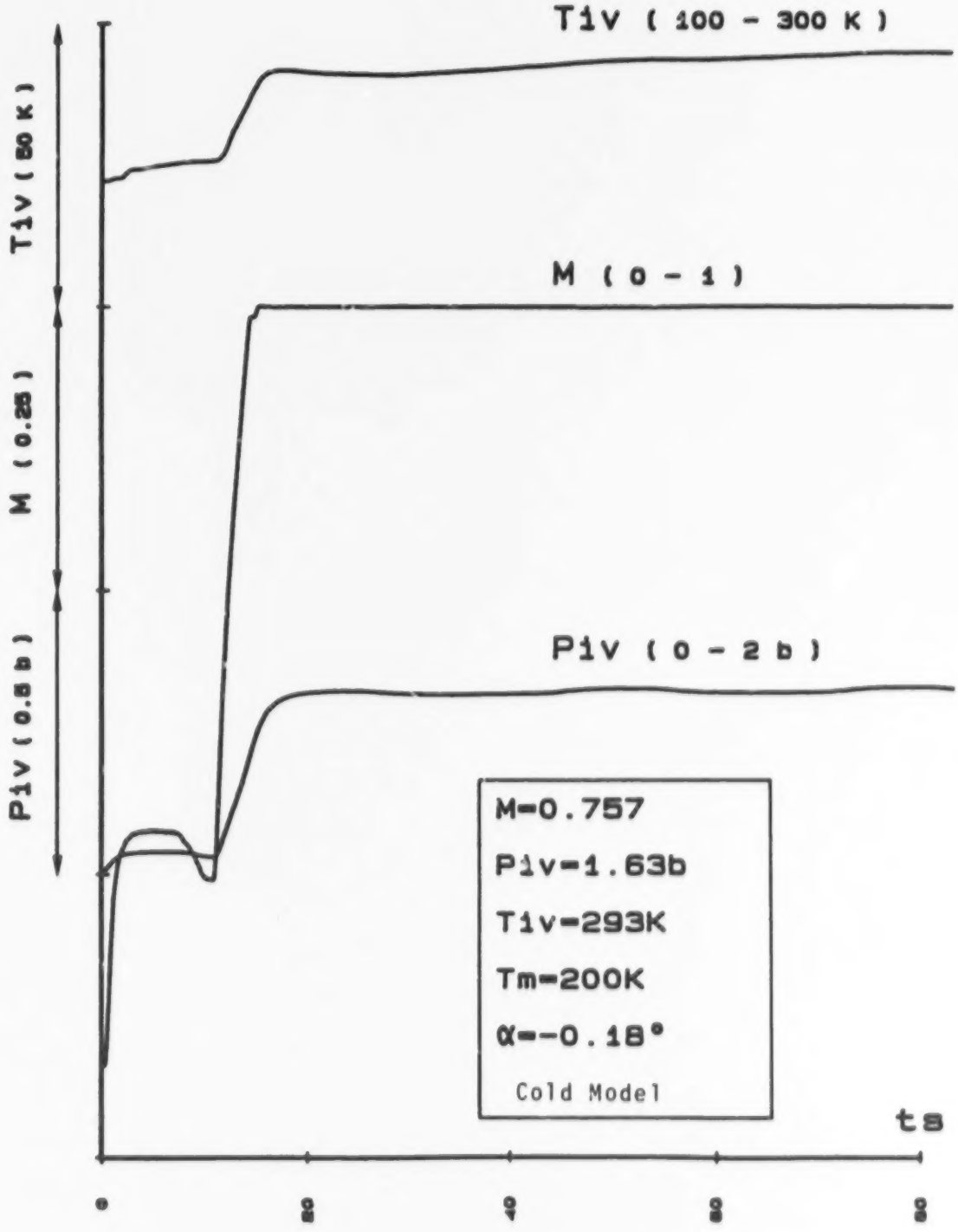

Fig. 22 - Variation of Gust Conditions (Test 28)

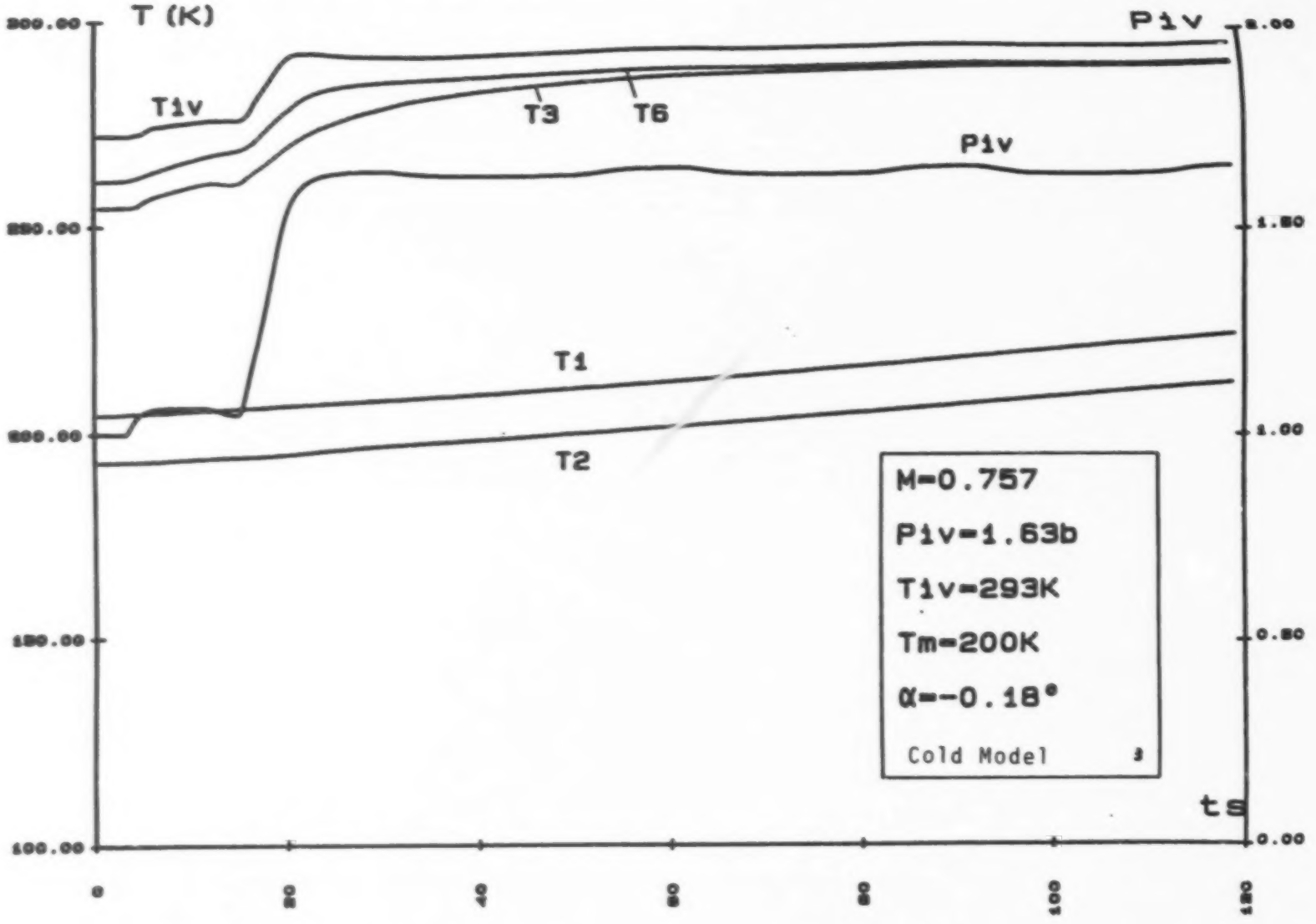

Pl. 23

Fig. 23 - Variation of Balance-Model Temperatures During Gust (Test 28)

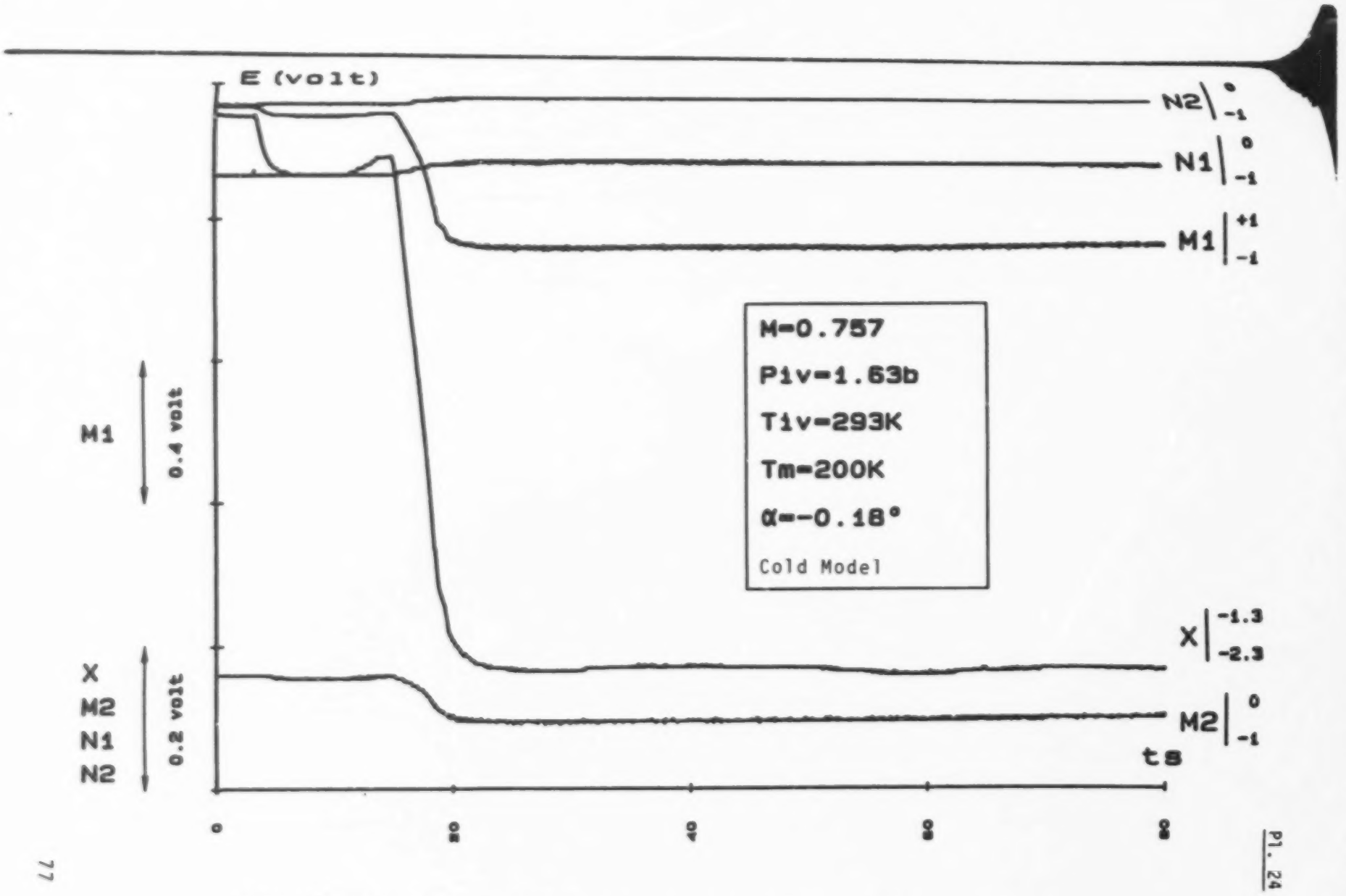

Fig. 24 - Variation of Bridge Tensions During Gust (Test 28)

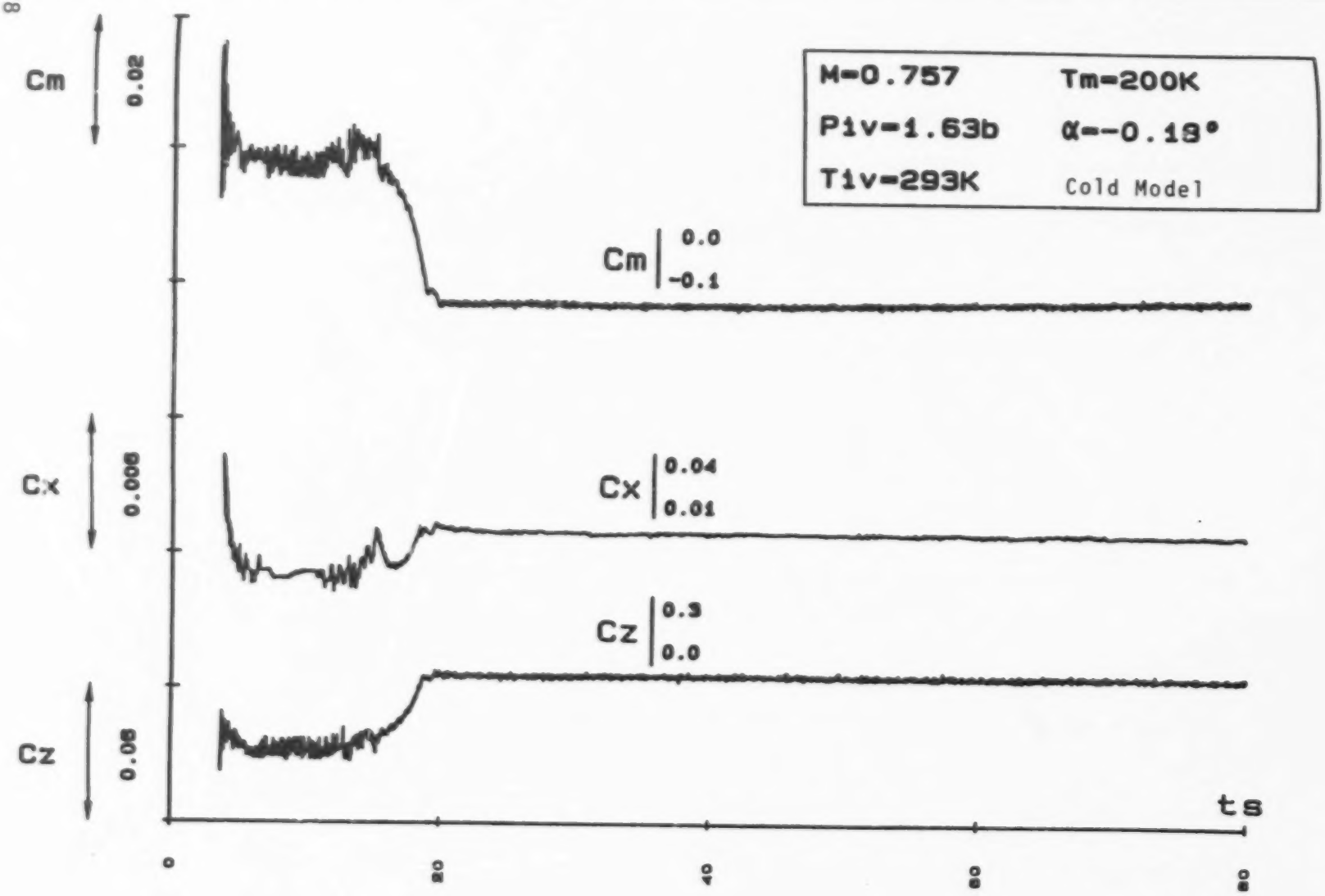

Fig. 25 - Variation of Balance Aerodynamic Coefficients (Test 28)

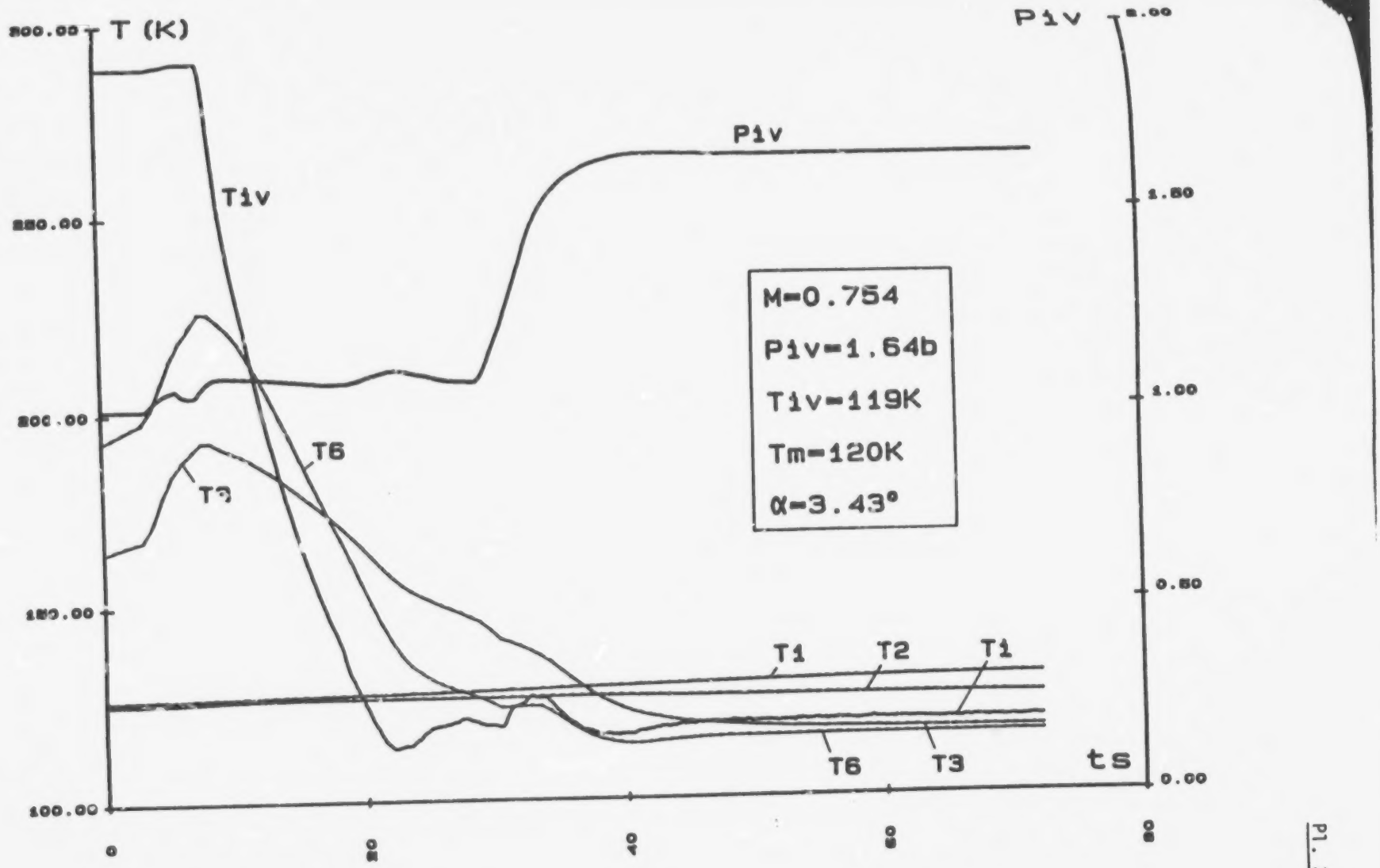

Pl. 26

Fig. 26 - Variation of Balance-Model Temperatures During Gust (Test 36)

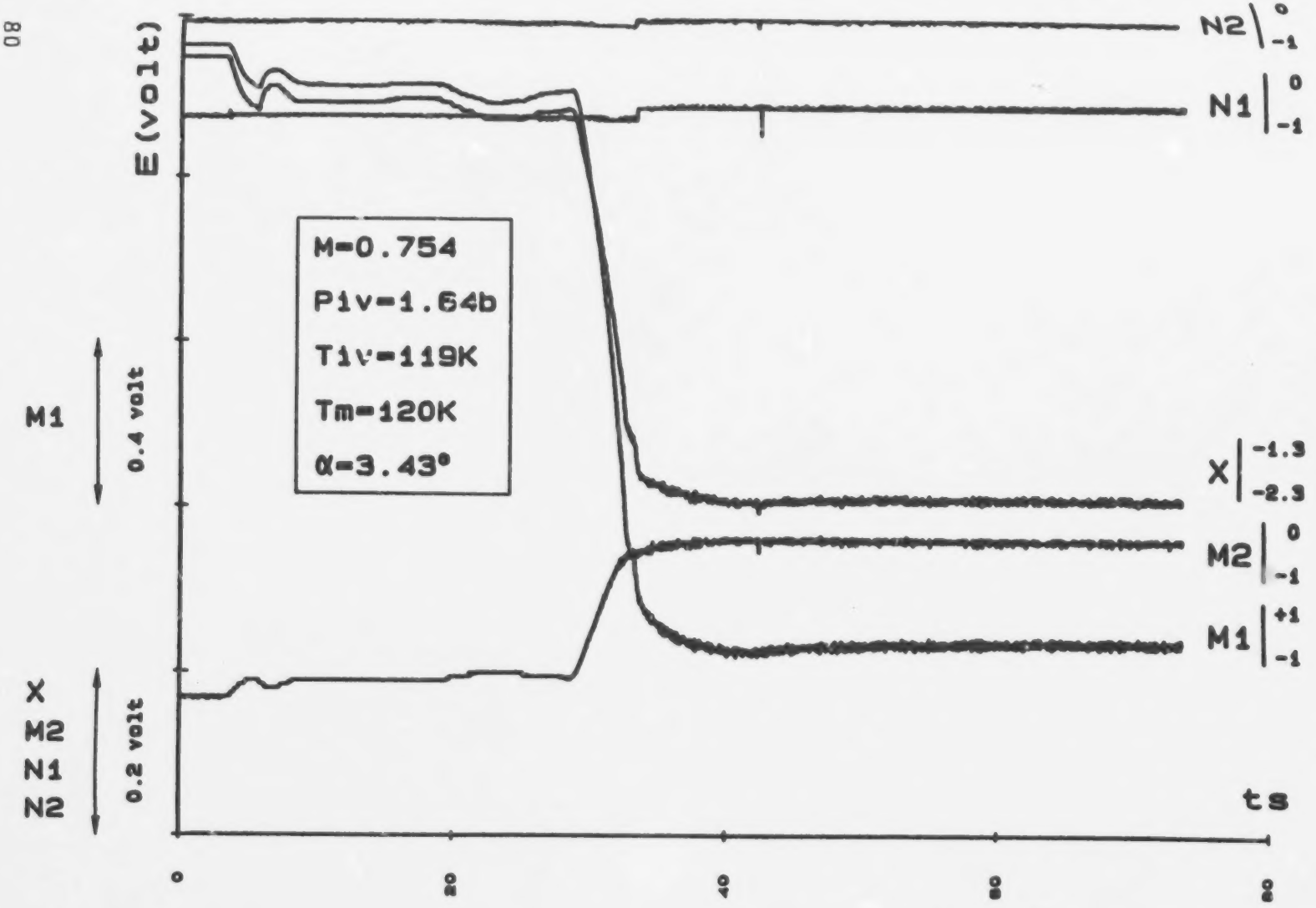

Pl. 27

Fig. 27 - Variation of Brdige Tensions During Gust (Test 36)

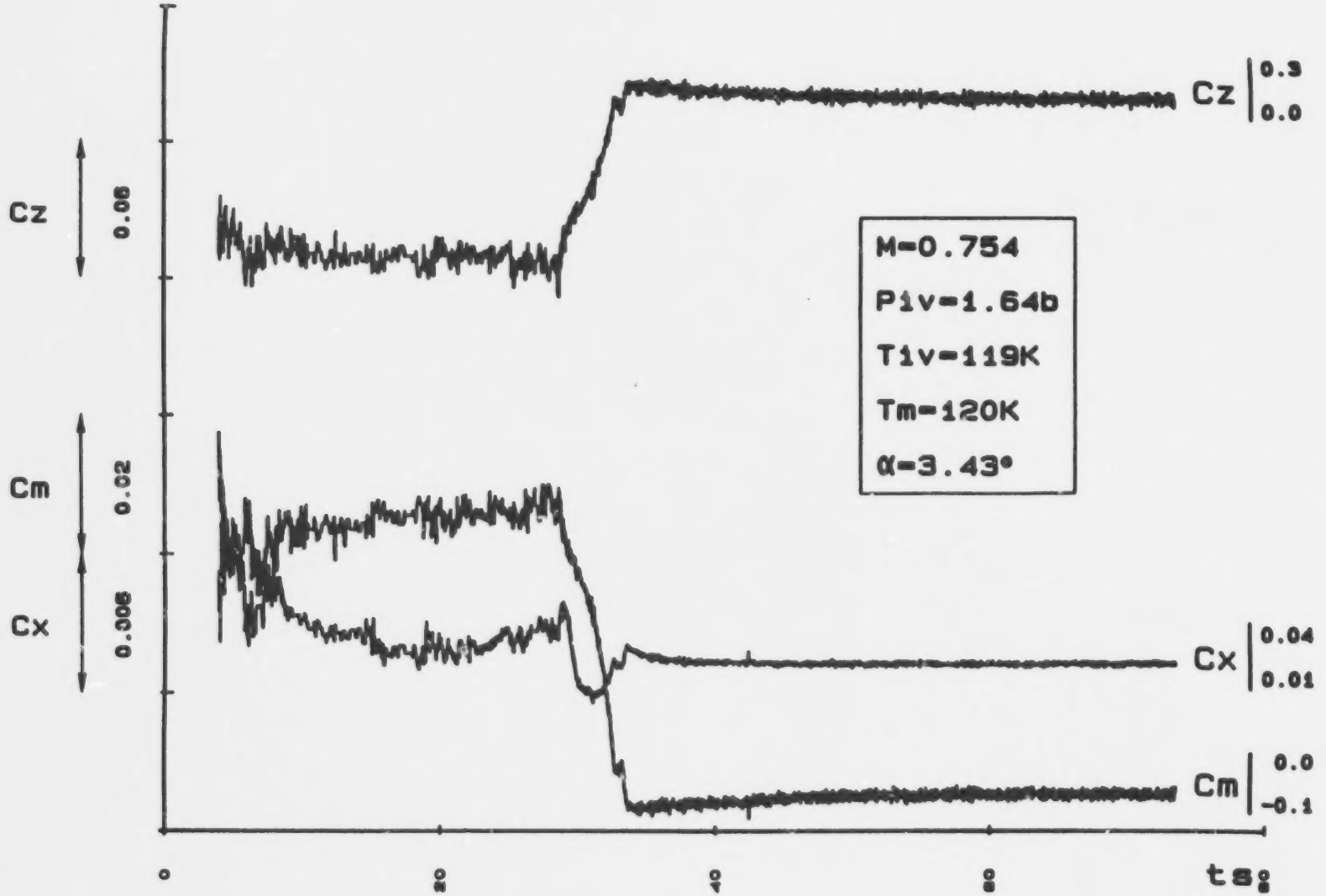

Fig. 28 - Variation of Balance Aerodynamic Coefficients (Test 36)

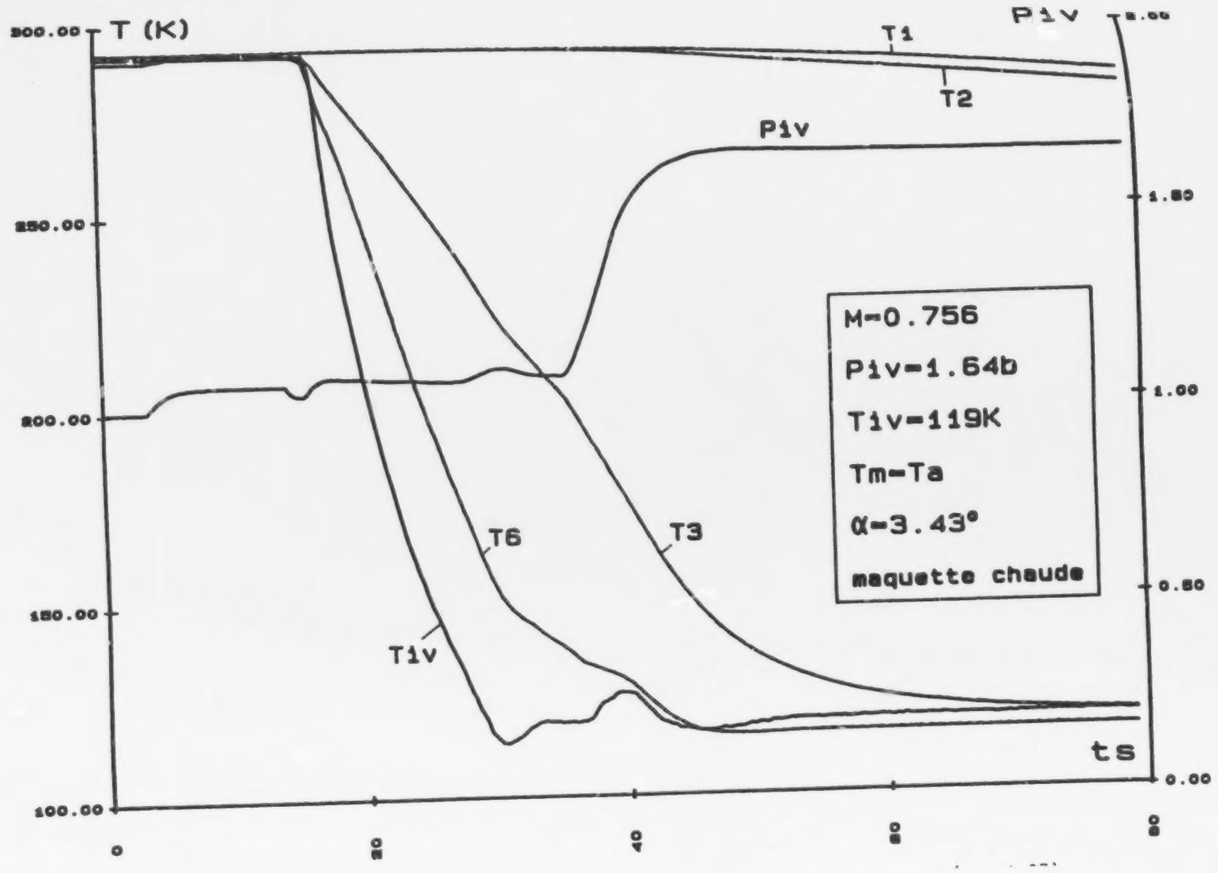

Pl. 29

Fig. 29 - Variation of Balance-Model Temperatures During Gust (Test 37)

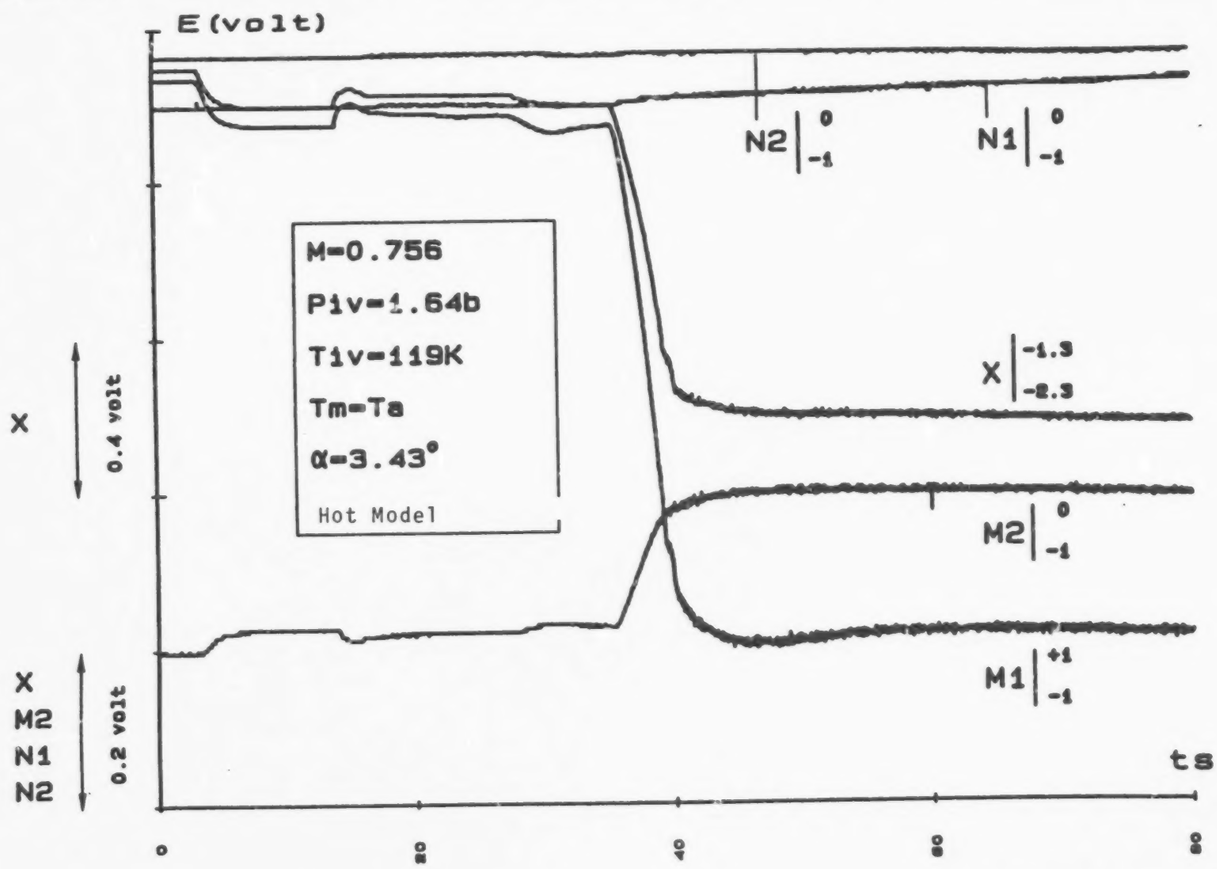

ORIGINAL PAGE IS
OF POOR QUALITY

Pl. 30

Fig. 30 - Variation of Bridge Tensions Duirng Gust (Test 37)

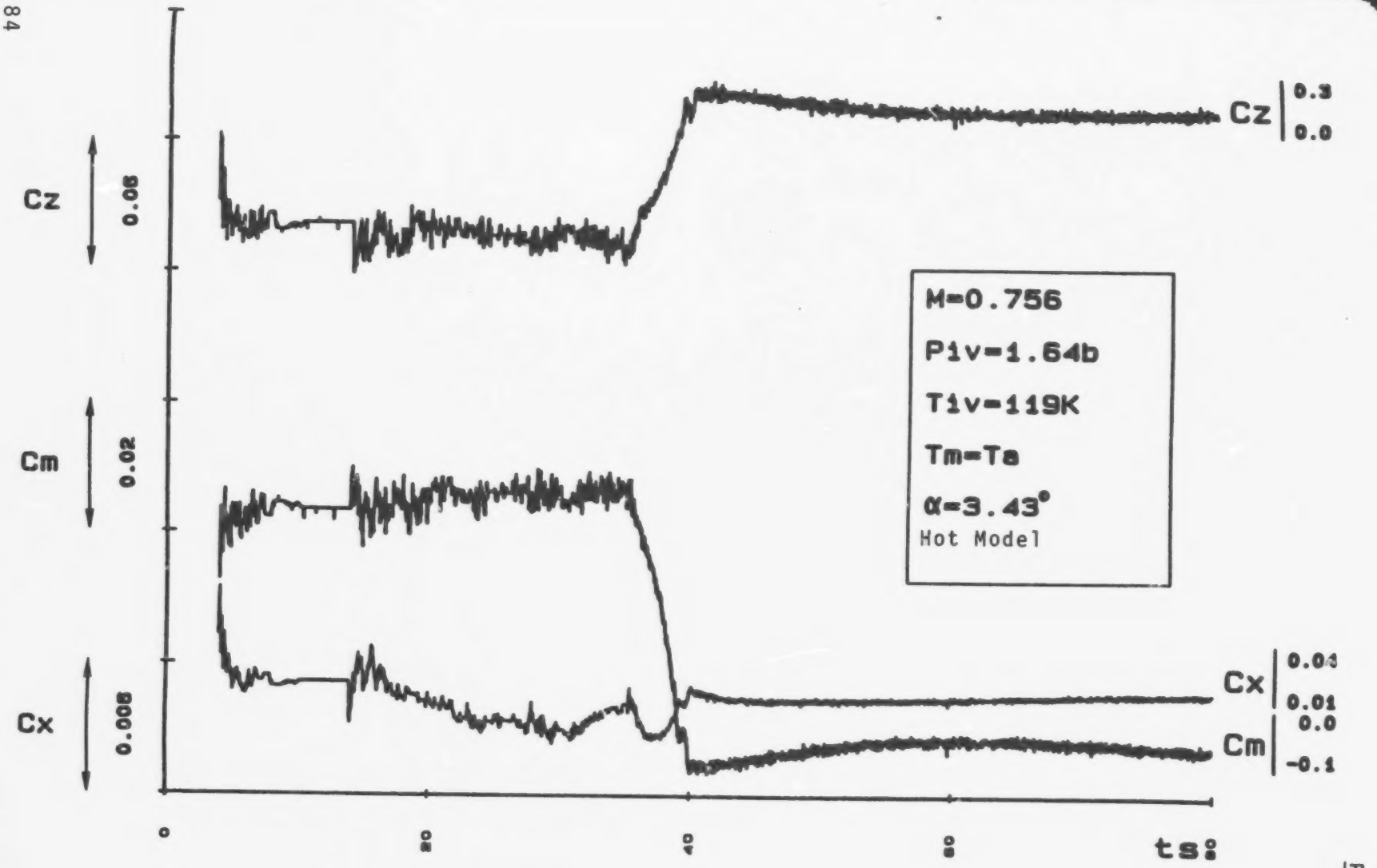

Pl. 31

Fig. 31 - Variation of Balance Aerodynamic Coefficients (Test 37)

BALANCE AERODYNAMIC COEFFICIENTS

α = -0.18°	Cx (M)	Plate 32
	Cz	Plate 33
	Cm	
α = 1.33°	Cx (M)	Plate 34
	Cz	Plate 35
	Cm	Plate 36
α = 3.43°	Cx (M)	Plate 37
	Cz	Plate 38
	Cm	Plate 39
α = 5.42°	Cx (M)	Plate 40
	Cz	Plate 41
	Cm	
	Cx (α)	Plate 42
	Cz (α)	Plate 43
	Cm (α)	Plate 44
	Cz (Cx)	Plate 45

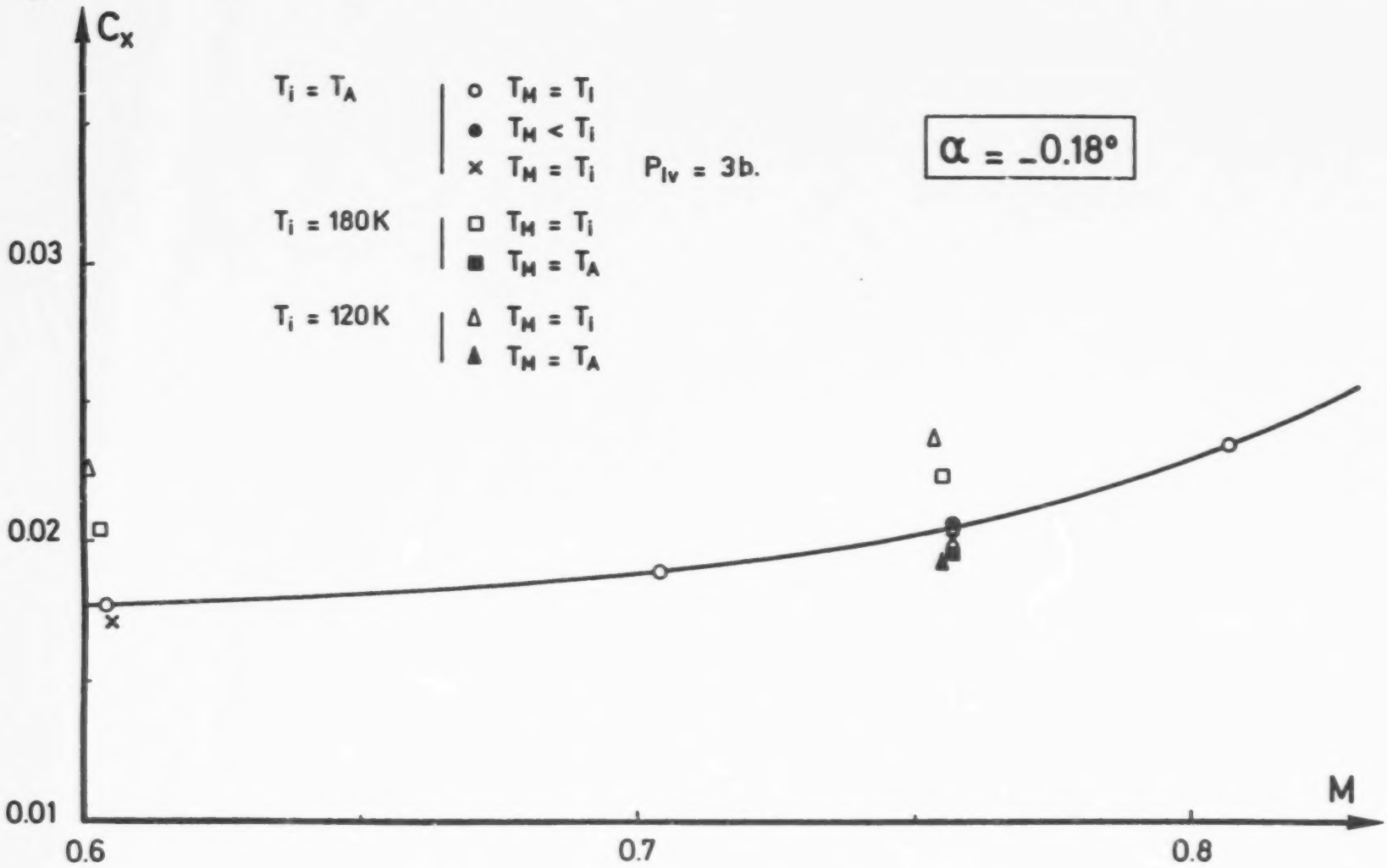

Pl. 32

Fig. 32 - Variation of Cx as a Function of the Macn Number

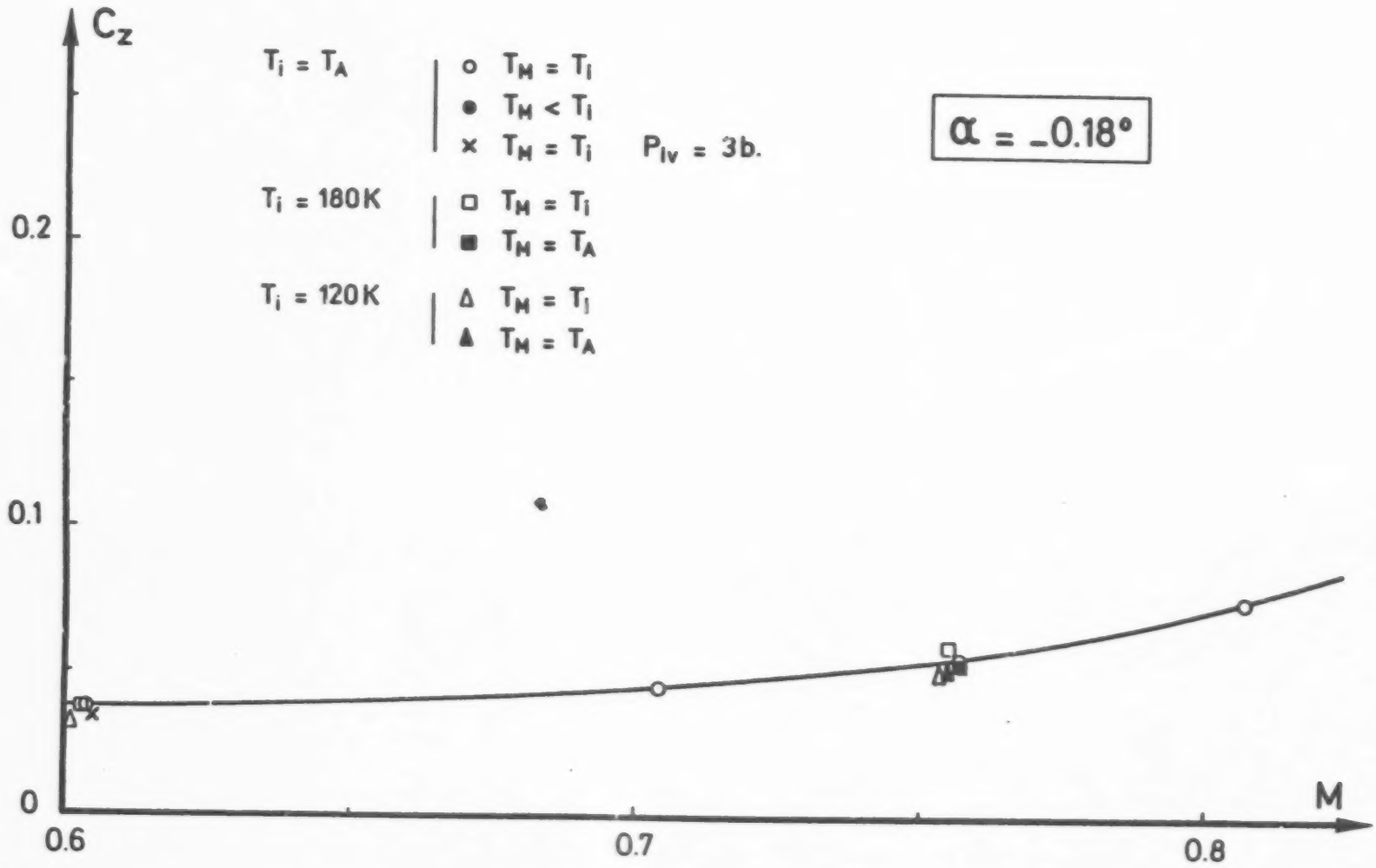

Fig. 33 - Variation of Cz as a Function of the Mach Number

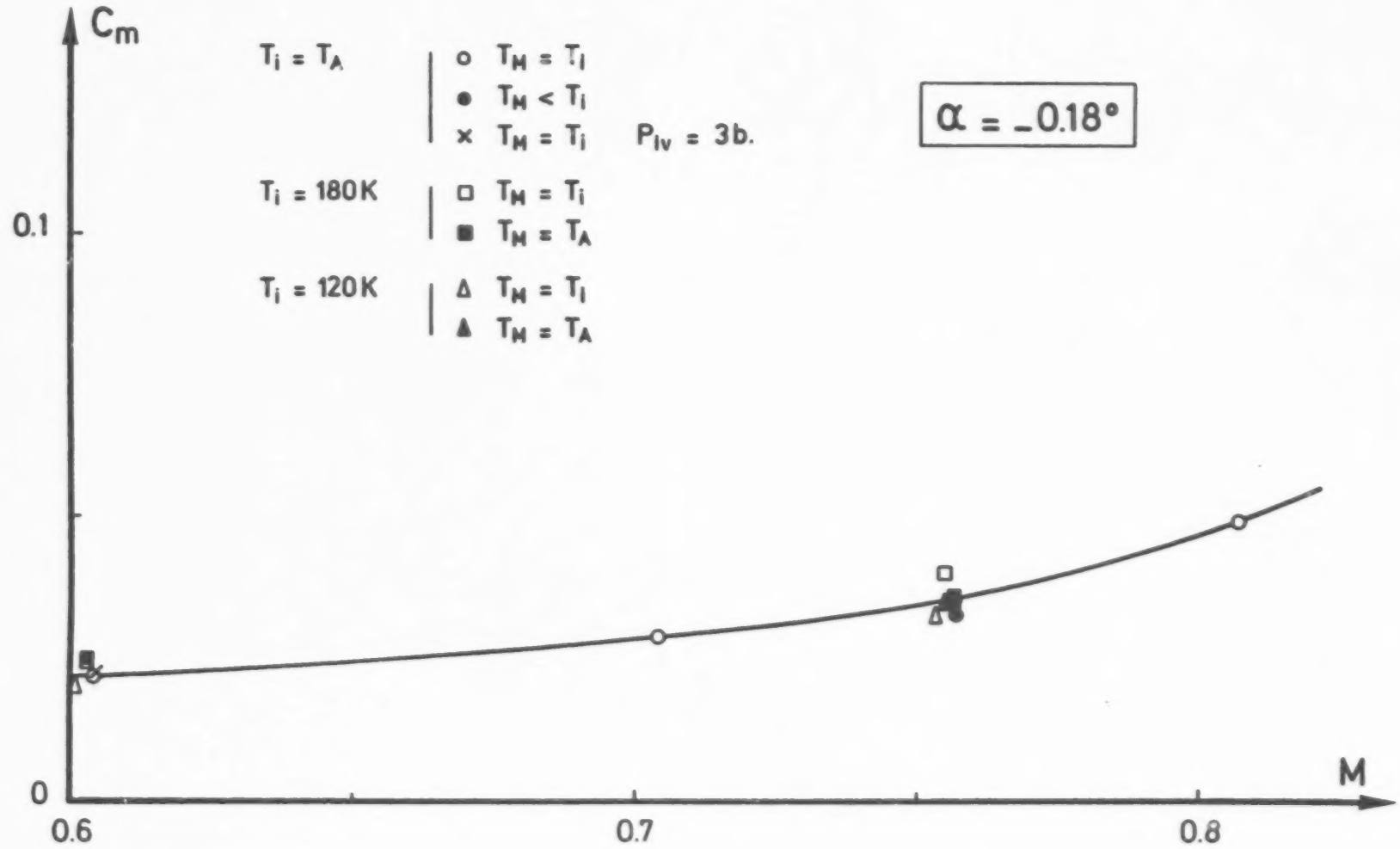

Pl. 34

Fig. 34 - Variation of Cm as a Function of the Mach Number

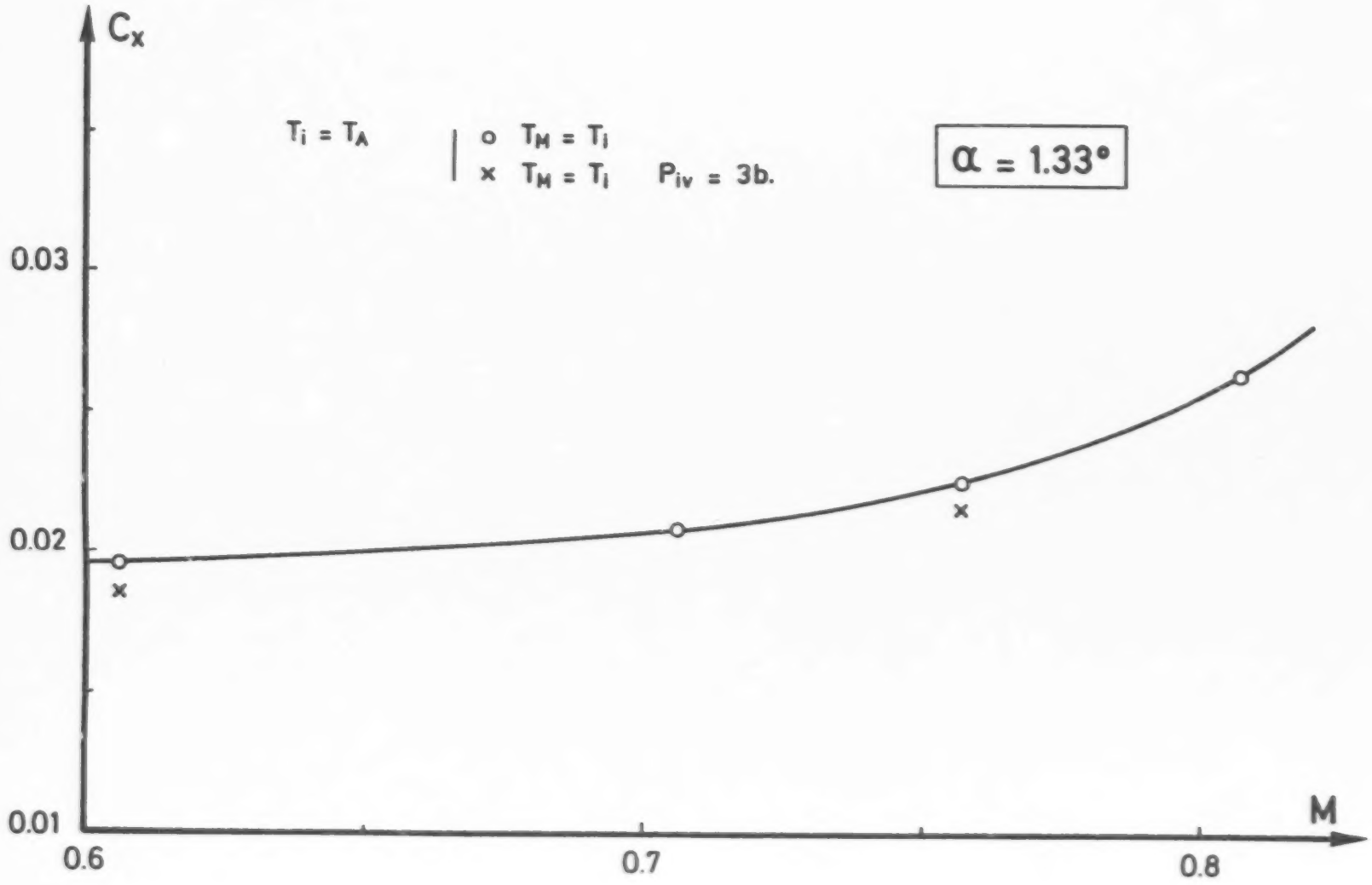

Fig. 35 - Variation of Cx as a Function of the Mach Number

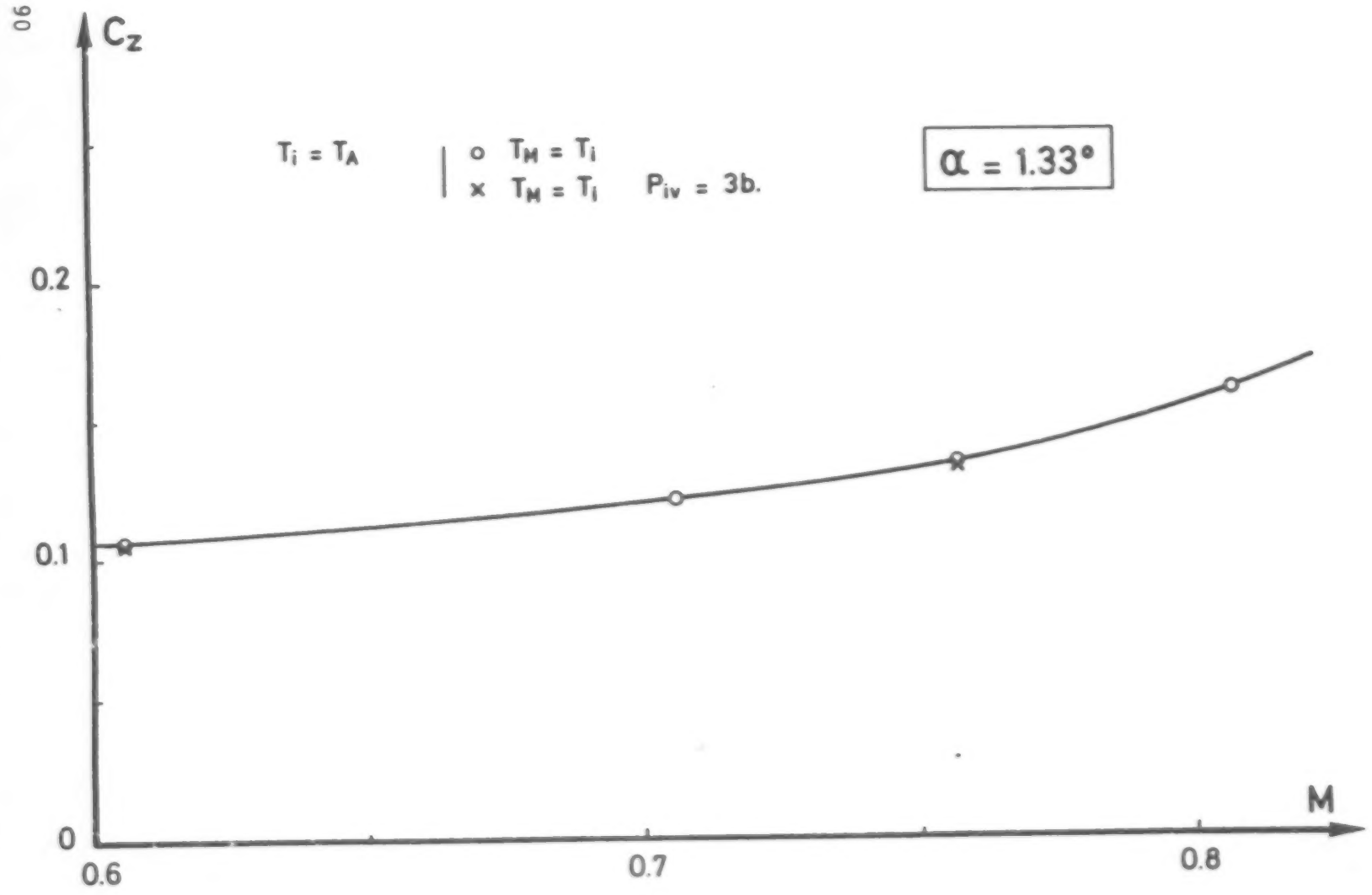

Pl. 36

Fig. 36 - Variation of Cz as a Function of the Mach Number

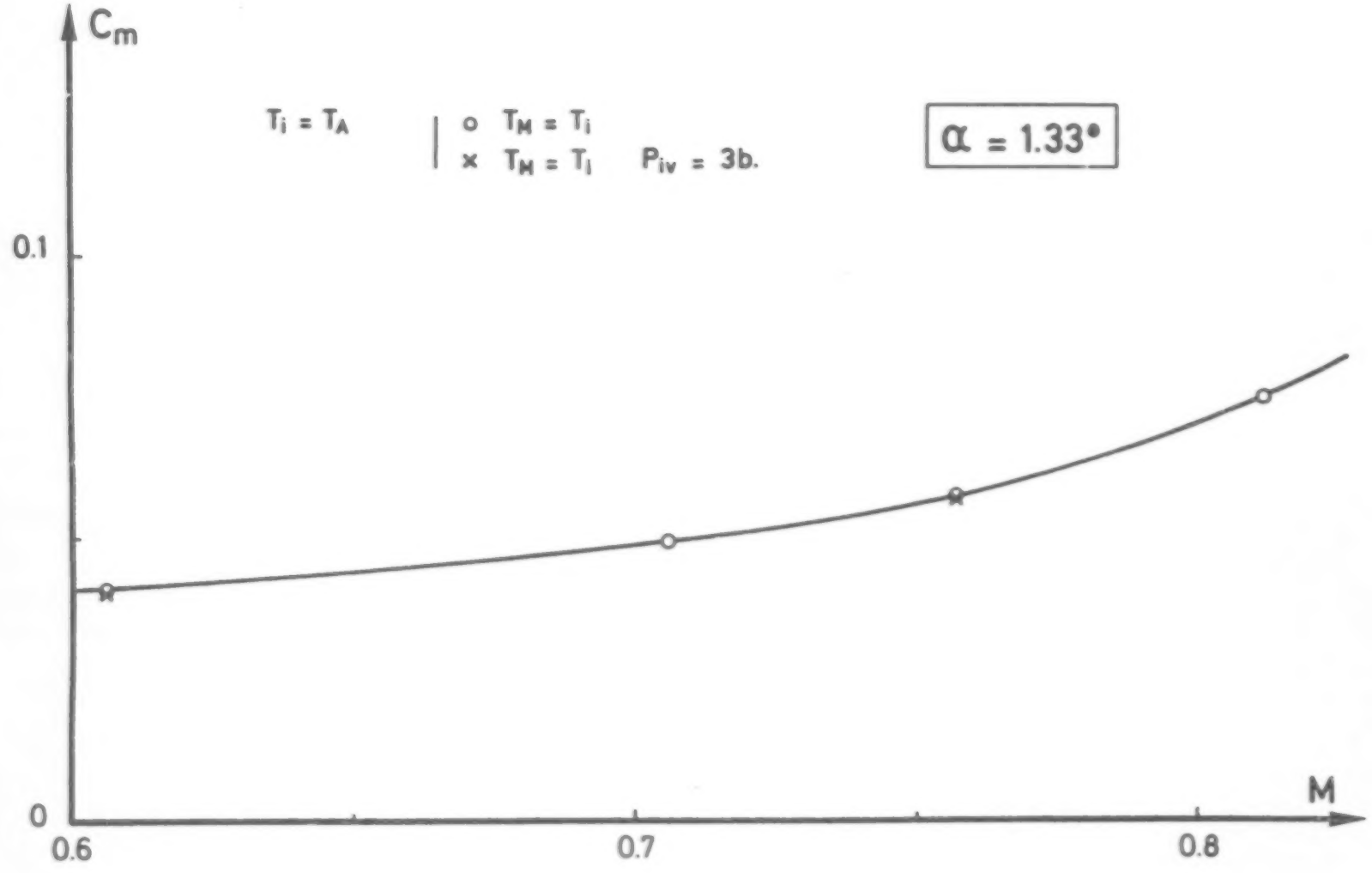

Fig. 37 - Variation of Cm as a Function of the Mach Number

Pl. 37

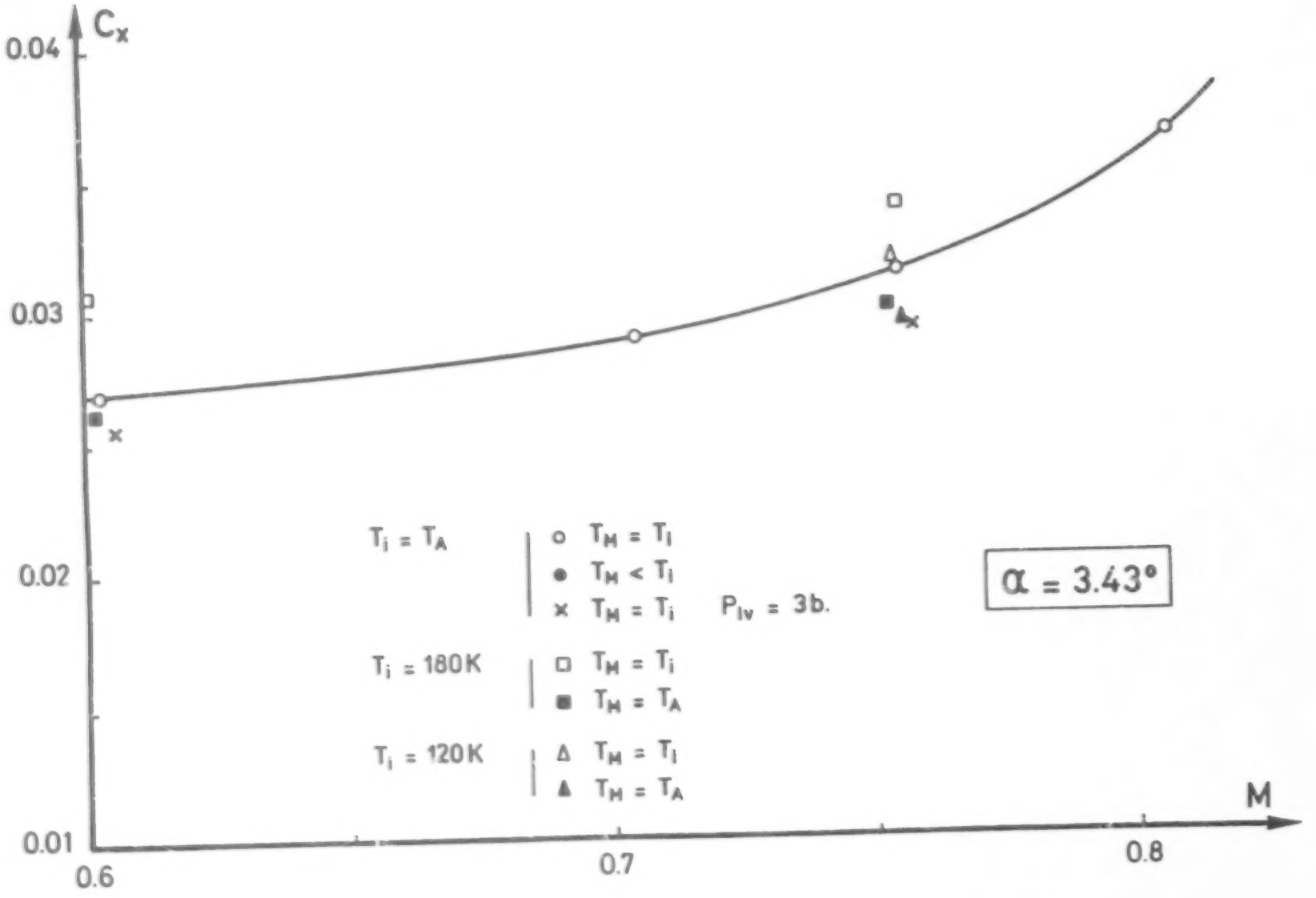

Pl. 38

Fig. 38 - Variation of Cx as a Function of the Mach Number

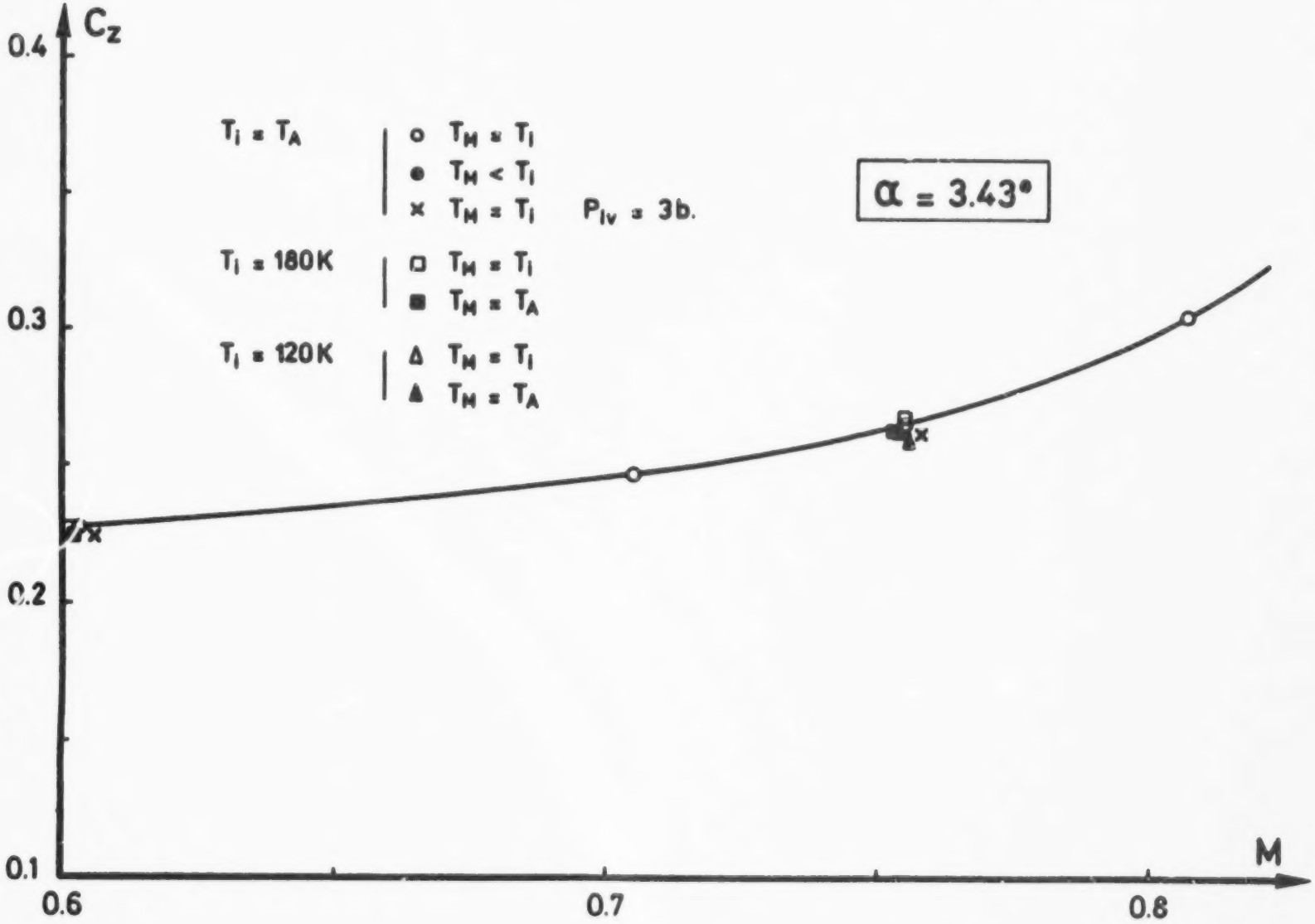

Fig. 39 - Variation of Cz as a Function of the Mach Number

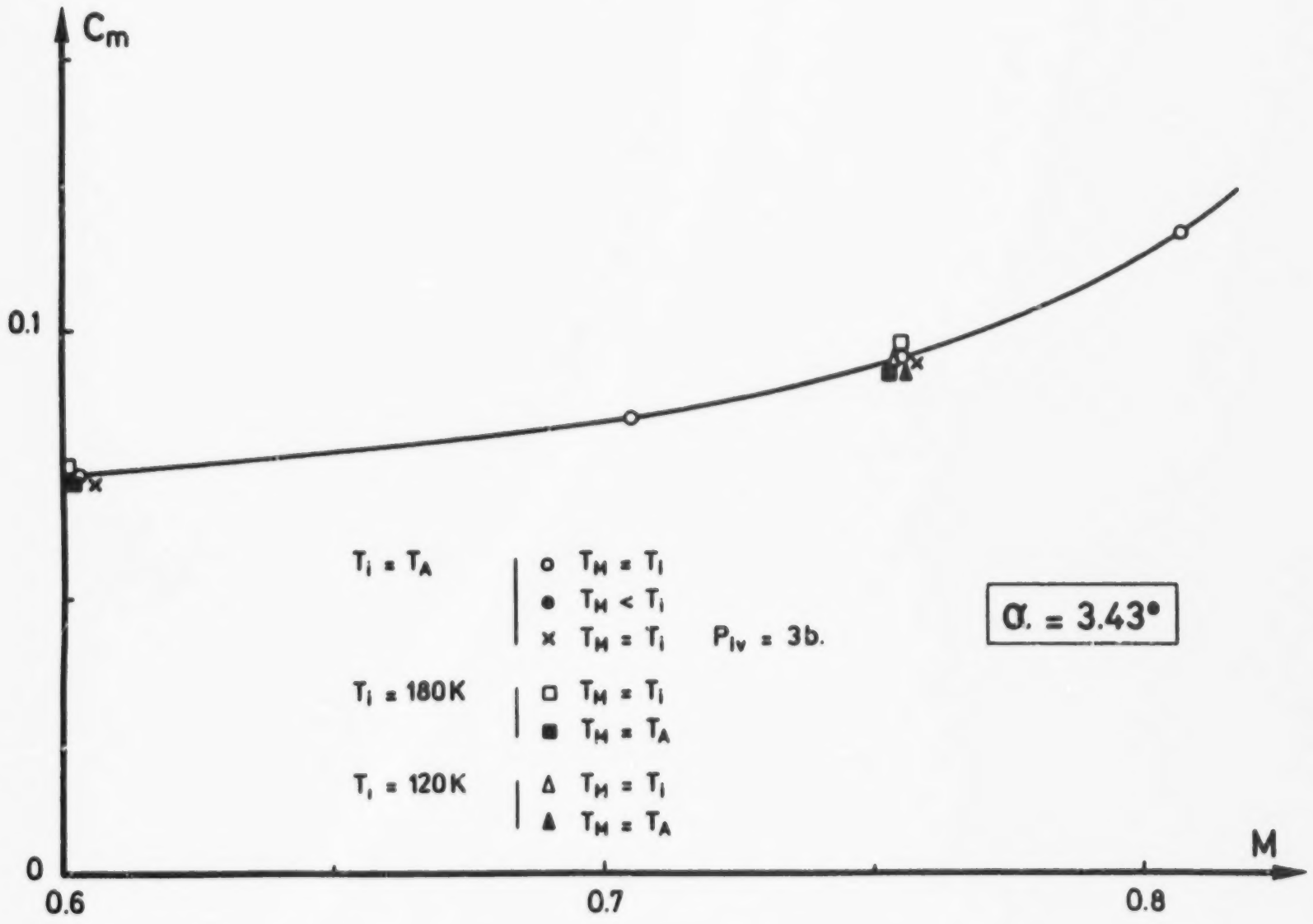

Pl. 40

Fig. 40 - Variation of Cm as a Function of the Mach Number

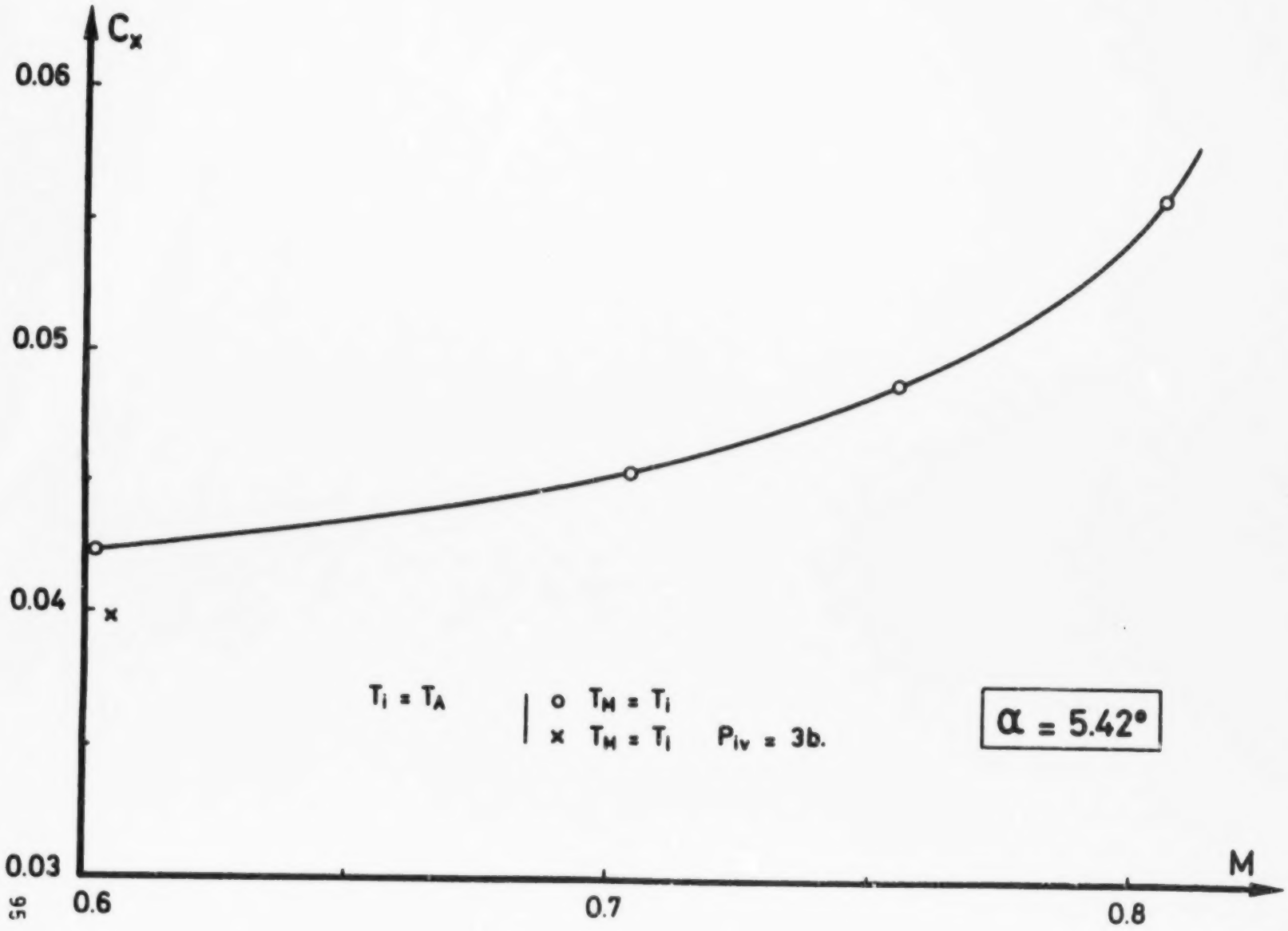

Fig. 41 - Variation of Cx as a Function of the Mach Number

Pl. 41

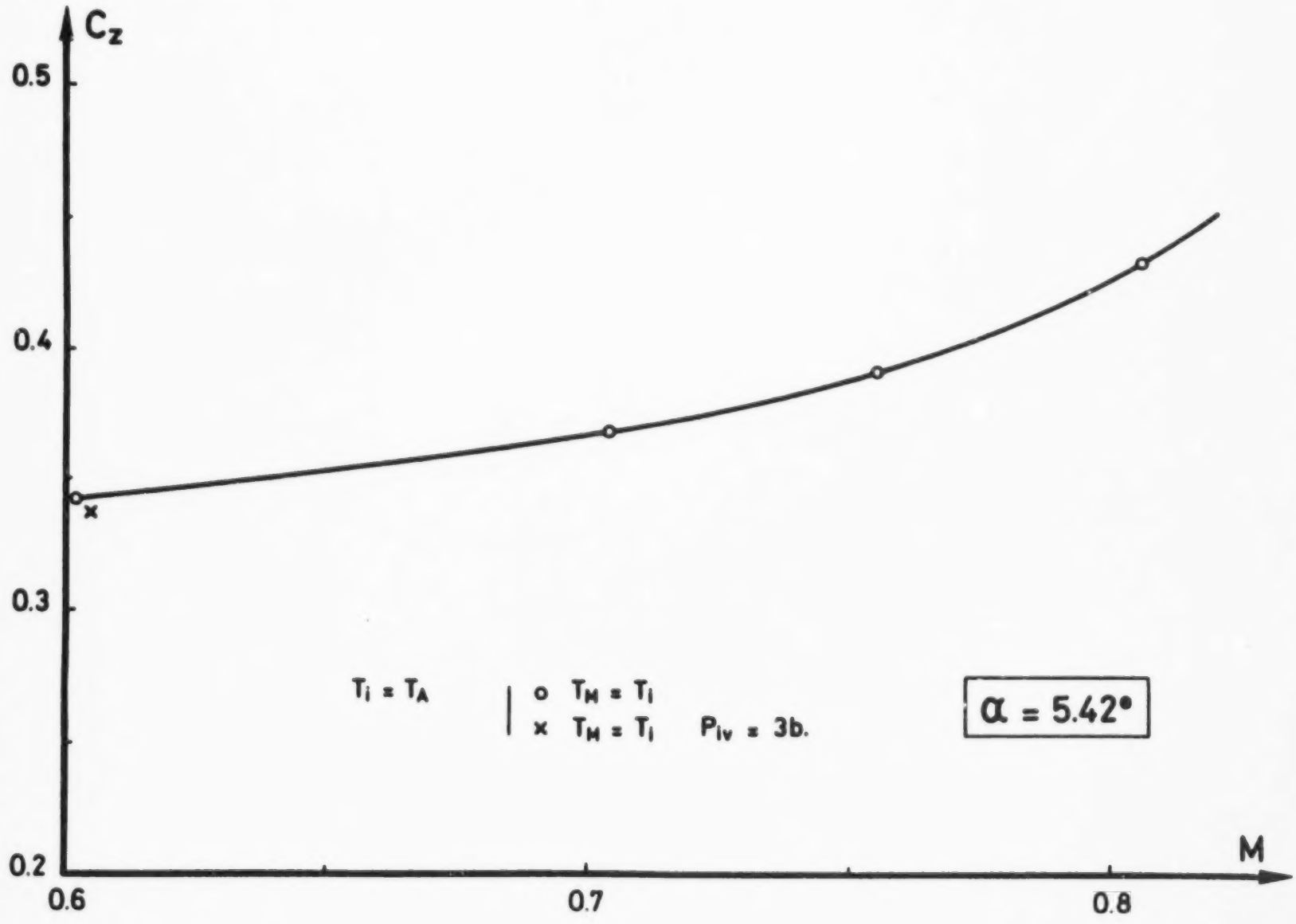

Pl. 42

Fig. 42 - Variation of Cz as a Function of the Mach Number

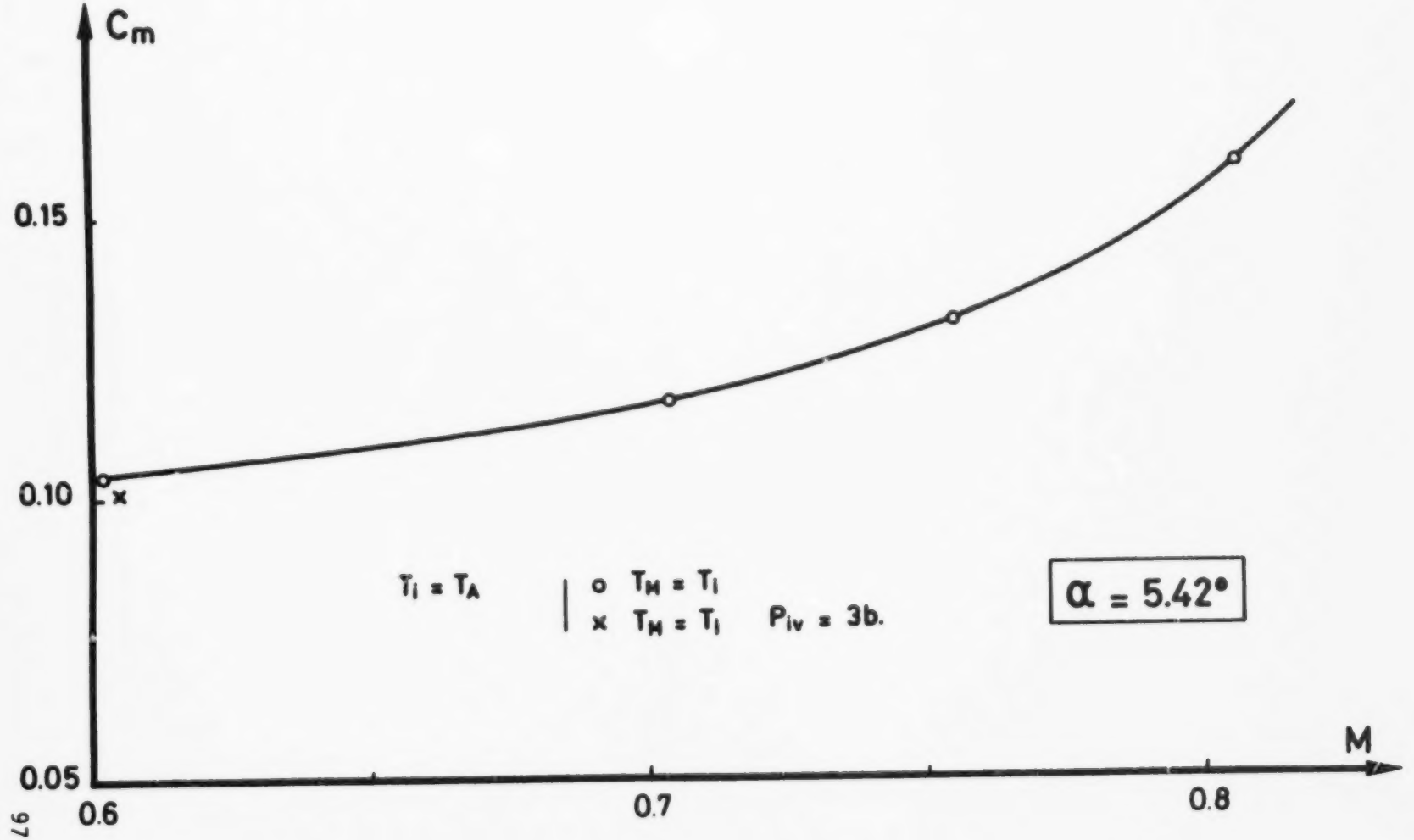

Fig. 43 - Variation of Cm as a Function of the Mach Number

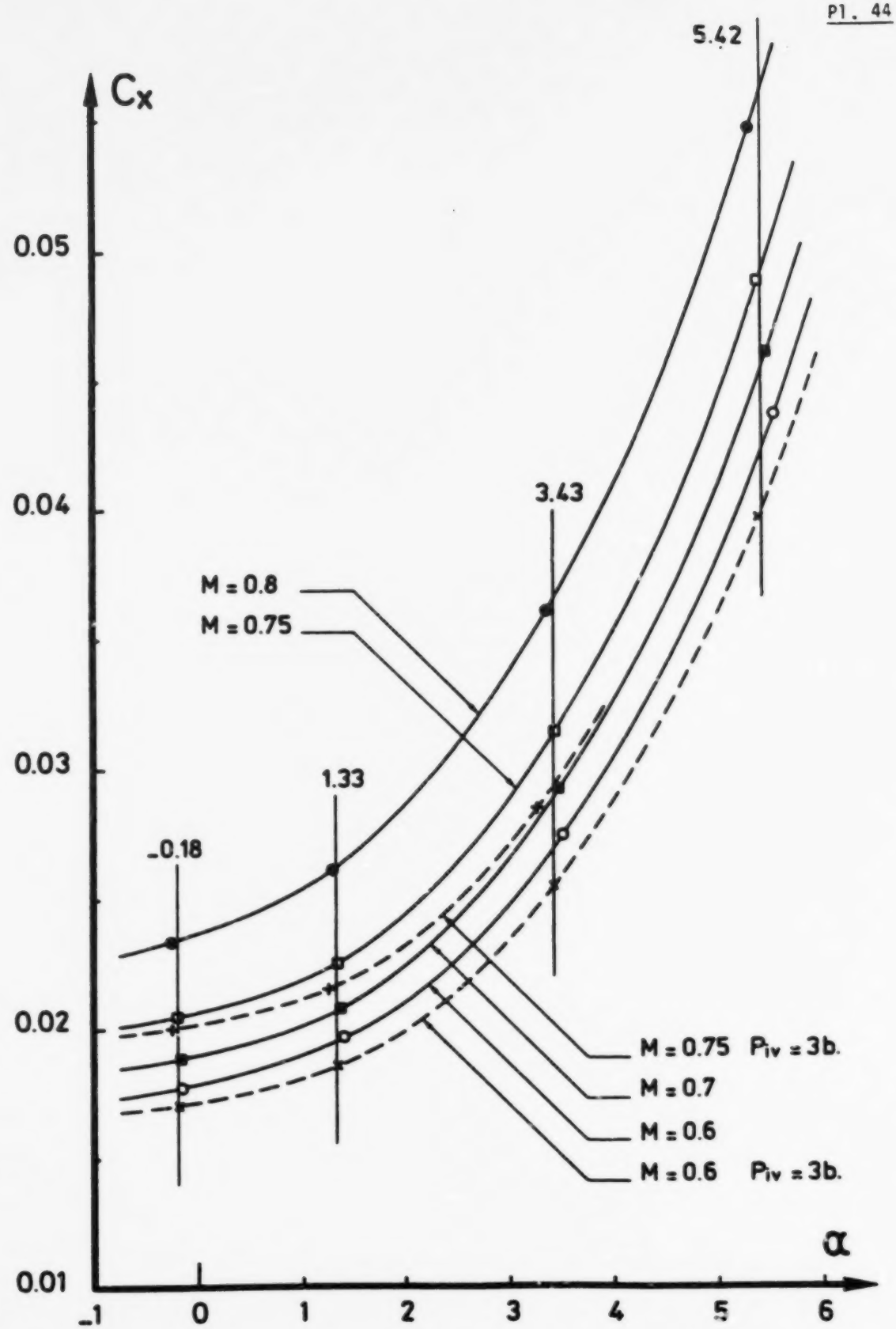

Fig. 44 - Variation of Cx as a Function of the Angle of Attack (Ti = Ta)

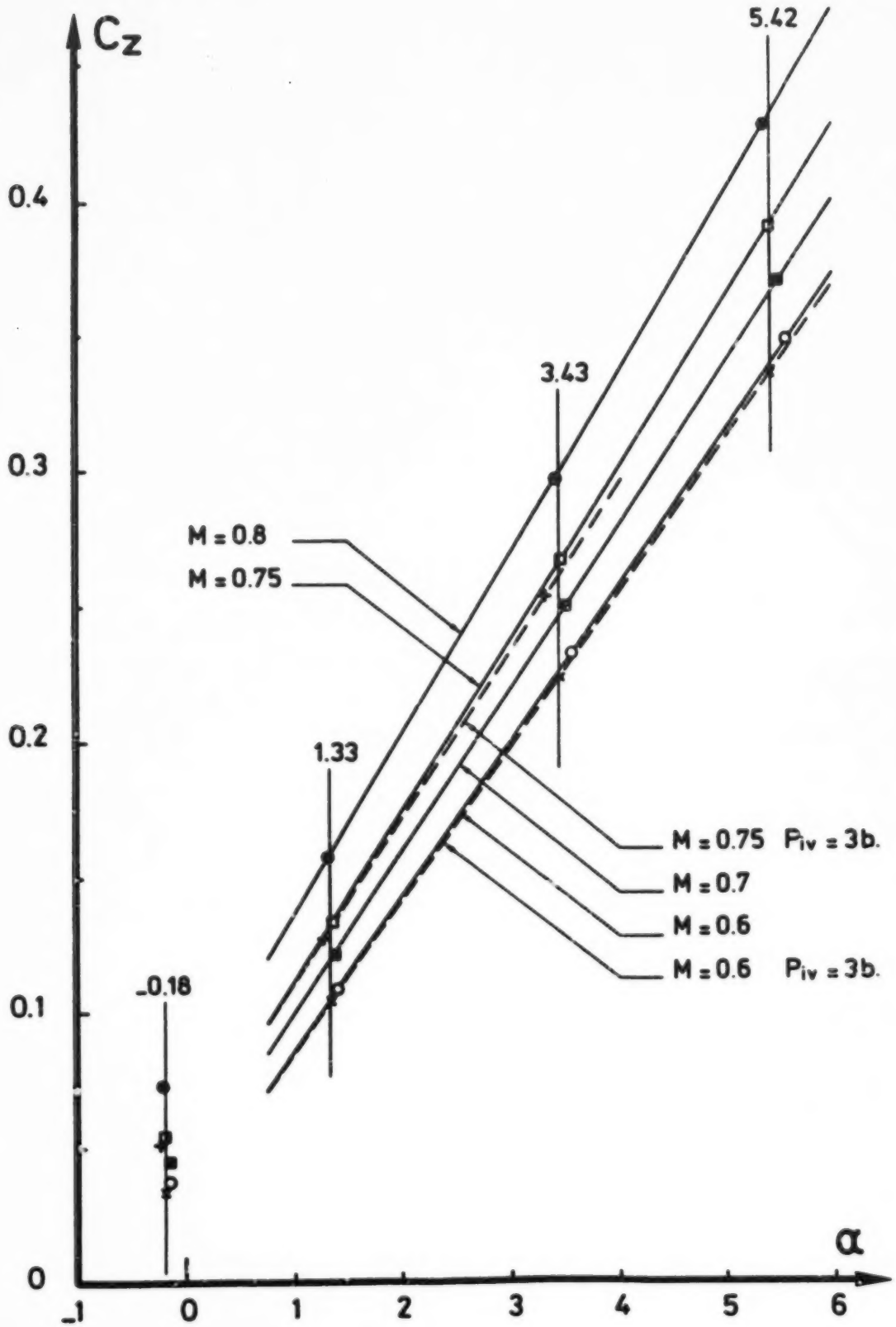

Fig. 45 - Variation of Cz as a Function of Angle of Attack (Ti = Ta)

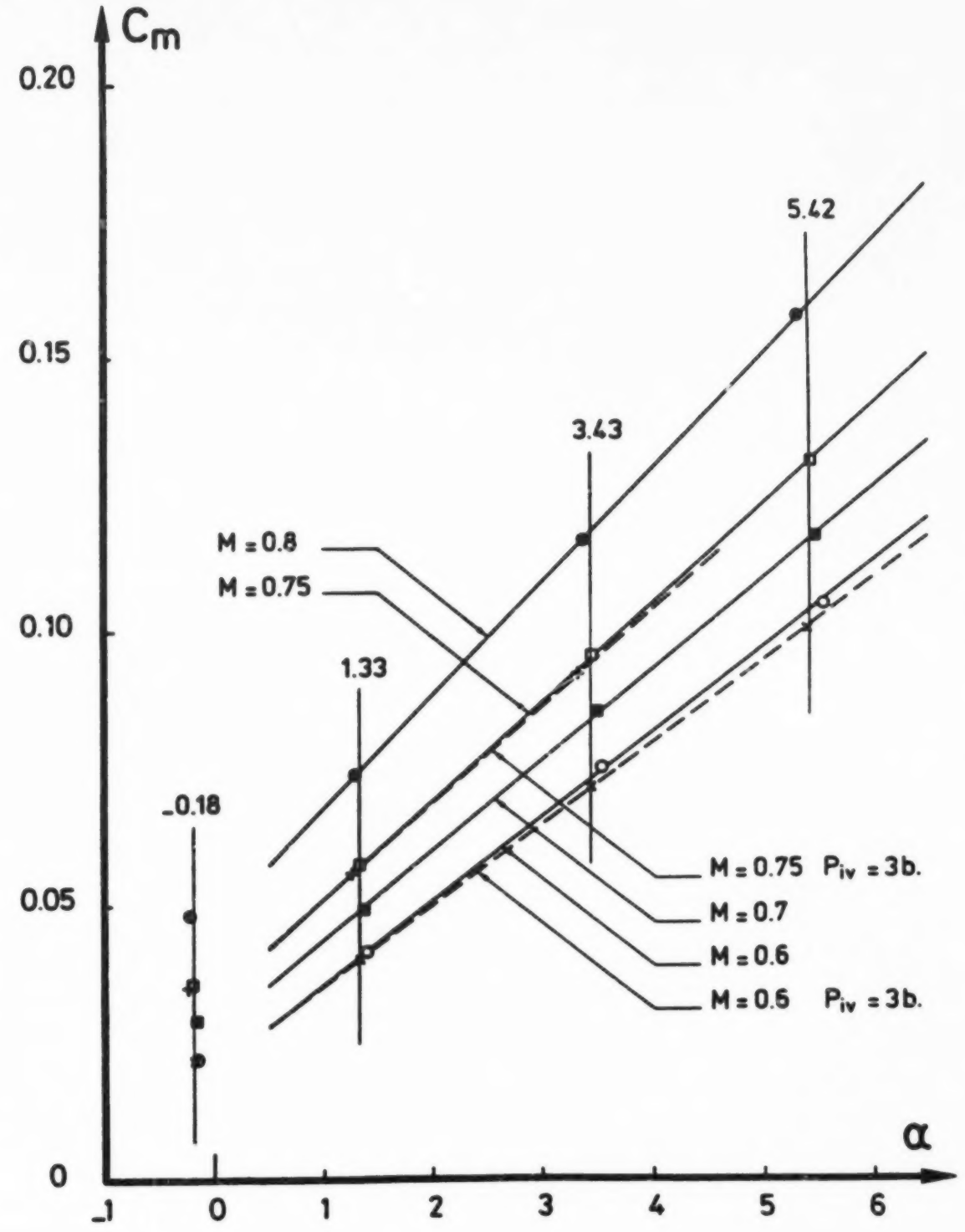

Fig. 46 - Variation of Cm as a Function of the Angle of Attack (Ti - Ta)

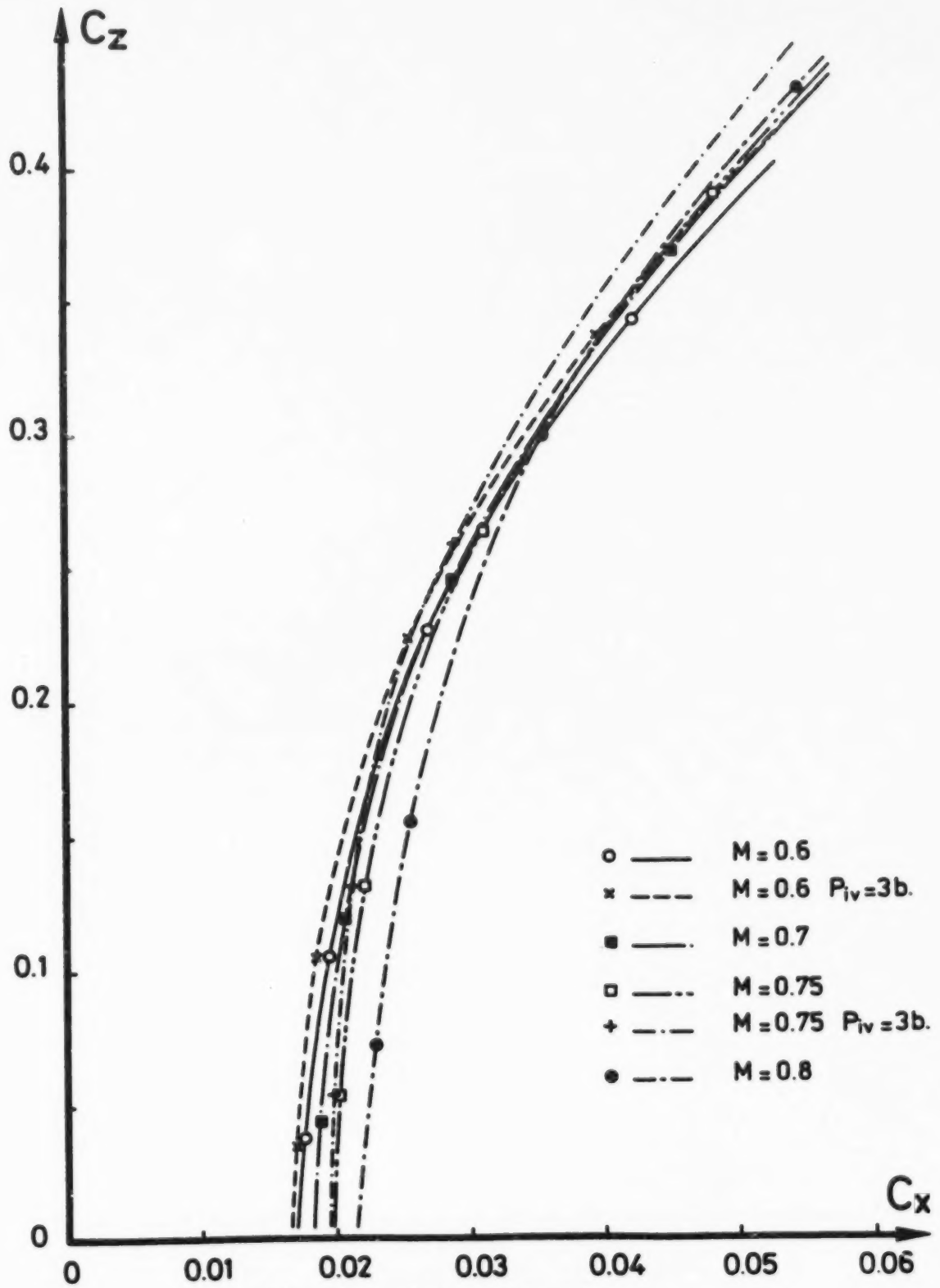

Fig. 47 - Polar (Ti = Ta)